Republic of Iraq
Ministry of Higher Education
and Scientific Research
Babylon University / College of Engineering
Civil Engineering Department

Flexural Behavior of Reinforced Concrete Beams Strengthened by Near Surface Mounted Bars and Carbon Fiber Reinforced Polymer Sheets

A Thesis
Submitted to the College of Engineering at the University of Babylon in Partial Fulfillment of the Requirements for the Degree of Master in Engineering \Civil Engineering \Structures

By

Hadeel Sameer Hamdi Hakeem

Supervised by

Asst. Prof. Dr. Hayder Mohammed Jawad Ali Alkhafaji

2022 A.D **1444 A.H**

To My Family

With Love and Respect

Hadeel S. AL-Ameedee

2022

(و يسألونك عن الروح قل
الروح من أمر ربي وما أوتيتم
من العلم إلا قليلا)

سورة الاسراء (الآية 85)

Certification

I certify that **Hadeel Sameer Hamdi AL-Ameedee** accomplished the preparation of this thesis entitled **" Flexural Behavior of Reinforced Concrete Beams Strengthened by Near Surface Mounted Bars and Carbon Fiber Reinforced Polymer Sheets "** under my supervision at the University of Babylon in fulfillment of partial requirements for the degree of Master in Civil Engineering (Structural Engineering).

Signature:

Name: Asst. Prof. Dr. Hayder Mohammed Jawad Ali Al-Khafaji

Date: / / 2022

Certificate of the Examining Committee

We certify that we have read this research entitled **" Flexural Behavior of Reinforced Concrete Beams Strengthened by Near Surface Mounted Bars and Carbon Fiber Reinforced Polymer Sheets "**, presented by **"Hadeel Sameer Hamdi AL-Ameedee "** and as an examining committee, we examined the student in its content and in what is connected with it, and that in our opinion, it meets standard of a thesis for the degree of Master of Science in Civil Engineering (Structures Engineering).

Signature:

Name**: Assist. Prof. Dr. Hayder Mohammed Jawad Ali Alkhafaji**

(Member and Supervisor)

Date**:** / / 2022

Signature:

Name: **Assist. Prof. Dr. Husain Khalaf Jarallah**

(Member)

Date**:** / / 2022

Signature:

Name: **Assist. Prof. Dr. Bahaa Hussain Al-Abbas**

(Member)

Date**:** / / 2022

Signature:

Name: **Prof. Dr. Haitham H. Muteb**

(Chairman)

Date**:** / / 2022

Approval of the Civil Engineering Department
Head of Civil Engineering Department

Signature:

Name: **Prof. Dr. Thair J. Mizhir Alfatlawi**

Date**:** / / 2022

Approval of the Dean of the College Engineering
Dean of the College of Engineering

Signature:

Name: **Prof. Dr. Hatem Hadi Obeid**

Date**:** / / 2022

Acknowledgments

In the name of Allah, the most gracious, the most merciful

All thanks and praise to Allah Who enabled me to achieve this research work.

Firstly, I would like to express my sincerest gratitude to my supervise or professor, ***Dr. Hayder M. Al-Khafaji****, for his invaluable insight, wisdom, and guidance. I am really indebted to him.*

I would like to thank the staff of the Department of Civil Engineering of Babylon University for their assistance with daily matters throughout my graduate academic life. Also, thanks to the technical staff of the structural laboratories for their assistance during the undertaking of my experimental program.

I would like to acknowledge the friendly support and assistance of my fellow graduate students who made my overall experience more gratifying.

I would like to thank ***Dr. Majid Muhammed Kazim*** *for his help, guidance and valuable opinions, which made my overall experience more enjoyable.*

I would like to thank ***Mustafa AL-Ameedee*** *and* ***Ola Mazin*** *for their kind help, support and guidance.*

Finally, a special thanks and gratitude to ***my family*** *for their care, and patience, in particular: my parents, and my brothers, who have been by my side throughout this entire endeavor. Without their love, encouragement, and support I would not have been able to complete this academic achievement.*

Hadeel S. AL-Ameedee

2022

Abstract

The strengthening and enhancing of structures represent an important aspect in the construction industry due to the growing need to increase the tolerability of origin to a specific level and within the required rehabilitation and maintenance work. The aim of the present study is to focus on the behavior of the reinforced concrete beams strengthened by two composite techniques (NSM) and (EBR) in flexure. In the present research, experimental and analytical studies have been devoted to investigating the behavior of two types of concrete (normal concrete and fiber concrete) simply supported beams strengthened with different types of bars, sheet, and composite products. The experimental work consists of the fabrication and testing of sixteen reinforced concrete beams with a cross section of (150x300mm) and a total length of (1500mm), which were tested under one-point loads. All beams are tested to failure with strain gages, dataloggers, and LVDTs, and their failure mode and ultimate load capacity are recoded. Besides, the strains, crack width, and crack pattern are measured in concrete at different load levels. The experimental results showed a significant increase in ultimate load capacity for all strengthened beams as compared to the control beams. Also, in group one, when using normal concrete for these strengthened beams, the use of CFRP is better than GFRP and steel reinforcing bar by about 2.41%. The use of NSM CFRP with CFRP sheet (EBR) technique strengthening is better than using CFRP (NSM) only, and the increase in the ultimate load is about 5.49%. Using micro steel fiber in group two in reinforcement in RC beams has a significant effect on the flexural strength and deflection of tested beams about (14.94%) better than in group one.

The strengthening of beams by CFRP composites reduces the maximum deflection under the same load the mid-span deflection is reduced by 55.92% for the beams with NSM CFRP. On the other hand, the maximum deflection is reduced by 60.02% for beams with EBR. The results showed that carbon fibers have a good ability to repair damaged beams, with an improvement in the bearing capacity of the beam. The optimum rehabilitation method is to use a CFRP bar with a CFRP sheet of about (44.08% -38.37%).

The theoretical investigation presents a three-dimensional nonlinear finite element model suitable for the analysis of reinforced concrete beams, which was produced using the ANSYS computer program (V. 19.2). A full bond is assumed between the CFRP, GFRP, and concrete surface and between the steel reinforcement and concrete. The brick elements SOLID65 and SOLID45 are used to represent concrete elements and steel plates, respectively. whereas LINK180 was used to represent steel reinforcement and Beam188 CFRP and GFRP bar, respectively. Shell 181 was used to represent CFRP composites, respectively. Based on the ultimate load, a comparison of the experimental and theoretical results showed that they were pretty close to each other.

List of Contents	
Subject	**Page**

The major symbols used in this thesis are listed below, the others are defined as they first appear.

Notation		
Symbol	**Definition**	**Unit**
A	Cross sectional area of a section.	mm^2
Ab	Area of reinforcement bar.	mm^2
Ac	Net area of concrete section.	mm^2
As	Area of longitudinal tension reinforcement.	mm^2
As`	Area of longitudinal compression reinforcement.	mm^2
Ast	Total area of longitudinal reinforcement.	mm^2
b, bw	Width of beam.	mm
d	Effective Depth.	mm
db	Diameter of bar.	mm
E	Modulus of Elasticity.	GPa
Ec	Modulus of elasticity for concrete.	GPa
Es	Modulus of elasticity of longitudinal steel reinforcement.	GPa
fcu	Compressive Strength of Concrete Cubes.	MPa
fcuf	Compressive Strength of Fiber Concrete Cubes.	MPa
fy	Yield stress of steel.	MPa
F'c	Cylinder compressive strength of concrete	MPa
fr	Flexural strength of concrete (modulus of rupture).	MPa
fct	Indirect tensile strength (splitting tensile strength).	MPa
fcu	Cube compressive strength of concrete.	MPa
fy	Yield stress of steel.	MPa
L	Total length of beam.	mm
Ln	Clear span of beam.	mm
Mu	Ultimate moment capacity.	kN.m
Mn	Nominal moment capacity.	kN.m
P	Maximum applied load.	kN
Pcr	Cracking load.	kN
Pu	Ultimate load.	kN
w/c	Water to Cement ratio.	
ϕ	Size of bar.	mm
ρ	Ratio of longitudinal tensile reinforcement.	
ρmin	Minimum ratio of longitudinal tensile reinforcement.	
Δmax.	Maximum deflection.	mm
Ɛ	Strain.	mm/mm
w/c	Water to Cement ratio.	
υ	Poisson's ratio of concrete.	
υs	Poisson's ratio of steel.	
εc	Axial applied load.	kN
εc	Ultimate load.	kN
εs	Volume to surface ratio.	

Abbreviations	
Symbol	**Definition**
ACI	American Concrete Institute.
ASCE	American Society of Civil Engineering
ASTM	American Society for Testing and Materials
B. S	British Standards (BSI: British Standard Institute)
IQs.	Iraqi Standard Specification
Ch.	Chapter
NSM	Near surface mounted
EB	External Bonded
ANSYS	Analysis system program
FE	Finite Element
F.E.A.	Finite Element Analysis
F.E.M.	Finite Element Method
RC	Reinforced Concrete
FRP	Fiber reinforcement polymer
CFRP	Carbon fiber reinforcement polymer
GFRP	Glass fiber reinforcement polymer
EBR	Externally Bonded Reinforcement
Rebar	Reinforcing Bar
SF	Steel Fiber
Eq.	Equation
N. A	Neutral Axis
fc ′	cylinder compressive strength
EXP.	Experimental
OPC	Ordinary Portland Cement
CF	Steel Fiber Reinforced Concrete
w/c	Water to Cement ratio
Kg	kilogram
MPa	Mega Pascal (N/mm2)
GPa	Gega Pascal (kN/mm2)
D	Dimension(s).
Max.	Maximum
Min.	Minimum.
No.	Number.
Vol.	Volume.
Fig.	Figure
c/c	center to center

Chapter One
INTRODUCTION

1.1 Introduction

Due to the growing requirement to increase the tolerability of origin to a particular level and within the needed repair and maintenance work, strengthening and enhancing structures is a key feature in the construction industry. The performance and effectiveness of the Near Surface Mounted (NSM) strengthening technology for hybrid steel fiber reinforced concrete beams were assessed in this study. The specimens were tested under point load to failure to determine the flexural behavior of the beams. The structural performance, deflection, ductility, stiffness, and modes of failure of the tested beams are presented and discussed.

Concrete is one of the world's most widely used construction materials. However, since the early 1800's, it has been known that concrete is weak in tension. Weak tensile strength combined with brittle behavior results in sudden tensile failure without warning. This is obviously not desirable for any construction material. Thus, concrete requires some form of tensile reinforcement to compensate for its brittle behavior and improve its tensile strength and strain capacity to be used in structural applications. Historically, steel has been used as the material of choice for tensile reinforcement in concrete [1].

In some cases, the structure needs to be strengthened or repaired to increase its strength to withstand any load increase or to restore its initial strength. Strengthening has been used in many structures. One of the ingenious strengthening techniques is Near-Surface Mounted (NSM), in which carbon fiber polymers are placed in the concrete cover at the tension side and bonded with high-strength resin (Epoxy) [2].

1.1.1 Benefits of concrete

There are numerous positive aspects of concrete:

- It is a relatively cheap material and has a relatively long life with few maintenance requirements.
- It has strong compression.
- Before it hardens, it is a very elastic substance that can easily be shaped.
- It is non-combustible [3].

1.1.2 Advantages of concrete beams

- Concrete beams have high compressive strengths as compared to other building materials. The reinforced concrete beam for the building system is more durable than any other building material or method.
- Due to providing reinforcement, concrete can also help a quality amount of tensile stress.
- The weather and fire resistance of reinforced concrete is excellent.
- The cost of maintaining reinforced concrete beams is minimal.
- Reinforced concrete can be molded into any shape, and it's usually used in precast structural component, beams applications shown in Figure (1-1).
- Compare to the steel in structured, and reinforced concrete cannot require skilled professional labor for the installing of structure [4].

Figure (1-1): beams application.

1.1.3 Disadvantages of Reinforced Concrete

The reinforced concrete tensile strength is 1/10 of all the Compressive Strength. There are plenty of steps using reinforced concrete in mixing, curing, and casting. These have an impact on the final gain strength. The cost of forms used in casting RC is comparatively higher [5]. The tensile strength of concrete is relatively low compared to other binding materials. Concrete is less ductile. The weight of the comparison is high compared to its strength. Concrete may contain soluble salts. Soluble salts cause efflorescence [6].

1.2 Fiber-reinforced concrete – Advantages, types and applications

Reinforced with fibers Concrete is a composite material consisting of fibrous material, which increases its structural integrity. It includes mixtures of cement, mortar or concrete and discontinuous, discrete, uniformly dispersed suitable fibers. Fibers are usually used in concrete to control cracking due to plastic shrinkage and drying shrinkage. They also reduce the permeability of concrete, and thus reduce the bleeding of water [7].

1.2.1 Advantages of Fiber-reinforced concrete [4].

- Fiber reinforced concrete may be useful where high tensile strength and reduced cracking are desirable or when conventional reinforcement cannot be placed.
- It improves the impact strength of concrete, limits crack growth and leads to a greater strain capacity of the composite material.
- For industrial projects, macro-synthetic fibers are used to improve concrete's durability. Made from synthetic materials, and are long and thick in size and may be used as a replacement for bar or fabric reinforcement. Show Types of Fiber Reinforced concrete in Figure (1-2).
- Adding fibers to the concrete will improve its freeze-thaw resistance and help keep the concrete strong and attractive for extended periods.
- Improved mix cohesion, improving pumpability over long distances.

- This increases resistance to plastic shrinkage during curing.
- Minimizes steel reinforcement requirements.
- It tightly controls the crack widths, thus improving durability.
- Reduces segregation and bleed-water.
- FRC's toughness is about 10 to 40 times that of plain concrete.
- Fibers increase the shear capacity of reinforced concrete beams[4].

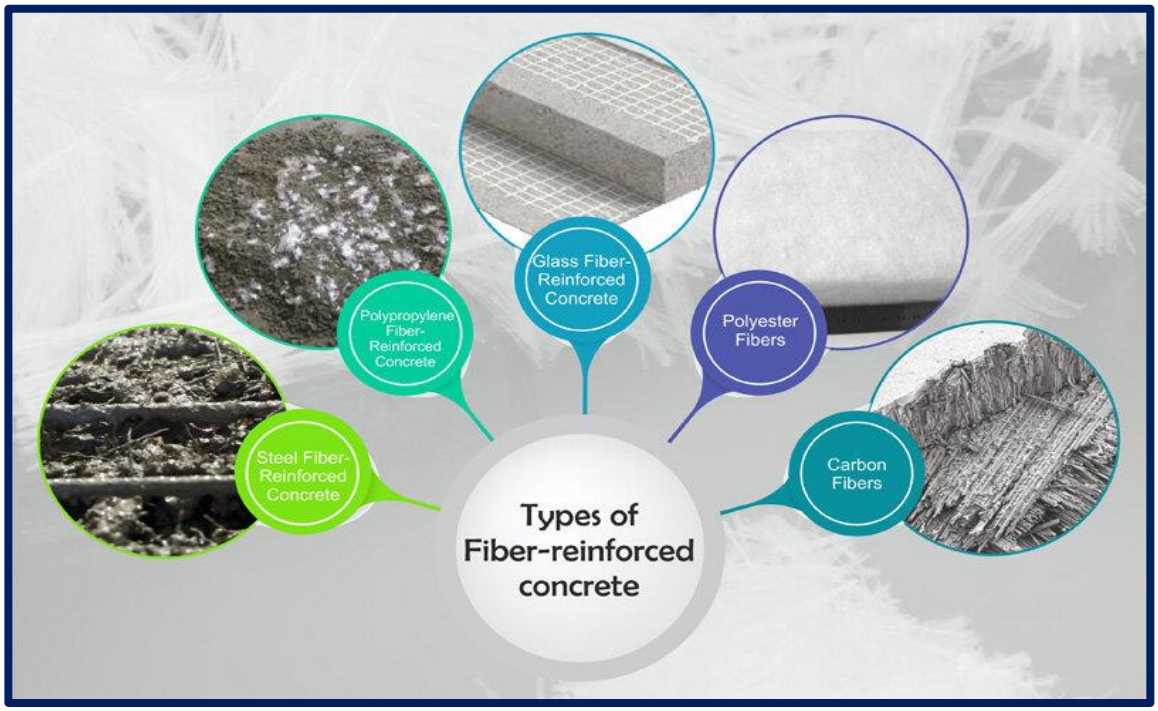

Figure (1-2): Types of Fiber Reinforced concrete [4].

1.2.2 Different types of fiber-reinforced concrete

Fibers for concrete are available in different sizes and shapes. The major factors affecting the characteristics of fiber-reinforced concrete are the water-cement ratio, percentage of fibers, diameter and length of fibers. Given below are different types of fiber-reinforced concrete used in construction.

- Steel-Fiber Reinforced Concrete.
- Polypropylene Fiber Reinforced (PFR) Concrete.
- Glass Fiber Reinforced Concrete.
- Polyester fibers.
- Carbon fiber.
- Macro synthetic fibers.

- Micro-synthetic fibers.
- Cellulose fiber.
- Natural fibers.

The use of natural fibers in making concrete is recommended since several types of these fibers are available locally and are plentiful as shown in Figure (1-3). The idea of using such fibers to improve the strength and durability of brittle materials is not new; for example, straw and horsehair are used to make bricks and plaster. Natural fibers can be used to make concrete stronger, and they are easy to find in developing countries [3].

Figure (1-3): Natural fiber.

1.2.3 Application of Fiber-reinforced concrete

The applications of fiber reinforced concrete depend on the application and builder in taking advantage of the static and dynamic characteristics of the material. Some of its areas of application are shown in Figure (1-4) below:

- Runway.
- Aircraft Parking.
- Pavements.
- Tunnel Lining.

- Pipes.
- Slope Stabilization.
- Thin shell.
- Walls.
- Manholes.
- Hydraulic Structure.
- Dams.
- Roads.
- Bridges.
- Elevated decks.
- Warehouse floors and other application.

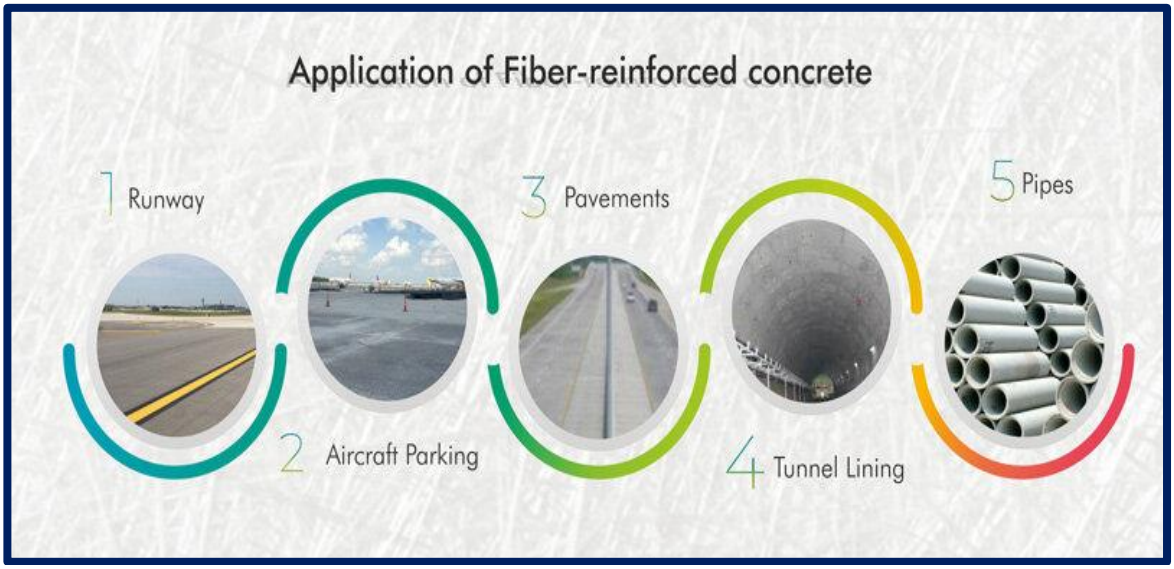

Figure (1-4): Application of Fiber-reinforced concrete.

1.3 Strengthening of structures

In the last decades, strengthening of buildings structural elements have been used widely worldwide. There are two methods of flexural strengthening of reinforced concrete members, such as externally bonded reinforcement (EBR), Externally Bonded Reinforcement of Groove (EBROG) or grooving method (GM), Externally Bonded Reinforced in Groove (EBRIG), near-surface mounted fiber reinforced polymer (NSM-FRP) rod or strips, and the holing method. EBR is one of the strengthening

techniques in which the surface should be prepared by removing the weak layer and the fiber sheets bonded to a plane tension face of concrete. Brittle failure was the main failure mode in this method. The advantages of the (EBR) method are the low cost and simple installation. However, the disadvantage of this method is the early debonding of fiber-reinforced polymer sheet from concrete as a result of exposure to external environmental conditions such as freezing, impact, and fire. The second method of strengthening is by (EBROG) or (GM). The grooves in this method have been invented to delay the debonding of CFRP from the concrete structure due to external conditions. This method was developed and renamed to the externally bonded on groove method. In which the slit is cleaned from dust by compressed air. Finally, the grooves are filled with epoxy, then fiber reinforced polymer is prepared and installed, and the excessive resin is then removed. The technique's advantages are: that the ultimate flexural strength is increased by up to 80% of the control beam, the debonding failure is eliminated, and a higher ultimate strain is obtained. The disadvantages of the (EBROG) method are: higher cost and preparation time[8]. The externally Bonded Reinforce in Groove (EBRIG) method appeared after the EBROG method by inserting the fiber reinforced polymer in the groove. The difference between the EBRIG, EBROG, and EBR is that the EBRIG gives a large contact area between the FRP and concrete layer compared to the two methods [9].

1.4 Fiber Reinforced Polymers (FRP)

Fiber-reinforced polymer (FRP) reinforcing products can effectively increase the flexural strength and stiffness of under-designed reinforced-concrete members when used as tension reinforcement; in particular, stiff FRP products such as plates, bars or laminates have been used so far in strengthening primarily the flexural properties of reinforced concrete beams

and plates[10] explain in Figure (1-5). The term "composite" often refers to a material compound of two or more featured parts working together. Often, one of the parts is harder and stronger, while the other is more of a force-transferring material. FRP is an abbreviation of Fiber Reinforced Polymers and is a composite of fibers and a polymer matrix. The material FRP holds many advantages over other materials in civil engineering. It has a very high stiffness-to-weight ratio and a high strength-to-weight ratio. The material exhibits excellent fatigue properties, non-magnetic properties, corrosion resistance, and is generally resistant to chemicals. The thermal is controllable and both material and geometrical can be tailored for the application. Fiber Reinforced Polymer, or FRP, is a composite material consisting of fibers and a polymer matrix. This study provides quantitative information about the strengthening of flexural members to contribute to developing the design procedure.

Figure (1-5): Carbon Fiber Reinforced Polymers for Concrete Construction.

1.4.1 Fiber Components

Many types of fibers are available, like glass, aramid, carbon. The most important applications for strengthening structures in civil engineering are

by carbon fibers, about 95%. Show some typical uniaxially loaded fiber materials and steel response. HM and HS are abbreviations of "high modulus of elasticity" and "high strength", respectively. Fibers have a linear elastic behavior until failure, which is brittle. The fibers are what make the FRP strong, and there are three things that control the mechanical properties of the FRP [11].

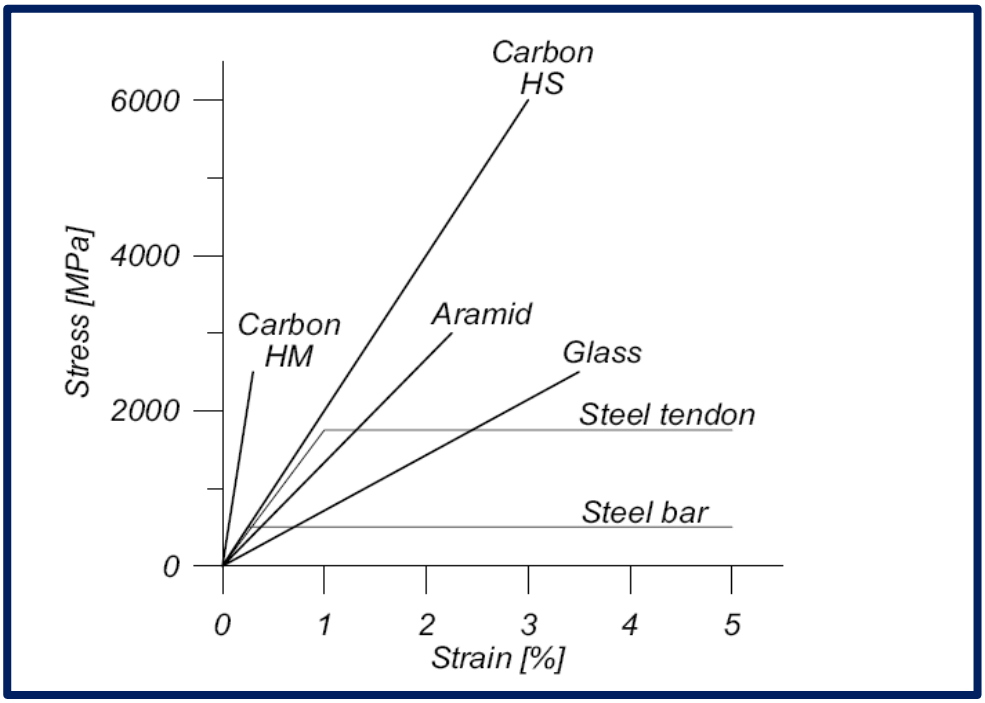

Figure (1-6): Fiber and steel stress-strain relationship [12].

1.4.2 Constituent substances

As mentioned earlier, there is a wide array of different materials to use. What is important to remember is that the fiber materials chosen, along with the polymer, determine the final quality, properties, and behavior of the FRP[13].

1.4.3 Fiber content

Regarding the amount of fiber used in the FRP, it is easy to say that the more fiber is used, the better properties will be achieved. This is somewhat true. With too high a fiber content, there will be manufacturing problems. If the fibers are tightly packed, the matrix will have problems enclosing the fibers, which might deteriorate the FRP [13].

1.4.4 Fiber orientation

The FRP will be stiffer and stronger in the fiber direction. For example, a rod with all the fibers is very strong in its fiber direction but in perpendicular direction the FRP has not as good properties. A typical FRP product for the construction industry has an isotropic behavior compared to steel which is isotropic [13].

1.5 CFRP in General

Carbon fibers have received considerable attention in recent years because of their high efficiency in producing ductile concrete. CFRP is a combination of carbon fibers and an epoxy resin matrix. CFRP laminates had unidirectional structural properties as they had very high strength and rigidity in the fiber direction and outstanding fatigue characteristics [14]. As shown in Figure (1-6), CFRP was used for strengthening and rehabilitation of beams, bridges, slabs, walls, columns, etc.

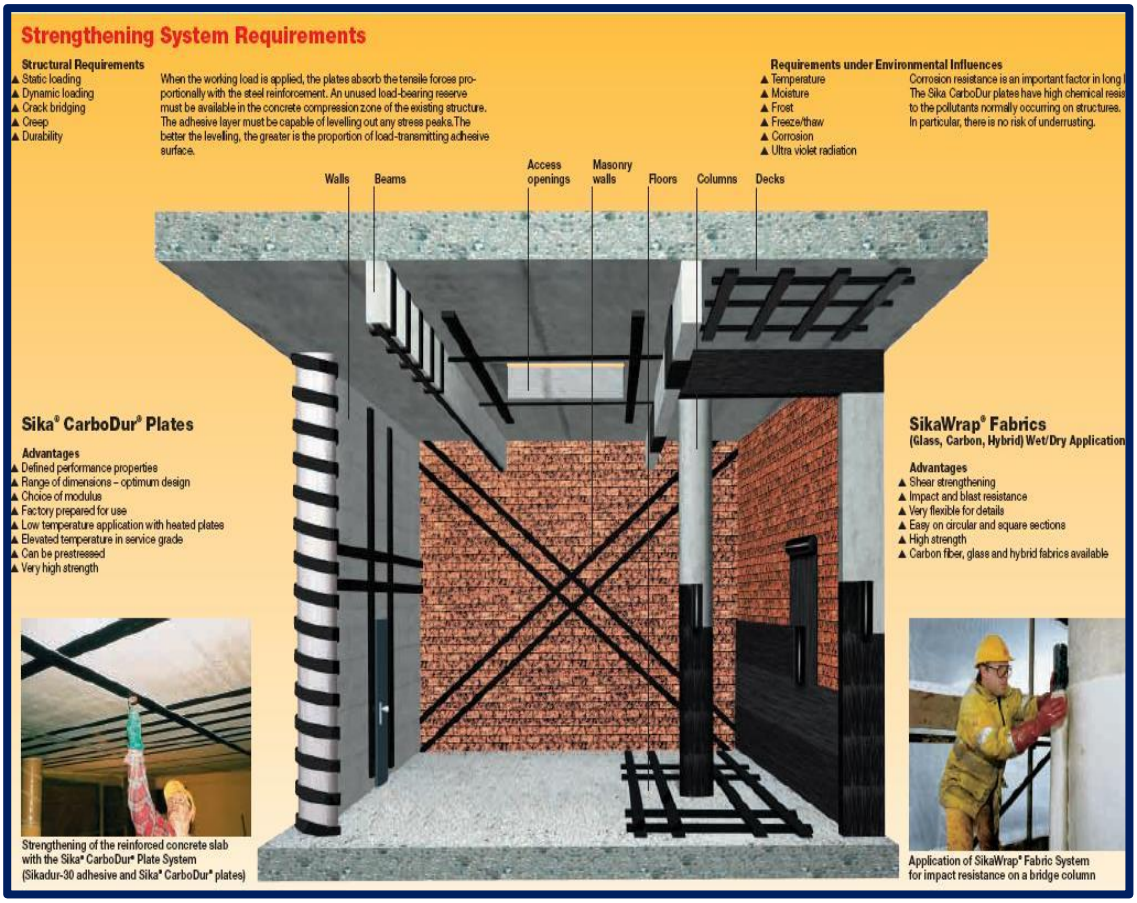

Figure (1-7): Applications of the CFRP strengthening system [13].

1.5.1 CFRP Advantages

The main advantages of CFRP were summarized in the following: -

- Very high strength (E > 165000 MPa, tensile strength > 2400 MPa).
- Outstanding fatigue strength.
- Reduced construction periods.
- Durability of the strengthening system (resistance to corrosion, alkalis, and other aggressive materials) .
- Available in any length and with the ability to be transported in rolls.
- Light weight.
- Reduced maintenance cost.
- Versatile design of systems.
- Improved fire resistance.
- Reduced mechanical fixing [15].

1.5.2 CFRP Disadvantages

The main disadvantages of CFRP are summarized in the following: -

- Erratic plastic behavior and less ductility.
- Susceptible to local unevenness.
- High cost [15].
- Need for epoxy (cohesion material) to work.
- It could be burnt easily [13].

1.6 Ductility

A concrete structure without any form of reinforcement will crack and fail with a relatively small load. In most cases of failure, it occurs suddenly and in a brittle manner. On the contrary, a heavily reinforced structure could also fail in a brittle manner. Ductility could be defined as the capability of a structure to deform while still carrying load even when the maximum bearing capacity has been reached. It was important to distinguish between material

ductility and structural ductility. A linear elastic material such as fiber reinforced polymers can, on the other hand, give a structure a ductile behavior. For an upgraded structure, the ductility depends on [16]:-

- Ductility of the original structure.
- Condition of the original structure (durability, deterioration, etc.).
- Choice of strengthening method, strengthening materials, amount of strengthening and design of strengthening.

1.6.1 Failure Modes of Concrete Beams Strengthened by Fibers

Failure of fiber reinforced polymer (FRP) strengthened concrete beams may take place through several mechanisms depending on the beam and strengthening parameters. Recently, ACI Subcommittee 440F[17] has developed a report specifically on the analysis, design, and construction of externally bonded fiber reinforced polymer (FRP) systems. The failure modes of beams in Figure (1-8) strengthened in flexure with external fiber reinforced polymer (FRP) reinforcement are classified as follows:

- Concrete crushing before reinforcing steel yields.
- Steel yielding followed by FRP rupture.
- Steel yielding is followed by concrete crushing.
- Cover delamination.
- FRP debonding.

In addition to these, shear failure occurs if the shear capacity of the beam cannot accommodate the increase in the flexural capacity [18].

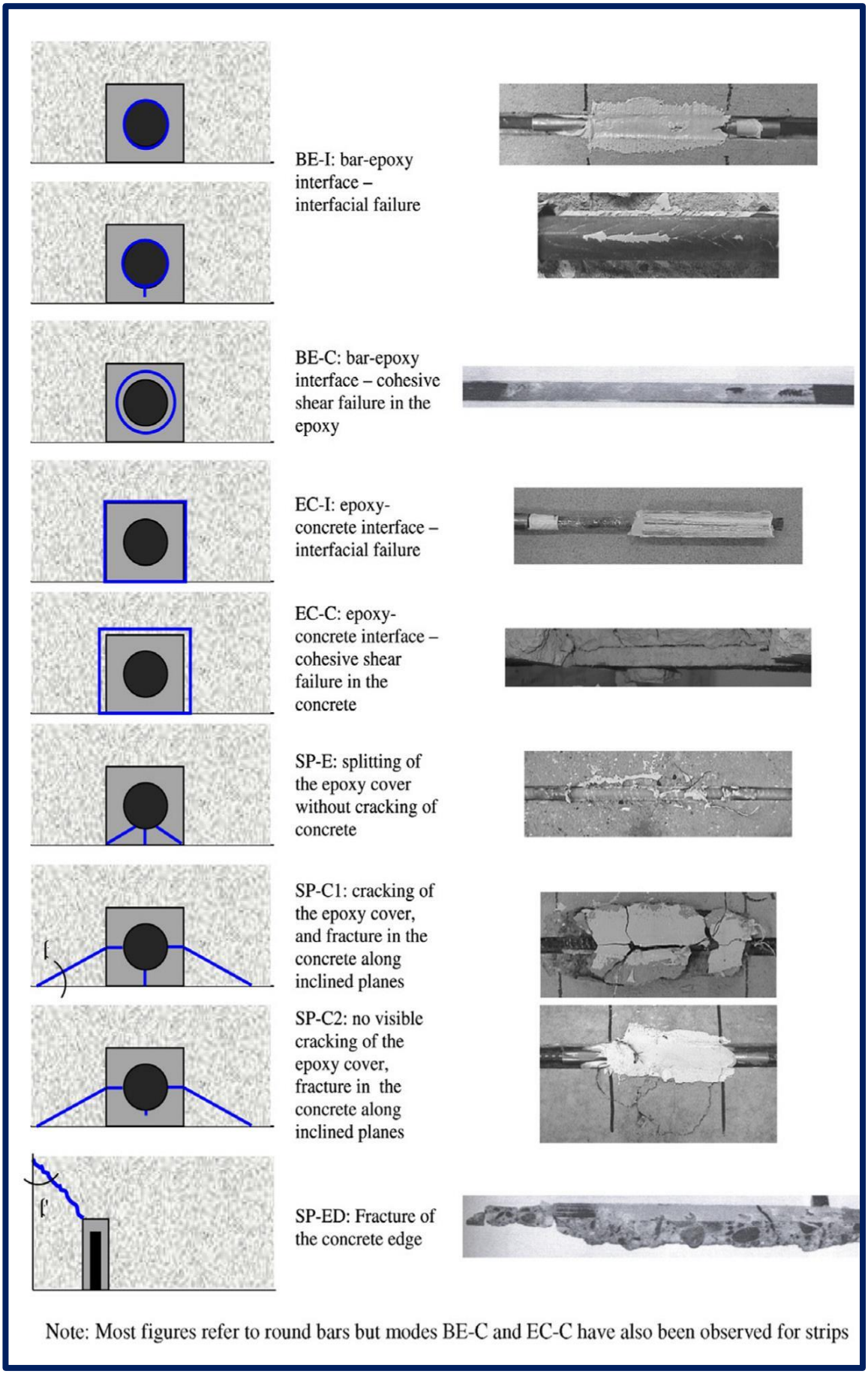

Figure (1-8): Bond failure modes of NSM systems observed in bond tests [19].

1.7 NSM FRP Method (Near Surface Method)

The technique of the NSM method, which is represented by the bar-shaped or strip-shaped FRP elements, is mounted in the groove made of concrete cover, and they are embedded in epoxy or cement resins (adhesives), which provide adhesion and mounting of the material [18]. Application of NSM FRP bar explain in Figure (1-9).

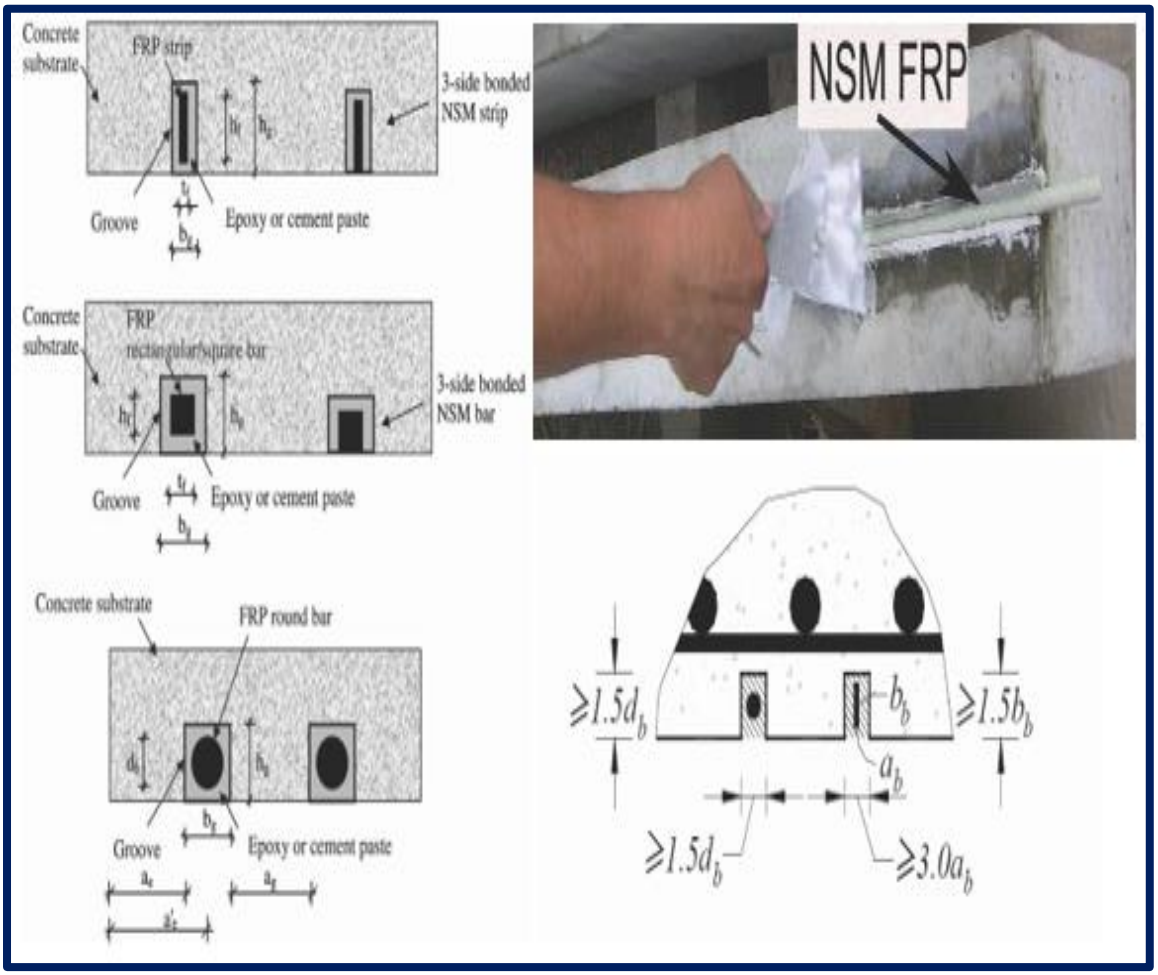

Figure (1-9): Application of NSM FRP "bar" elements [18].

1.8 Benefits of Near Surface Mounted (NSM) over Externally Bonded (EB)

The NSM system has several advantages compared to externally bonded FRP: -

- The effort at the site could be minimized because the surface was not prepared except for the grooves. For example, it is not necessary to remove plaster and the poor layer.

- NSM reinforcement is less exposed to deboned from the concrete surface.
- NSM can be easily pre-stressed.
- This method is effective in connecting NSM in adjacent members, as in the frame joints between beams and column. The method connects NSM effectively in order to prevent debonding failure at the end of the member.

The concrete cove protected the NSM bars, making them less vulnerable to accidental impacts and mechanical damage. Suitable for enforcing negative moment regions [20].

1.9 The Study's Objective

The main purpose of this thesis is to study the flexural behavior of reinforced concrete beams. Some of these beams are reinforced concrete beams that are strengthened with steel fiber and bars, utilizing the ANSYS computer program. Summarized as follows: -

- Experimental investigation of the flexural behavior of normal concrete simply supported beams strengthened with External Bonded Reinforcement (EBR CFRP) composites was used along the length of the beam under static loading.
- Experimental investigation of the flexural behavior of normal concrete simply supported beams strengthened with Near Surface Mounted (NSM CFRP, GFRP, Steel reinforced) composites throughout was used along the length of the beam under static loading.
- A comparison between the EBR CFRP and NSM CFRP systems.
- Study the behavior of beams strengthened with carbon fiber sheets (CFS) under one-point loads and compare results with unstrengthened beams.
- Using the finite element analysis program ANSYS to compare the experimental results with the numerical analysis results.
- Experimentation on a variety of factors, including: - (First cracking load, Load-deflection behavior at mid span, Ultimate load carrying capacity,

Ductility factor, and cracking pattern at failure, The bond properties between concrete and CFRP).

1.10 Thesis layout

This thesis will include five chapters and be carried out by the following sequential organization: -

Chapter One: Provides a general introduction to concrete, some properties and benefits of steel fiber, advantages, Fiber Reinforced Polymers (FRP) and introduces a strengthening with CFRP application.

Chapter Two: reviews the most of the previous studies (experimental and theoretical investigation), which are related to the present study.

Chapter Three: Explain the experimental program, test setup. Details of tested beams, material properties and concrete mix design, and procedures adopted for the test program.

Chapter Four: shows the test results and discussion. The observed crack patterns, crack width, and mode of failure were reported for the beam specimens.

Chapter Five: Deals with the numerical analysis in the finite element analysis of our beam's elements used, real constant and boundary condition under consideration by using the finite element method using ANSYS software.

Chapter Six: Shows the conclusions and recommendations drawn from the research work for future work.

Chapter Two
LITERATURE REVIEW

2.1 Overview

This chapter provides a general review of experimental and theoretical studies on the (NSM, EB) techniques, including reinforcement technique progressions and a review of studies on the strengthening of RC Beams. Many researchers studied the history of Near-Surface Mounted (NSM) and external bonded (EB) research, theories, and codes. Summarized according to the main studies in this field.

2.2 Review of Research on Reinforced Concrete Beams

In NSM **DeLorenzis (2000)**[21] FRP rods emerged as a promised technique for enhancing the flexural and shear strength of deficient RC and prestressed concrete (PC) members. The objective of study was to see how effective NSM FRP rods are as a strengthening system for RC structures. Rods are a promising technology for increasing the flexural and shear strength of deficient RC and PC members. The ability to attach the rods into adjacent members and reduced installation time are two advantages of employing NSM FRP rods over externally bonded FRP laminations.

Arup Maji et al. (2001)[22] because of the employment of a carbon fiber overwrap on the normally smooth pultruded rods, flexural cracking was prevented by a good bond between the FRP and the concrete. Even though the FRP rods and concrete are both brittle, their combined behavior demonstrates ductility far beyond what is generally expected of reinforced concrete. The ductility of concrete is related to the substantial fraction of total strain energy utilized in the creation of distributed cracking, according to an analytical analysis of fracture energy.

De Lorenzis (2002)[23] to improve the flexural and shear strength of RC elements, a promising technology is the use of FRP rods that are NSM. The bond is essential because it permits the transfer of stress from the concrete to the FRP reinforcement, which in turn results in composite action. In the course of the experiments, three distinct failure modes manifested themselves: the epoxy cover splitting, the concrete around the groove cracking, and the FRP rod being removed. Bond strength is affected by surface shape of FRP rods; in other cases, multiple failure mechanisms were observed.

Hakan Nordin(2003)[11] FRP, was a composite material made up of fibers and a polymer matrix. CFRP (Carbon Fiber Reinforced Polymer), GFRP (Glass Fiber Reinforced Polymer), and AFRP (Aluminum Fiber Reinforced Polymer) are the most commonly used FRPs in civil engineering applications (Aramid Fiber Reinforced Polymer). Polyester, Vinyl Ester, or Epoxy are the most common polymer matrixes employed.

In recent years, **Jose and Joaquim(2004)** [24] Department a strengthening technique based on NSM laminate strips of CFRP has been introduced to increase the load-carrying capacity of concrete and masonry structures by introducing laminate strips into precut grooves on the concrete cover of the elements to be strengthened.

R. Gussenhoven and S.F.Breña(2005)[25] presented a methods of beams were strengthened using different thicknesses and widths of composite laminates, those parameters would generate different failure modes.

J.A.O. Barros and A.S. Fortes (2005)[26] the load carrying capacity of concrete beams collapsing in bending was doubled by utilizing NSM strengthening approach using CFRP laminate strips. This goal was met, and the strengthened beams' deformational capacity was comparable to that of the reference beams. The NSM approach increased the load at the serviceability limit condition as well as the stiffness following concrete

cracking by a significant amount. A numerical algorithm was designed to simulate the deformability of RC beams strengthened using the NSM technology. The load-carrying capability of the tested beams, as well as the related deflection, are accurately predicted.

In the **L.Vasseur et al.(2006)** [27] structural behavior of reinforced concrete beam strengthened in flexure with externally bonded FRP reinforcement has been thoroughly examined. However, there is a scarcity of information on the behavior of continuous beams reinforced with composites. The non-linear behavior of the beam is explored through an analytical analysis. It is determined how much moment redistribution remains when using this strengthening procedure.

According to **Q. L. MA et al.(2007)**[28] static behaviors of CFRP-strengthened beams are prioritized over fatigue phenomena. The high strength of CFRP sheets without pre-stress, on the other hand, can only be exploited after the steel reinforcement has yielded, which has no influence on boosting the service capacity of strengthened beams. Experiments on the fatigue behavior of RC beams reinforced with prestressed CFRP sheets are carried out in this research, and a design proposal for fatigue life is established based on the local stress-strain relationship of steel reinforcement in the beams.

R.J. Gravinaa and S.T. Smithb(2008)[29] showed model was used to estimate the bending moment distribution, as well as the progressive creation of flexural cracks and associated crack spacings and crack widths, in continuous beams reinforced with FRP bars. The model's ability to predict deformations in highly stressed sections of the beam is particularly intriguing. In comparison to concrete beams reinforced with steel bars, comments are given based on theoretical studies about the ductility and overload behavior of concrete beams reinforced with FRP bars.

In **M. Mustafa Önal (2009)**[30] concrete beams with low bending and shear strengths were strengthened by covering them in CFRP. The work was done on rectangular-section beams that were found to need reinforcing after a thorough inspection and statistical analysis. The goal was to reinforce beams with insufficient shear strengths.

Slobodan Ranković et al. (2010)[31] has examined the use of FRP materials in current reinforcement methods for RC beams. The NSM method and the basic features of FRP materials are provided, as well as the way of mounting FRP bars within concrete, that is, near the surface of the beams. The technology's features and advantages over the EBR has been investigated.

Amjad Kreit et al.(2011)[32] behavior of RC beams damaged and strengthened using CFRP rods NSM has been studied experimentally. The RC beams were damaged by increasing loads to create varied degrees of cracking, according to the experimental program. The strengthened RC beams with NSM CFRP rods were then bent along the same loading path and carried out to failure under increasing loads.

In **Shuaib H. Ahmad et al.(2012)**[33] load-deflection was responded of flexure-critical RC beams externally strengthened with NSM CFRP laminates is predicted using a computerized analytical model. The analytical model uses concrete, reinforcing steel, CFRP laminate materials, strain compatibility, and sectional analysis to produce moment-curvature relationships, which are then used to generate load-rotations and load-deflection of flexure-critical RC Beams reinforced with NSM CFRP laminates. The predictions of the analytical model are compared with the experimental results of flexure-critical RC beams strengthened with NSM CFRP laminates for validation of the analytical model, and the comparisons are considered to be good.

Ricardo Perera et al.(2013) [34] used FRP to reinforce steel structures has become a popular choice, potentially resulting in more confident retrofitting of existing structures. The FRP strengthened steel constructions was presented link between steel and FRP, the strengthening of steel hollow section parts, and fatigue crack propagation in the FRP steel system are three areas that have seen rapid development.

According to **I.A.Sharaky et al.(2014)** [35] behavior of RC beams enhanced in flexure by different combinations of externally bonded hybrid (GFRP&CFRP) sheets is investigated experimentally and analytically. Multiple tensile coupon tests were performed to determine the mechanical characteristics of the hybrid sheets. It was also discovered that the ductility of beams reinforced with glass and hybrid sheets is higher than that of beams reinforced with a single carbon sheet at failure stresses. In addition, an analytical model was created to estimate the load-deflection response of the tested specimens, and the findings were compared to experimental data. The results revealed that the constructed analytical model accurately anticipated the reaction of the tested beam specimens.

I.A. Sharaky et al.(2015)[36] NSM reinforcement was made of CFRP bars and strips, as well as GFRP bars. The impact of end anchorage and transverse wrapping on the behavior and load capacity of strengthened beams was also investigated. The RC beams enhanced with fully bonded NSM FRP exhibited stronger stiffness and bearing capacity than the beams strengthened with partially bonded NSM FRP, according to the findings. The usage of NSM FRP for the reinforcement of RC beams with end anchorage or transverse wrapping increased their load-carrying capability and rigidity. The behavior of the tested beams was well predicted by the analytical model.

Several traditional methods for strengthening in **A.H. Abdullah and M.R. AbdulKadir(2016)**[37] have been utilized , including jacketing for reinforced columns, adding steel plates at tensile stress areas, and pre-

stressing key locations to improve the member's strength. FRP have recently surpassed steel plates as a better material for externally applied reinforcing material for beams to boost their shear and flexural capacities, as well as for columns to reduce warping and confinement. Inside pre-prepared grooves, NSM FRP is applied to the tension zone of the beams. The presence of bars or strips inside grooves in the NSM process would provide a better bond between the FRP and the substrate.

Shi Shun Zhang(2017)[38] when employing the NSM,FRP technology to strengthen existing weak structures, a set of parallel NSM FRP strips is normally required to meet the capacity augmentation needs. The adjacent grooves and FRP strips have a negative impact on the bond behavior of each NSM FRP strip. Such negative effects should be considered for a safe design of the NSM FRP strengthening system. Two FPP strips are separately implanted in two parallel grooves in this investigation for NSM bonded joints. Based on the results of the parametric analysis, a reduction factor is proposed and applied to NSM bonded joints with three or more uniformly spaced FRP strips to account for the harmful effect of insufficient groove spacing on bond strength.

Mario Coelhoa et al.(2018)[39] The design processes for FRP systems inserted into the cover of concrete elements using the NSM technique was presented. The bond strength of such a strengthening mechanism is crucial. The bond strength of NSM FRP systems in concrete is estimated using two known design formulas. The findings demonstrate that existing rules can be expanded and used within the Eurocodes framework. However, the diversity of the probabilistic distributions discovered is extremely significant owing to their limits in addressing individually all probable failure modes. The results in high partial coefficients of safety. The behavior of beams strengthened with NSM FRP bars and external CFRP strips under four-point bending was examined. Eight T-beam specimens with a span of 2700 mm, a

height of 300 mm, a flange thickness of 50 mm, a flange width of 300 mm, and a web width of 150 mm were examined.

In **H.M.Abdzaid and H.H.Kamonna(2018)**[20] the number of bars, the type of FRP, the groove dimension, and the strength of the FRP were all considered. Variables that were investigated by an external evaluator were used to compare the effectiveness of NSM techniques. The amount of FRP materials used in bonded specimens was the same as in NSM. It was decided to employ reinforced beams. Flexural stiffness and load capacity have increased dramatically. One NSM was discovered.

Tarek Hassan and Sami Rizkalla (2020) [40] used of FRP bars and strips as near-surface mounted reinforcement, especially for strengthening purposes. The bond properties of FRP CFRP strips were investigated using both experimental and analytical methods. A quantitative criterion for the debonding failure of CFRP strips positioned near the surface has been established. Various characteristics such as internal steel reinforcement ratio, concrete compressive strength, and groove width are discussed.

Yajun Zhao et.al (2020)[41] NSM strengthening system was used to protect FRP rods from external threats. When using a pre-stressed near-surface mounted steel–basalt–fiber-reinforced polymer composite bar to compensate for the inferior stiffness and ductility of FRP bar compared to steel rebar. A steel rod is wrapped in a basalt-fiber-reinforced polymer cover to create a steel–basalt fiber–reinforced polymer composite bar. The breaking load is appropriately predicted using standard-based load analysis; however, the ultimate strength of the beams is underestimated. To create a more efficient load-bearing solution, finite element technique modeling is used.

In **Francesco Micelli and Laura De Lorenzis(2013)**[42] FRP materials were currently available in a variety of designs and are commonly used to strengthen and remodel concrete structures and bridges. Experimental and

analytical investigations were carried out to evaluate the bond qualities of near-surface mounted carbon FRP CFRP strips. A total of nine concrete beams were fabricated and tested under monotonic static stress with NSM CFRP strips. The development length required for optimal utilization of near-surface mounted CFRP strips was evaluated using various embedment lengths. The debonding failure of CFRP strips positioned at the surface is governed by a quantitative criterion.

2.3 NSM (Near Surface Mounted Reinforcement)

2.3.1 Fiber Reinforced Polymer (FRP) Strengthening Technique

Near surface mounted (NSM) reinforcement dates to the early 1940s. This method is used to place steel reinforcement in grooves in concrete cover or in additional concrete cover cast onto the structure. The steel bars were then placed in grooves. Then the grooves were mortared into the concrete frame. Another way of using steel bars; is as the basis of the structure surface and the shotcrete surface.

L. DeLorenzis et al.(2006)[43] method has some disadvantages; a strong bond to the original building is always difficult to achieve, and it is difficult to cast concrete around steel reinforcement in certain cases. an enhanced the bonding process of the steel reinforcement. However, because of the susceptibility to corrosion of the steel reinforcement, it also needs an external cement cover. Steel insulation as a protective layer needs to be epoxy coated. The NSM system has certain advantages compared to externally bonded FRP strengthening.

However **Md. Akter Hosen et al. (2018)[44]** NSM has some limitations. The width of a beam to be strengthened can limit the number of bars that can be used due to the needed groove width spacing between adjacent grooves. A problem that can occur is debonding due to stress overlapping. This contributes to the amount of rebar to be used.

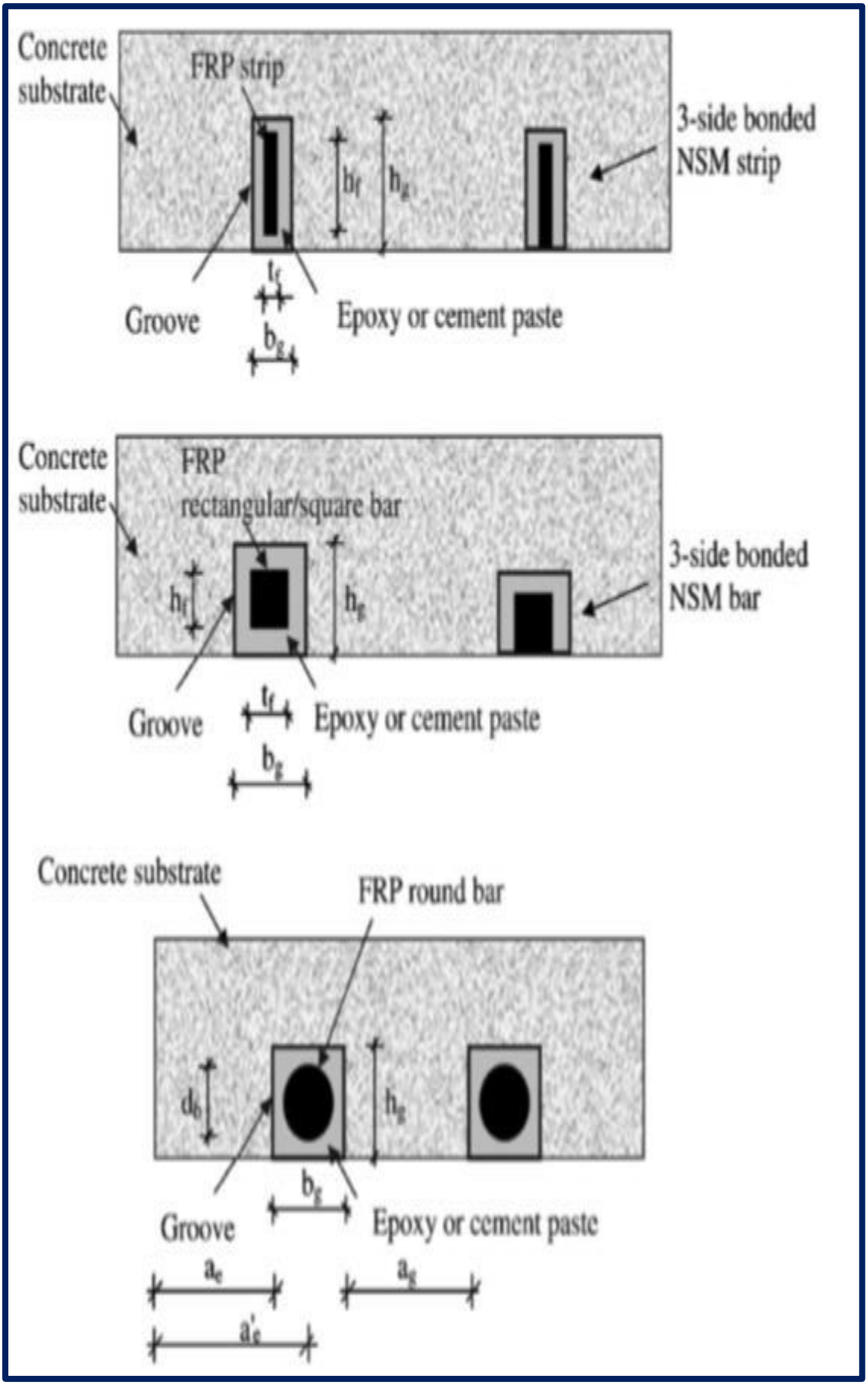

Figure (2-1): Various NSM and nomenclature schemes[45].

2.3.2 Mode of Flexural Failure

The possible failure modes of beams strengthened with the (NSM) technique are as follows: -

1. Brittle Failure: This mode of failure may occur in a single material such as concrete (crushing) or in FRP (rupture or debonding). Concrete crushing happens because concrete members have a high reinforcement ratio or the concrete strength is too low. Also, CFRP rupture or debonding happens when fiber strength or bond strength is exceeded as a result of improper design. This type of failure should be avoided.

2. Ductile failure: This mode of failure happens when steel yielding starts first, followed by concrete crushing. However, steel yielding may be followed by CFRP rupture or debonding, which is difficult to prevent. Figure (2-2) shows the types of debonding failure that may happen in CFRP[40].

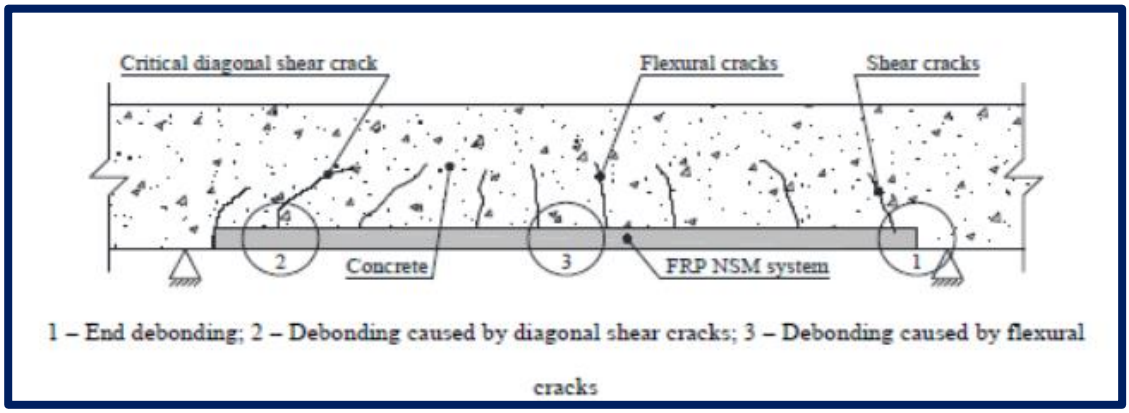

Figure (2-2): Principle failure in a beam strengthened with a CFRP NSM system [40].

2.4 Conclusion Remakes

1. use of FRP rods that are NSM. The bond is essential because it permits the transfer of stress from the concrete to the FRP reinforcement, which in turn results in composite action.
2. increase the load-carrying capacity of concrete and masonry structures by introducing laminate strips into precut grooves on the concrete cover of the elements to be strengthened.
3. The amount of FRP materials used in bonded decided to employ reinforced beams. Flexural stiffness and load capacity have increased dramatically.

Chapter Three
EXPERIMENTAL WORK

3.1 General

This chapter gives detailed information about the experimental work carried out, including preparing and testing of the materials used and the test setup used for this study. All tests have been carried out at Babylon University in the Civil Engineering Department Laboratory.

3.2 The Experimental Program and Beam Specimen Description

The experimental program consisted of testing (16) specimens with dimensions of 150 mm in width, 300 mm in height, and 1500 mm in length. The specimens are divided into two groups. All the specimens have the same steel reinforcement and are tested under the same one-point load. The first group consisted of eight beams, which were made of normal strength concrete and served as control specimens (without any strengthening). The second group consisted of eight beams, which were cast as a hybrid concrete (steel fiber reinforced concrete with a volume fraction of fiber of 1%). This shows each case is shown below in Table (3-1).

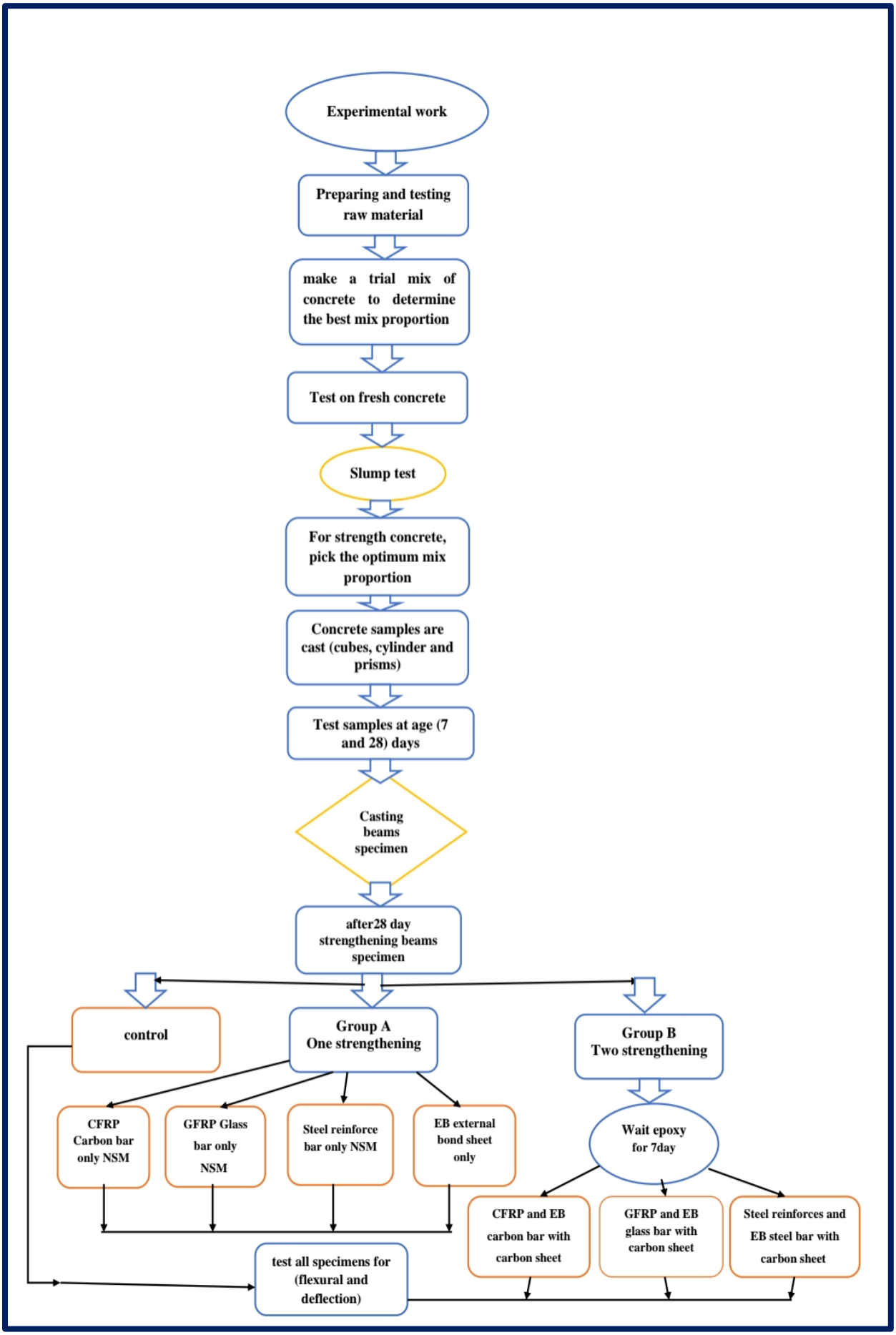

Figure(3-1): Study Plan Flowchart.

Table(3-1): All specimens details.

Group	Specimen symbol	Specimen type	NSM Strengthening				NSM length	Percentage of fiber (%) by volume
			Bars			Sheet		
			Number	Diameter	material			
Group (1) Specimens with Normal Concrete	NC	Normal control	-	-	-	-	-	-
	NT	EB external bond sheet only	-	-	-	FRP	1200	-
	NCb	CFRP carbon bar only NSM	1	6	CFRP	-	1200	-
	NGb	GFRP Glass bar only NSM	1	6	GFRP	-	1200	-
	NSb	Steel Reinforce only NSM	1	6	Steel bar	--	1200	-
	NCbT	CFRP and EB carbon bar with carbon sheet	1	6	CFRP	FRP	1200	-
	NGbT	GFRP and EB carbon bar with carbon sheet	1	6	GFRP	FRP	1200	-
	NSbT	Steel Reinforce and EB steel bar with carbon sheet	1	6	Steel bar	FRP	1200	-
Group (2) Specimens with Fiber Concrete	CF	Control fiber	-	-	-	-	-	1
	FT	EB external bond sheet only	-	-	-	FRP	1200	1
	FCb	CFRP carbon bar only NSM	1	6	CFRP	-	1200	1
	FGb	GFRP Glass bar only NSM	1	6	GFRP	-	1200	1
	FSb	Steel Reinforce only NSM	1	6	Steel bar	-	1200	1
	FCbT	CFRP and EB carbon bar with carbon sheet	1	6	CFRP	FRP	1200	1
	FGbT	GFRP and EB carbon bar with carbon sheet	1	6	GFRP	FRP	1200	1
	FSbT	Steel Reinforce and EB steel bar with carbon sheet	1	6	Steel bar	FRP	1200	1

3.3 Material Characteristics

The qualities of the material are determined using standard tests according to the American Society for Testing and Materials (ASTM) and Iraqi specifications (IQS).

3.3.1 Cement

Ordinary Portland cement OPC **(Type I)** from an Iraq plant named Mass has been used for casting all specimens. The cement was saved in good condition to prevent the effect of humidity. Table (3-2) and Table (3-3) show the physical and chemical properties of the **OPC** used in accordance with **IQS** the **Iraqi specification No.472/1984**. The obtained results confirmed the limitations of the Iraqi Standards Specification [46]. tested at the University of Babylon in the construction.

Table (3-2): Chemical composition of cement compared with I.Q.S(472:1984)

Compound Composition	**Chemical Composition**	**% By Weight**	**I.Q.S. (5:1984) limit**
Lime	CaO%	62.42	----------
Silica	SiO2%	20.88	----------
Alumina	Al2O3%	4.07	----------
Iron oxide	Fe2O3%	5.40	----------
Magnesia	MgO%	1.6	≤ 5%
Sulfate	SO3 (%)	1.18	if C3A < 5% ≤ 2.5% if C3A > 5% ≤ 2.8%
Free Lime (%)	Free CaO	0.84	----------
Loss of Ignition. (%)	L.O.I	2.68	≤ 4%
insoluble residue. (%)	I.R	0.36	(1.50%)
Lime Saturation Factor	L.S.F	0.91	0.66 to 1.02
	M.S	2.21	
	M.A	0.75	
Main compounds			
Tricalcium Silicate	C3S%	53.57	----------
Dicalcium Silicate	C2S%	19.45	----------
Tricalcium Aluminate	C3A%	1.62	≤ 3.5%
Teracalcium Alumminoferrite	C4AF%	16.43	----------

Table (3-3): Physical properties of cement compared with I.Q.S. (5:1984) limitations.

Properties	**Test result**	**I.Q.S. (5:1984) limit**
Setting time **Initial (hour: min.)** **Final (hour: min.)**	 2:23 3:25	 ≥00: 45(hour: min) ≤ 10:00(hour: min)
Fineness ($m2/kg$)	326	≥ 250 m3/Kg
Compressive strength (MPa) **3days** **7 days**	20.33	 ≥ (15 Mpa) ≥ (23 Mpa)

3.3.2 Fine Aggregate (Sand)

Natural sand from the **(Al-Akaidur)** region was used for concrete mixes in this research. The sand was washed, cleaned by water, and dried before use. The grading of the fine aggregate shows specific gravity=2.6. The test results for sieve analysis of sand were obtained within the limitations of Iraqi standards **I.Q.S.45/1984 (zone3)**. Physical and chemical test results are given in Table (3-4) while the grading of fine aggregate used is illustrated in Table (3-5). Fine aggregate has been tested at the University of Babylon in the Construction, Material, and Environmental Laboratories of the Civil Engineering Department.

Table (3-4): Physical and chemical properties of the fine aggregate.

Properties	**Test result**	**I.Q.S. (45:1984) limit**
Sulfatecontent (SO3) %	0.13	≤ 0.75
Specific gravity (Gs)	2.56	---
Absorption%	0.75	---

Table (3-5): Sieve analysis of fine aggregate (sand).

Sieve analysis (mm)	**Passing %**	
	Fine aggregate	**I.Q.S. (45:1984) limit**
Size		**Zone 3**
10	100	100
4.75	95.8	90-100
2.36	88.4	85-100
1.18	76.8	75-100
0.6	66	60-79
0.3	22.8	12-40
0.15	5	0-10

3.3.3 Coarse Aggregate (Gravel)

Crushed gravel from the AL-Naba'ee region was used in this study.Table(3-6) shows the gradation of the coarse aggregate used, while Table (3-7) gives the physical and chemical properties of the aggregate. All the results confirmed the requirements of the Iraq specifications I.Q.S.(45:1984)[47]. The chemical and physical tests were conducted in the Environmental and Constructional Materials Laboratories of College Engineering at the University of Babylon, respectively.

Table(3-6): Sieve analysis of coarse aggregate.

Sieve analysis (mm)	**Passing %**	
	Coarse aggregate	**I.Q.S. (45:1984) limit**
Zone B		
37.5	100	100
20	97.52	95-100
10	34.68	30-60
5	3.16	0-10

Table (3-7): Properties of physical and chemical properties of coarse aggregate.

Properties	**Test result**	**I.O.S. (45:1984) limit**
Sulfate content (SO3) %	0.05	≤ 0.1
Specific gravity	2.59	---
Absorption%	0.74	---

3.3.4 Water for mixing and curing

The tap water was used in the work for concrete mixing and curing all the specimens.

3.3.5 Steel Reinforcement

In this study, three types of steel reinforcing deformed bars of Ukrainian origin are used (ø12mm, ø10mm and ø6mm). The samples for each size are tested according to **ASTM A 615/A 615M – 04a** [48]. The reinforcing bars with a diameter of 12mm are used as main reinforcement and are employed as tension and compression reinforcement. While the bars with a diameter of 10mm are used as ties, the bars with a diameter of 6mm are used as NSM.Table (3-8) gives the results of the tensile tests for reinforcement bars

that were performed in the engineering laboratories at Al-Musayyib Technological Institute's material laboratory.

Table (3-8): Details of steel bars.

Diameters (mm)	Measured Diameters (mm)	Yield Strength Fy, (MPa)	Ultimate Strength Fu, (MPa)	Modulus of Elasticity Es (MPa) *	ASTM Specification	
					Fy (MPa)	Fu (MPa)
12	11.95	678	731	200000	420	620
10	9.94	580	724	200000	420	620
6	5.95	460	510	200000	515	585

*Assumed value, ACI 318M-08.

Plate(3-1): Tensile testing of steel bars.

3.3.6 Steel Fibers

In this study, micro steel fibers (typeWSF0213) commercially available are employed. A company in Jiangxi Province made these steel fibers as shown in Plate (3-2). That appear to be straight short brass coated gold colored steel fibers with an aspect ratio (Lf/Df) of 65. The physical properties are listed in Table (3-9).

Plate(3-2): Micro steel fibers.

Table (3-9): Properties of the steel fibers.

Property	Specifications
Type	WSF0213
Surface	Brass coated
Relative Density	7860 kg
Tensile Strength	Minimum 2300MPa
Modulus of Elasticity	203 GPa
Form	Straight
Melting Point	1500°C
Average Length	13 mm
Diameter	0.2mm±0.05mm
Aspect Ratio	65

3.3.7 Epoxy Adhesive

The building and construction industries represent some of the largest users of adhesive materials, many applications are non-structural in the sense that the bonded assemblies are not used to transmit or sustain significant stresses (e.g., crack injection and sealing, skid-resistant layers, bonding new concrete to old. The epoxy-resin (Sikadur®-330), manufactured by Sika Company, was employed in this study to paste the bars inside NSM-grooves. This material consisted of two parts (Resin part A+ Hardener part B), as shown in Plate (3-3). Technical properties of epoxy material are displayed as provided by the manufacturer in Table (3-10).

Table (3-10): Epoxy Adhesive(Sikadur® 330) properties [4]**.**

Properties	**Sikadur® 330**
Modulus of elasticity in flexure	3800 N/mm2(7 days at +23 °C)
Tensile strength	30 N/mm2 (7 days at +23°C)
Modulus of elasticity in tension	4500 N/mm2 (7 days at +23 °C)
Tensile strain at break	0.9 % (7 days at +23 °C)
Tensile adhesion strength	Concrete fracture (> 4 N/mm2) on sandblasted substrate
Density	1.3Kg/Ltr (mixed)
Appearance	Comp. a: white, comp. b: grey Components A + B mixed: light grey paste
Mixing ratio	A: B=4:1(by weight)
Open time	30 min (at+35C)
Viscosity	Pasty, not flowable
Application temperature	+15 C to +35V (ambient and substrate)

Plate(3-3): Two component epoxy adhesive (Sikadur® 330).

3.3.8 Carbon Fiber Reinforced Polymer (CFRP)

The chosen carbon fiber as reinforcement material has high specific strength and excellent mechanical performance. It is widely used in prestressed structures. When loaded in tension, FRP fibers did not demonstrate any plastic behavior (yielding) before rupture. Up until failure, which is rapid and can be disastrous, tensile behavior is defined by a linearly elastic stress-strain relationship. As for flexural reinforcement employed rough bar made of CFRP. The mechanical properties were determined using testing procedures in accordance with ACI 440.3R-04. Beams, bridges, slabs, walls, and columns are strengthened and rehabilitated using CFRP and GFRP show in Plate (3-1). The properties are shown in Table (3-11).

Table(3-11): Properties of CFRP, GFRP.

Properties	CFRP	GFRP
Size	2	2
Diameter (mm)	6	6
Nominal Area (mm)	31.67	31.67
Tensile load (kN)	71	28
Tensile strength ((kN)	2241	896
Modulus of elasticity (GPa)	124	46

The concrete, glue, and CFRP material models are programmed to act linearly elastic until the tensile strength is reached. To create an isotropic material model, the CFRP bar is simplified. The modulus of elasticity, Poisson's ratio, and tensile strength are the material properties examined for the concrete and adhesive. The tensile strength of the CFRP is not reached in the pullout test, so only the modulus of elasticity and the Poisson's ratio are considered.

Plate(3-4): NSM bars: - (a)CFRP, (b)GFRP, (c)Steel Reinforce.

3.3.9 Glass fiber reinforced polymer (GFRP)

Many elements of structures can be easily and effectively rehabilitated using the NSM approach. Rough bar made of GFRP is summarized in **Appendix B**. The mechanical properties were determined using testing procedures in accordance with **ACI 440.2R-02** [18]. The results are shown in Plate (3-4), Table (3-11). Glass Fiber Reinforced polymer (GFRP) has been employed in the majority of NSM applications to construction structures. GFRP properties are as below:

- **Mechanical strength:** GFRP has a specific resistance greater than steel.
- **Lightweight:** It is 9 times lighter than steel means less structural framing, faster installation, and lower shipping costs.

- **High resistance:** Its t is not rust, oxidation or corrosion, so it gives concrete its life span not less than twice that of conventional concrete.
- **Incombustibility:** Being a mineral material, GFRP is naturally incombustible. It does not propagate or support a flame, and it does not emit smoke or toxicity when exposed to heat, the risk of fire, it maintains the cohesion of concrete from collapsing because it is not heat expandable and non-conductive for electricity.
- **High durability:** high durability resin reached to high durability of GFRP bar. Withstands twice as much tensile stress as traditional steel.

3.3.10 Carbon Fiber Reinforced Polymer (CFRP Sheet)

The unidirectional woven carbon fiber fabric with mid-range strengths is designed for installation using the dry or wet application process. The polymer (CFRP) sheet (SikaWrap®-300 C) used in this study has been reported by the manufacturers to be linear up to failure. The Properties of the Carbon Fiber Reinforced Polymer sheet are not determined in the laboratory. However, the properties published by the manufacturer (BASF The Chemical Company) are used to define the material models for the analytical studies. The values of the parameters of carbon fiber reinforced polymer sheet are summarized in **Appendix B** for the composites used in this project. The thickness, tensile strength, modulus of elasticity, and elongation are 0.167mm, 4000Mpa, 230000GPA, and 1.7% respectively. Plate (3-5) shows the CFRP sheet used in the present study.

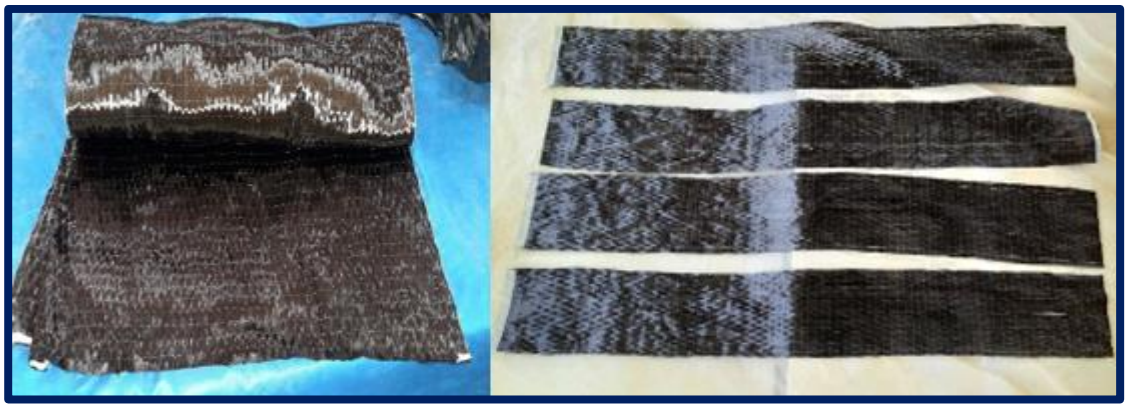

Plate(3-5): CFRP sheet.

3.3.11 Matrix of Bonding

The Sikadur® 330 Epoxy Paste was used as the adhesive epoxy paste. Epoxy adhesive is used as a bonding material between carbon fiber and concrete. The epoxy adhesive consists of two parts based on a combination of epoxy and special filler, part A (white) and part B (grey). The mix ratio was 4A:1B by weight. The mechanical and physical properties of the epoxy resin are presented in Table (3-10) by the manufacturer.

3.4 NSM-FRP Bond Behavior

This study has been conducted in two steps. The first study looked at the strengthening behavior between normal concrete and the bonding material, while the second step was to study the strengthening behavior between fiber concrete and the bonding material, in two-way NSM and EB. The experimental work of the present study consisted of testing sixteen beams with dimensions of**(150mm*300mm*1500mm)**. The material properties used for the test specimens are presented in the following sections.

3.5 Mix Proportion of Normal Strength Concrete

The American approach of selecting mix proportions is used to design the normal strength of concrete (ACI Committee 211.1-91). At age 28, the desired concrete strength (f'c) for all beams is 35 MPa. With the trial mix, the mixed design ratio is changed to provide the requisite compressive strength. This explains the optimum mixes with the weight proportions used in this work for $1m^3$. The mix proportion of normal strength concrete is shown in Table (3-12).

Table (3-12): Mix proportion of concrete.

Concrete type	Cement (kg)	Fine aggregate (m^3)	Coarse aggregate (m^3)	W/C ratio	Fiber (By volume)
NC	400	700	1056	0.437	-----
SFC	400	700	1056	0.437	1%

3.5.1 Fresh Normal Strength Concrete Testing

3.5.1.1 Slump Test

According to the manufacturer, the following test is done to determine the fresh qualities of normal strength concrete (ASTM C143-15)[50] as shown in Plate(3-6).

Plate(3-6): Slump test.

3.5.2 Hardened Normal Strength Concrete Test

3.5.2.1 Compressive Strength Test

The compressive strength of typical concrete is determined using cubes with dimensions of (150*150*150mm) loaded uniaxially using a compressive machine type (BS1881-116) as shown in Plate (3-7). Cubes were tested at different ages (7 and 28 days) to determine the fcu value, and then the value of (f'c) is determined using the equation (3-1) according to (IRAQI Code 1/1987). using automatic compression testers for cubes and cylinders with a capacity of 2000kN, the load was applying perpendicular to the direction of casting at rate of 0.3 MPa per second. The tests were carried out at the structural laboratories of Babylon University.

$$f'_c = f_{cu} * 0.8 \qquad (3\text{-}1)$$

3.5.2.2 Flexural Strength Test

On normal-strength concrete specimens, flexural strength (modulus of rupture) tests are performed in accordance with (ASTM-C78-02)[51]. After curing for 28 days in a water tank inside the laboratory, flexural strength tests are performed on (6) prism specimens (100*100*400 mm). The tests were performed as a simply supported beam with a third point load. using the machine shown in Plate (3-8). The results are calculated using the equation below: -

$$Fr=(P*L)/(b*d^2) \quad (3\text{-}2)$$

where:

fr = *The modulus of rupture (MPa).*

P = *The ultimate load (N).*

L = *The length of span (mm) [in this test, L=300 mm].*

b = *The average width of the specimen (mm).*

d = *The average depth of the specimen (mm).*

3.5.2.3 Splitting test

According to ASTM C496[52], split tensile strength is tested using cylindrical concrete specimens with a diameter of 100 mm and a height of 200 mm. At 28 days of age, the specimens are evaluated using automatic compression testers for cubes and cylinders with a capacity of 2000kN. Plate(3-9) shows the splitting tensile test setup. The splitting tensile strength is calculated using equation(3-3).

$$\boldsymbol{ft = (2 * P) \ / \ (\pi * d * L)} \quad (3\text{-}3)$$

where:

ft = *The Splitting tensile strength (MPa).*

P = *The Max. applied load recorded by the testing machine (N).*

d = *Cylinder diameter (100mm).*

l = *Cylinder length (200mm).*

Plate(3-7): Compressive strength test.

Plate(3-8): Flexural strength test.

Plate(3-9): Splitting tensile test.

Table (3-13): Ordinary test.

Test type	Average of all specimens at test time	Group one	Group two
Compressive Strength (MPa)	**Cubes (150×150×150) mm**	35	40
flexure Tensile Strength (MPa)	**Prisms (100× 100× 400) mm**	5.153	6.07
Splitting Tensile Strength (MPa)	**Cylinder (100 × 200) mm**	4.07	6.113

3.6 Concrete Mixing Procedure

3.6.1 Normal Strength Concrete Mixing Procedure

Before mixing normal strength concrete, all amounts of the raw materials (gravel, sand, and cement) are weighed and packed in a clean plastic container. Dry sand and saturated surfaces of dry gravel are mixed for several minutes in an electrical horizontal mixer rotating drum with a capacity of (0.5) m^3. Following that, the cement is poured into the mixer, and weighted water is progressively added to the mix. The total time required for the mixing operation is about (8-10 min.). After initial mixing, by sifting, the fibers are gradually added to the fresh concrete and mixed until a homogeneous mixture is achieved.

Plate(3-10): Mixing at rotary mixer.

3.7 Preparation of Testing Specimens

This section covers reinforcement cages and mold preparation, as well as mixing, casting, and curing test specimens.

3.7.1 Preparation of Reinforcement Cages and Molds

The reinforcement cages for all beam specimens are made from two sizes of deformed steel reinforcement bars. Steel bars with a diameter of 12mm are used as longitudinal reinforcement, while steel bars with a diameter of 10mm are utilized as stirrups to increase the specimen's strength, as shown in Plate (3-11).

Plate(3-11): Manufacturing cage of steel longitudinal and stirrup reinforcement.

Sixteen plywood molds are prepared so that the reinforcement cages can be accommodated. The mold is made up of seven sections that may be easily collected. The mold can be used multiple times; it is constructed to be simple to collect or disassemble without affecting the cast specimen. This formwork is lubricated and leveled horizontally prior to casting. The beam specimen

reinforcement remained firmly in place inside the mold when the mold preparation was completed. Small plastic spacers were utilized to place the reinforcement cage at the proper bottom and side distance from the molds to obtain the cover, as shown in plate (3-12).

Plate(3-12): The reinforcing cage is installed inside the mold and it is ready for casting.

3.7.2 Mixing, Casting, and Curing of Specimens

Each beam is cast using one batch of concrete. A horizontal rotary mixer with a capacity of (0.5 m^3) is used to make the concrete. Concrete is mixed in accordance with ASTM C192-07[53]. All the ingredients are weighed and placed in a clean container before being mixed. The coarse and fine aggregates are stoked and blended for one minute in 2/3 of the needed water in all mixtures. Then, for three minutes, cement and the remaining water were added and blended. Multiple beams are cast together with control samples on the day of each casting. Then, for three minutes, cement and the remaining water were added and blended. Multiple beams were cast together with control samples on the day of each casting.

On the day of each casting, several beams are cast together with control samples, six-cylinder specimens of 150mm in diameter and 300mm in height, three (150×150×150) mm cubes, and (50×50×50) mm to determine the concrete mechanical properties. After mixing, the concrete was poured into the lightly oiled mold in three layers and well compacted by a plunger mechanical vibrator (3500 rpm), for (5seconds) for each insertion. The surface of the concrete is leveled off and finished with a steel trowel. Due attention was paid not to move the cage. As shown in Plate (3-13).

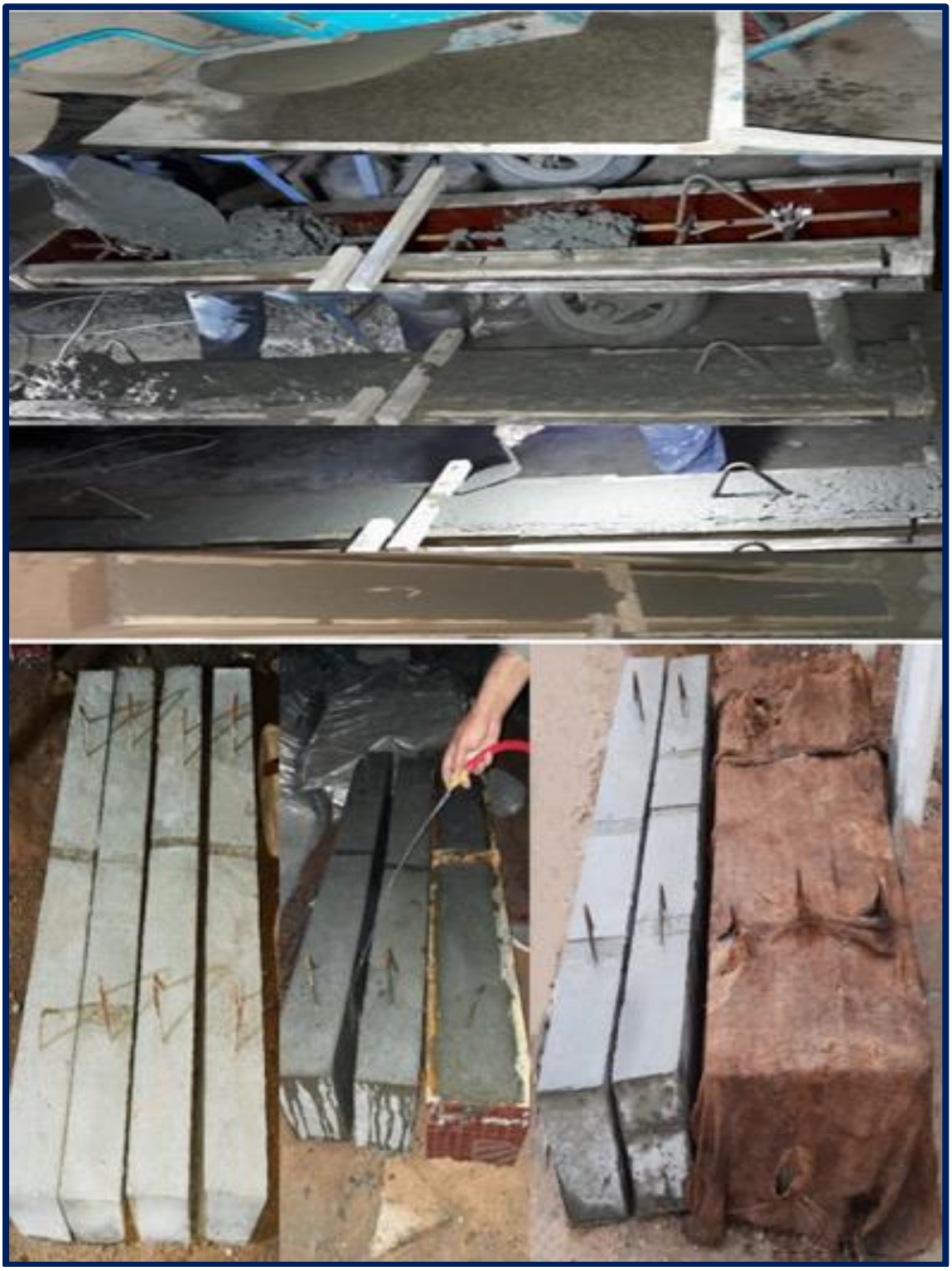

Plate(3-13): The casting and curing stages of NC and fiber concrete beam specimens.

All specimens were demolded after 24 hours of the casting, and then burlap sacks were placed over the beams and kept wet until 28 days. Cylinders, cubes, and prisms are placed in a curing water tank and kept wet in accordance with the standard specifications. After (28) days, they are taken out of the curing basin and then tested. On the other hand, the concrete

surfaces of the beam specimens were painted white, then marked with their symbols, and prepared for testing. See Plate (3-14).

Plate(3-14): (a): Demolding and curing, (b) prepare, (c): painting the beam specimens.

3.8 Hardened Concrete Mechanical Properties

All the samples (cubes and cylinders) are given a 24-hour rest period. They are then taken out of the molds and placed in a basin of clean water. They are taken out of the container after 28 days and tested with each beam specimen at the same time using a universal testing machine with a capacity of 2000kN, according to the standard specifications BS1881-116-89 [54] and ASTM-C496-11[52] to obtain the compressive and splitting tensile strengths, respectively.

The first step was the selection of materials, prepared and weighed according to the required volume of the mix. All specimens in this work are cast in plywood molds with a clear dimension of (150*300*1500 mm). After the mold was greased, the main steel reinforcement cage was placed in the mold at the middle of the beams for normal strength concrete, and the fiber concrete followed the same stages. Then vibration is used to remove the gaps and to achieve complete bonding between the concrete components.

The following stages describe the casting process:

1. Plywood formwork is provided before each casting by proper cleaning and lubrication of the inner surface with oil to prevent hardened concrete from sticking and laying on flat ground.
2. After the formwork is prepared, a pre-prepared reinforcing steel cage is placed in the middle with a cover 30 mm from the bottom and 25 mm in the other directions.
3. Concrete with regular strength is poured with fiber concrete in the same way.
4. To prevent caking or voids in the leaking concrete fibers, a steel rod with a diameter of (3mm) is used to compact each layer. This step is repeated until the mold is completely filled to the required level.
5. After filling in all the required samples, it is necessary to use a vibrator for concrete with normal pressure to compress and achieve bonding. Between

the concrete components inside the molds, cube samples are poured to determine the concrete pressure strength. Cubes (150*150*150mm) for regular-strength concrete. After (24) hours, the plywood template is removed. The traditional processing method is used to simulate the site conditions. Then, the beams are covered with impregnated burlap to avoid the evaporation of the treatment water.

3.8.1 Strengthening of Test Specimens

Two of the sixteen test specimens are strengthened with carbon fiber strips (CFRP). The surface of concrete was smoothed before the installation of CFRP. The installation procedure recommended by the manufacturer is described as follows:

• After 28 days of curing, grooves with (**3ab**) width and (**1.5bb**) depth [55][18] were cut in concrete cover by using diamond cutter then the grooves are washed by water and cleaned by compressed air to remove the dust and gain better bonding as shown in Figure(3-2).

ab: is the thickness of strip.

bb: is the width of strip

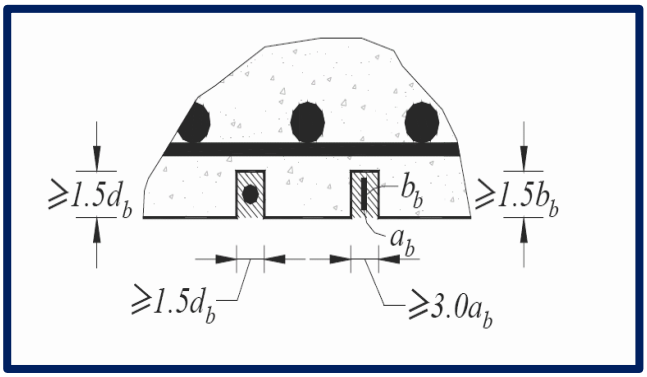

Figure(3-2): Minimum dimension of grooves[5].

• Before installation, CFRP is cut to the required lengths and cleansed of dust, oil, grease, and other contaminants.

• Epoxy glue is a two-part epoxy adhesive (A white and B black). At a 35°C ambient temperature, the two parts were mixed until a grey color was obtained in the proportion (4A: 1B) without exceeding the mixing time (3 minutes).

• After allowing the adhesive to cure in the air for seven days, all specimens are painted white to identify and observe the breaking pattern. Plate (3-14) illustrates the installation process.

3.9 Specimen Testing

All specimens are put through their paces on a machine with a maximum load capacity of (3000kN). A digital load cell and a data logger acquisition system were installed on the machine, which recorded the load and deflection every second and saved the data in the form of an excel sheet. The specimens are simply supported along a span length of 1500mm, and each specimen is tested at mid-span under a single concentrated force, as shown in Plate(3-16).

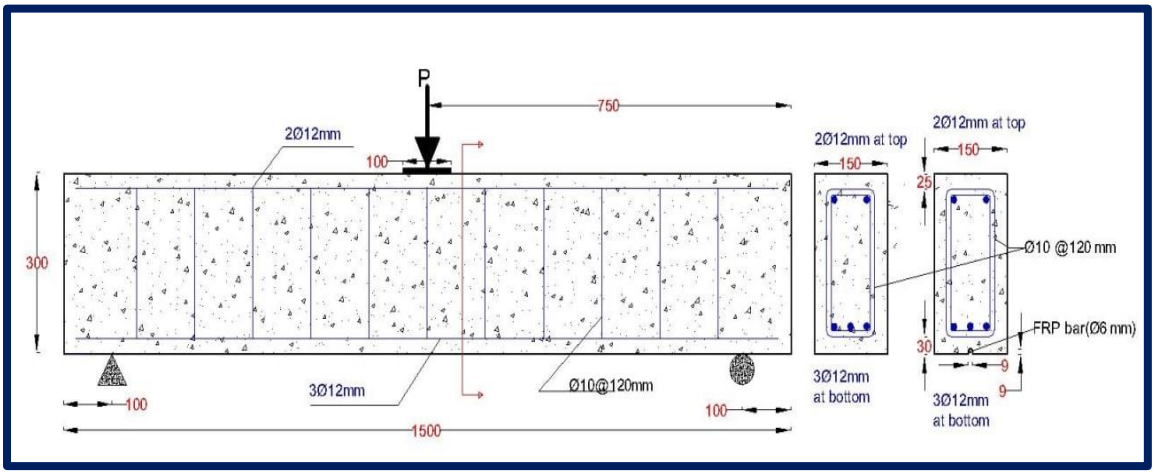

Plate(3-15): Beam dimensions and reinforcement.
details: a) Elevation, b) Section1control beam, c) Section 2 strengthening beam.

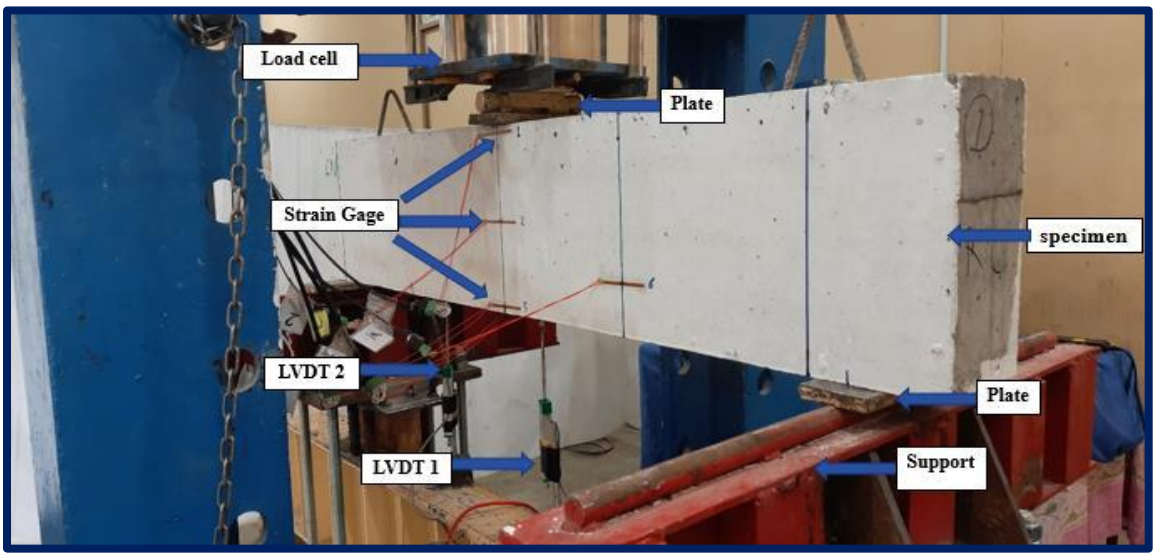

Plate(3-16): Specimen dimensions and reinforcement in test setup.

Chapter Four
EXPERIMENTAL RESULTS AND DISCUSSION

4.1 General

In this chapter, the most relevant results obtained from experimental program that described in chapter three are summarized and discussed.to study the flexural behavior of such specimens testing under one point load.

The main objective of this study was to test the structural behavior of beams strengthened or repaired in flexural directions. The experimental program consisted of sixteen (16) tested beams divided into two groups. All the reinforced concrete beams had the same length and cross-sectional area. Test results are analyzed based on cracking behavior, vertical midspan deflection, and strain distribution across the depth of the reinforced concrete beam at midspan section and failure mode. In this chapter, the general behavior and test observations of such beams are reported and discussed. In addition, the effects of various parameters on the behavior are investigated.

4.2 Experimental Results of Beams

4.2.1 Cracking Behavior

The creation of cracks is tracked during the testing to compare the behavior of the reinforced specimens to that of the unstrengthen control beams. In the sections that follow, all models' first cracking loads, cracking patterns, and crack widths are given.

4.2.1.1 First Cracking Load

In models, the first cracking loads of RC beams strengthened near their surfaces were found to be significantly higher than those of reference control beams and externally strengthened RC beams.

Group One NCb, NSb, showed higher first cracking loads when compared with NGb.

External Strengthening showed better enhancement in first cracking loads in model NT compared with reference control. While NCbT and NSbT demonstrated higher initial cracking loads than NGbT.

4.2.1.2 Cracking Patterns

The following sections discuss the cracking pattern of each beam specimen: -

Group One

- ***Control Beam Specimen (CN)***

The CN control beam is evaluated as an unstrengthen beam to compare to the strengthened beams. The control beam behaved in expected fashion under flexural loading. It was gradually loaded until the initiation of cracking. Flexural cracks first appeared at 30kN, within the constant moment zone. As the load increased, flexural cracks occurred and expanded.

The crack width is measured at the value of the load 176kN as the last value.

It was found it difficult to measure the width of the cracks, because the model is in advanced stages of loading and may cause harm to the reader. The beam failed when the concrete crushing at the tensile cracks flexural at load (191.505KN) as shown in Plate (4-1).

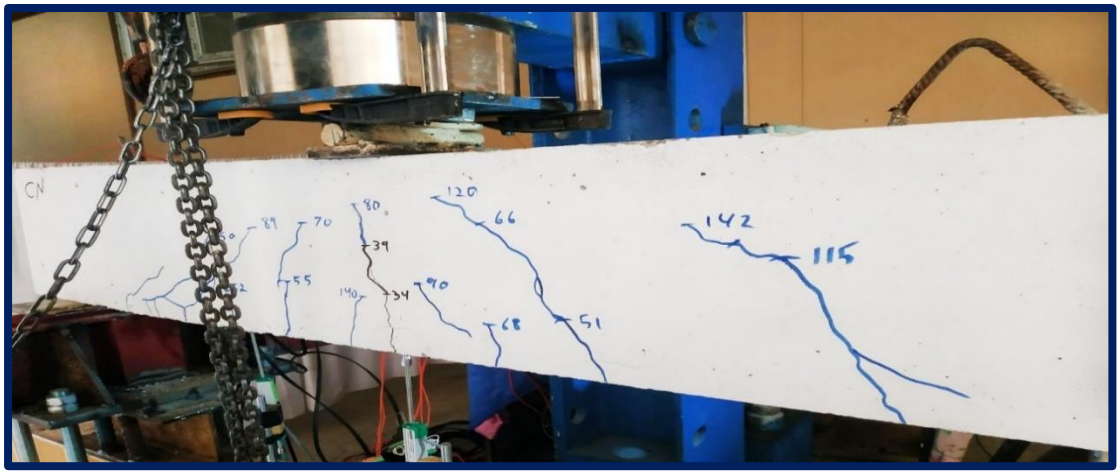

Plate (4-1): Crack pattern after failure for beam CN.

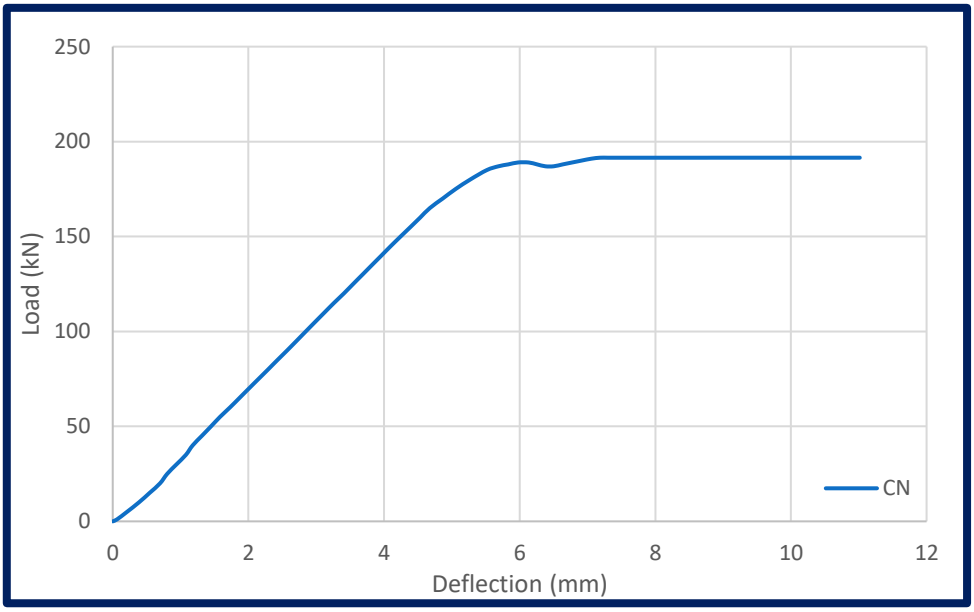

Figure(4-1): Load-Deflection curve for control beam specimen CN.

- ***strengthened Beam Specimen (EBR-CFRP Sheet (NT))***

For the strengthened beam specimen NT, which is strengthened with only one CFRP sheet of length (1200mm) and width (150mm). The first crack was observed at a load of 38kN. New cracks were observed along the beam specimen as the load was increased. Finally, debonding failure occurred at (257.562kN). which is greater than the control beam (CN) by 34.49%. Debonding occurs in FRP-strengthened RC members at areas with significant

stress concentrations, which are frequently coupled with material discontinuities and cracks. Debonding failure is a phrase used to denote a considerable reduction in member capacity caused by the onset or propagation of a large crack near the interface region. As shown in Plate (4-2).

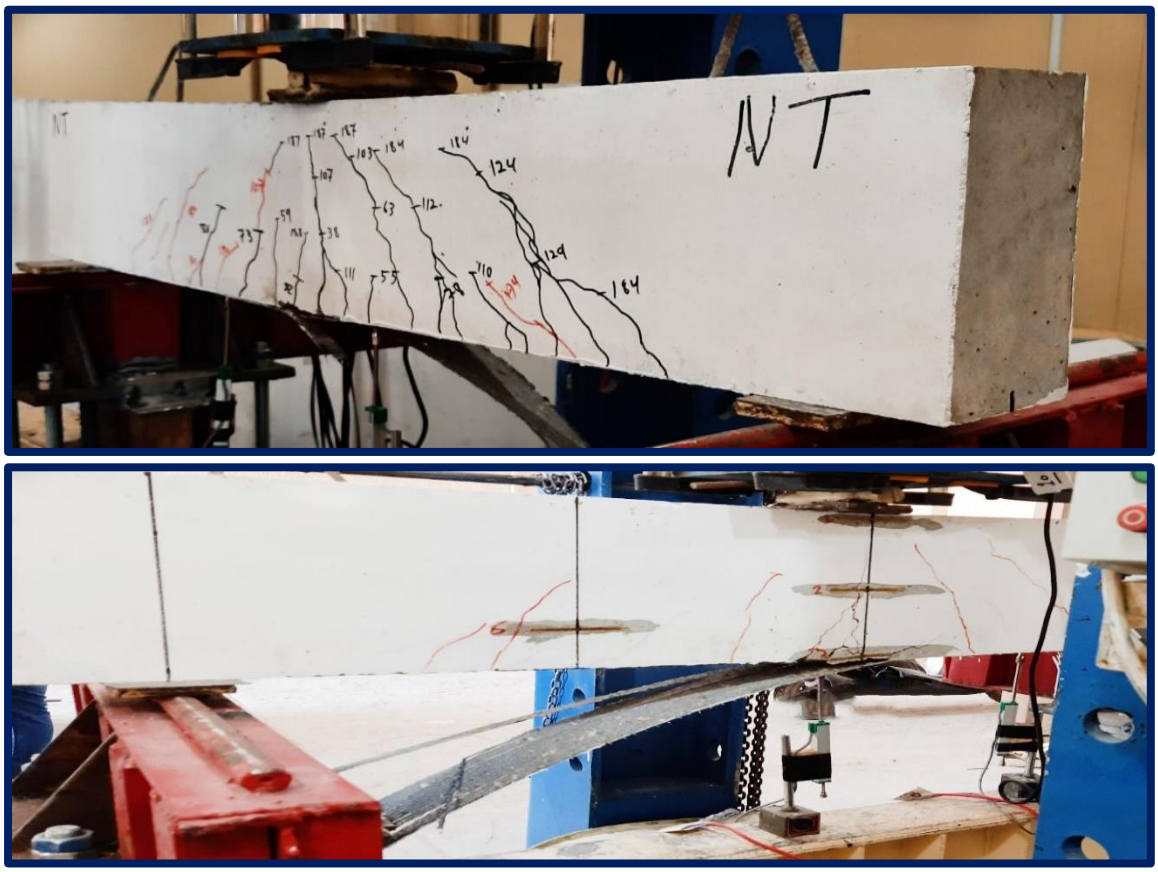

Plate (4-2): Crack pattern after failure for beam NT.

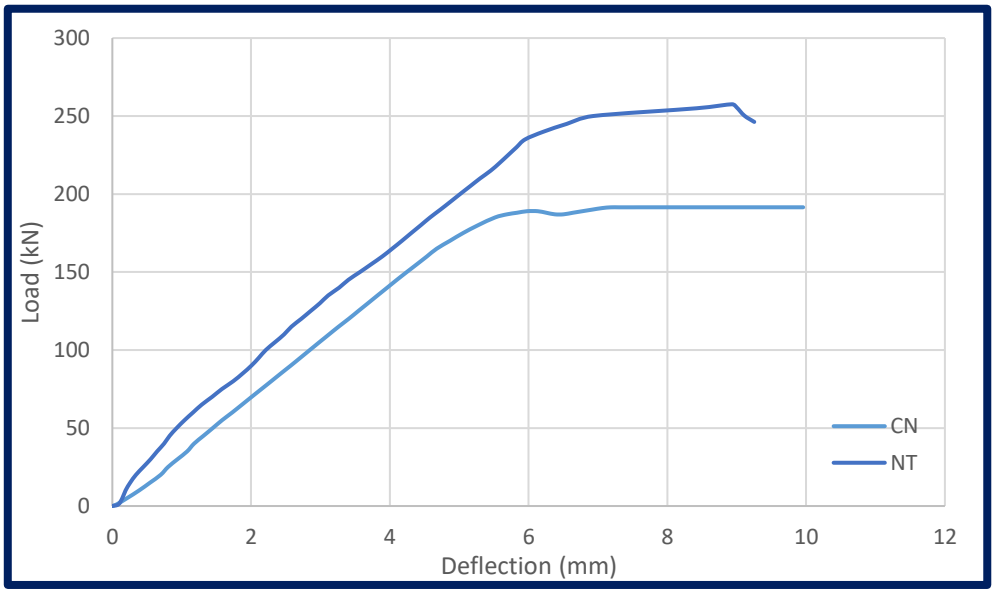

Figure(4-2): Load-Deflection curve for specimen NT.

- ***Strengthened Beam Specimen (NSM-CFRP(NCb))***

To study the effect of the near surface mounted technique, the beam specimen **NSM-CFRP** is strengthened with only one CFRP bar of length (1200mm) and a diameter of 6 mm. The first crack, as shown below in Plate (4-3), is observed at a load of (30kN) (is like the control beam). As the load is increased, new cracks form along the beam specimen. The beam failed due to splitting in CFRP at load (268.0787 kN), which is greater than the control beam (CN) by 39.98%. Failure occurred because of a combination of interfacial crack-induced debonding and full cover separation. If the force in the FRP cannot be supported by the substrate, cover delamination or FRP debonding can occur. Regardless of where the failure plane propagates within the FRP adhesive-substrate area, this behavior is referred to as debonding. ACI440.2R-08[56] provides behavior and failure modes.

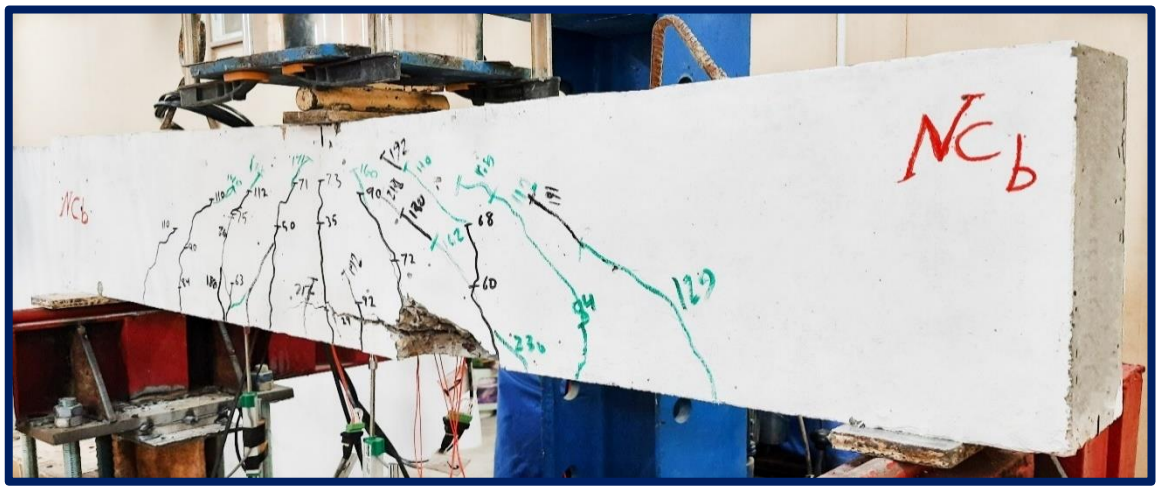

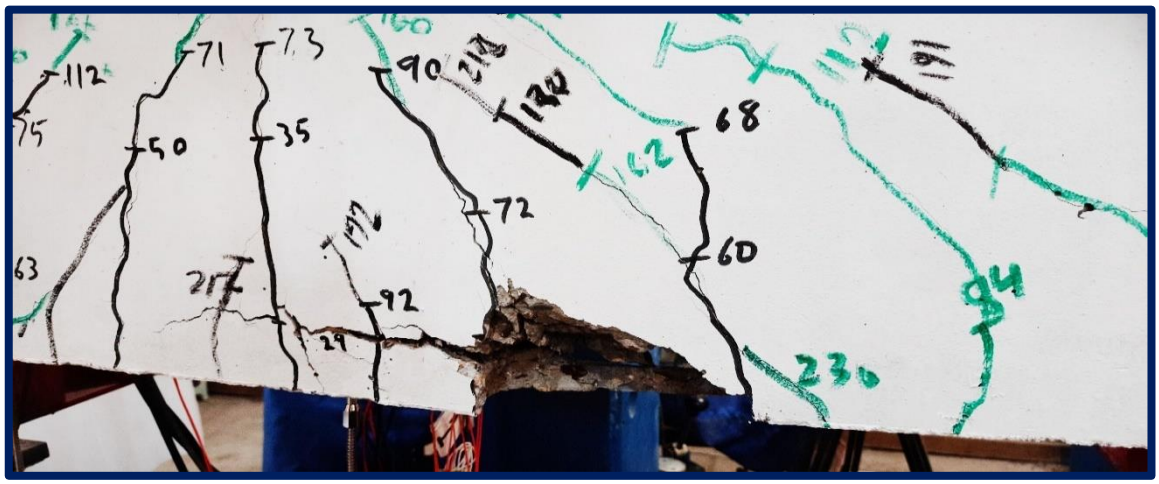

Plate (4-3): Crack pattern after failure for beam NCb.

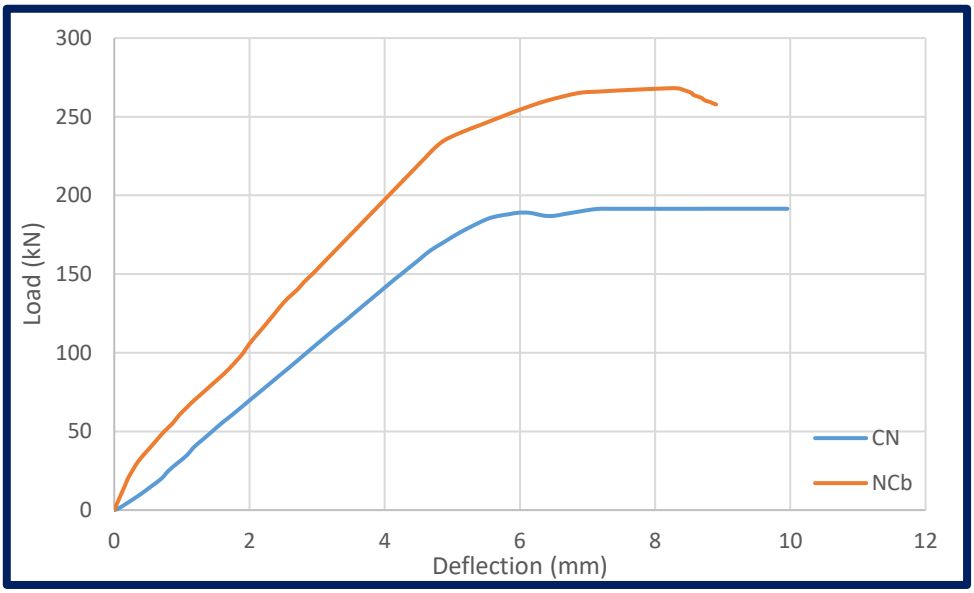

Figure (4-3): Load-Deflection curve for beam specimen NCb.

- ***strengthened Beam Specimen (NSM- GFRP(NGb))***

The beam specimen ***NSM-GFRP*** is strengthened with GFRP bar of length (1200mm) and diameter (6 mm), which are installed on the tension bottom face of the reinforced concrete beam. The crack pattern of this beam specimen is shown in Plate (4-4). The first crack occurred at a lower load than that of the unstrengthened beam specimen CN, which is noticeable when a load of (28kN) is applied. The number, width, and depth of flexure cracks increased as the load is increased. Finally, the beam failed when it reached an ultimate load of 242.1188kN, which is 26.43% larger than the control beam (CN). cover delamination or FRP debonding can occur, this behavior is referred to as debonding.

Plate (4-4): Crack pattern after failure for beam NGb.

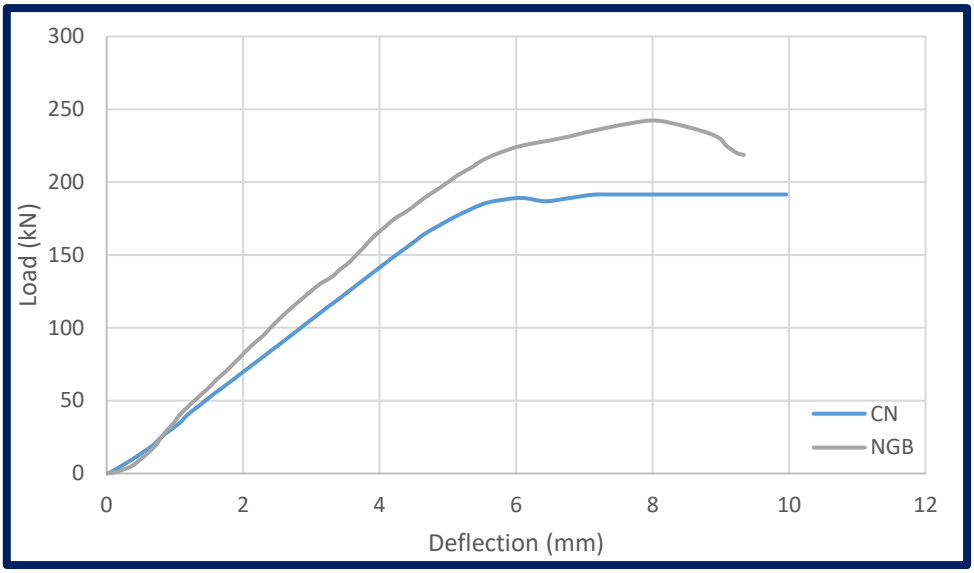

Figure (4-4): Load-Deflection curve for specimen NGb.

- ***Strengthened Beam Specimen (NSM- Steel Reinforce bar (NSb))***

The beam specimen **NSM-Steel reinforce bar** is strengthened with steel reinforcement bar of length (1200mm) and diameter (6mm), which are installed on the tension bottom face of the reinforced concrete beam. The crack pattern of this beam specimen is shown in Plate (4-5). The first crack appeared at a lower load than the unstrengthened beam specimen CN, and it is discovered when a load of (31kN) applied. As the load is raised, the number, width, and depth of flexure cracks are increased also appear shear cracks. The beam finally collapsed when it achieved an ultimate load of 223.2563kN, which is 39.98% greater than the control beam (CN). This behavior is known as debonding, and it occurs anywhere in the FRP-adhesive-substrate region where the failure plane propagates.

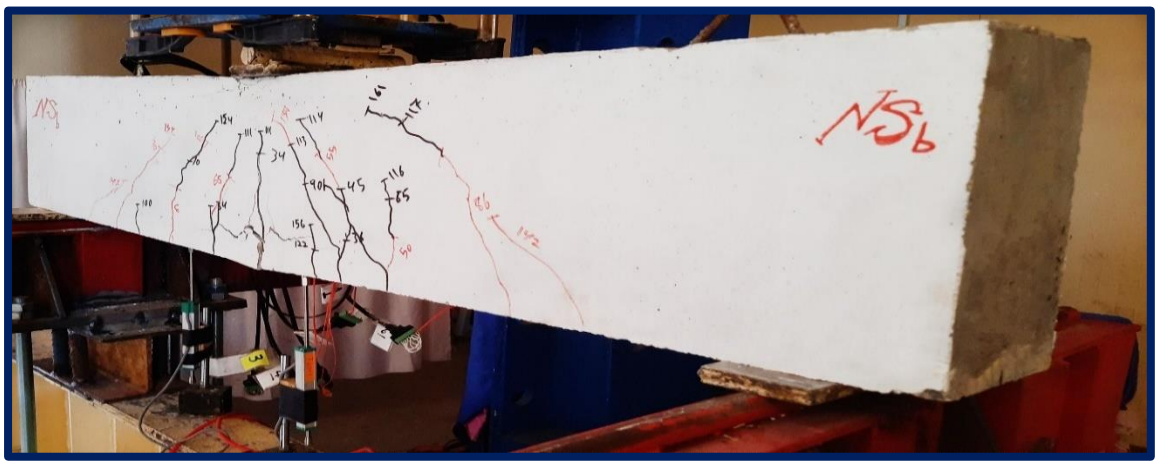

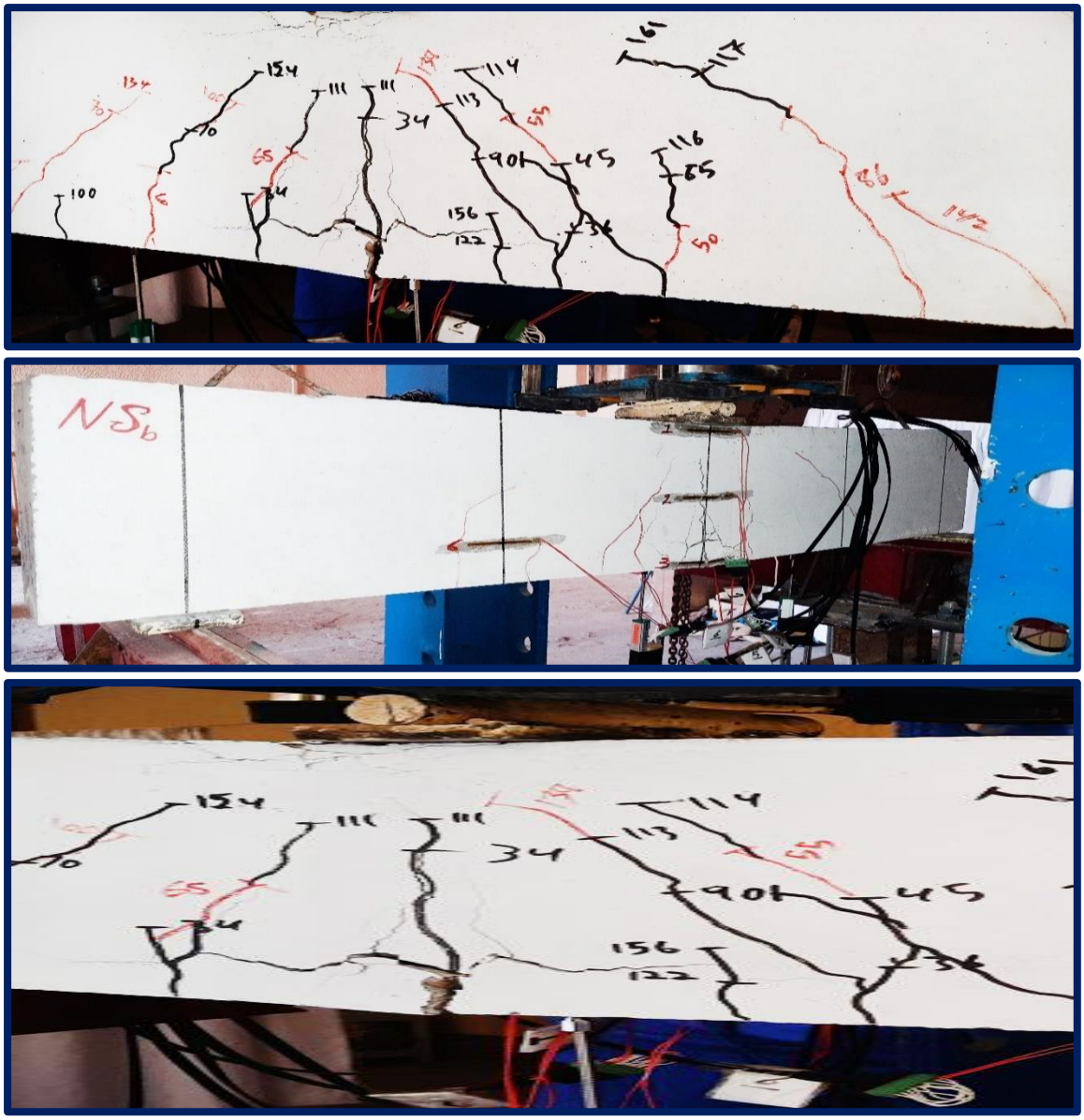

Plate (4-5): Crack pattern after failure for beam NSb.

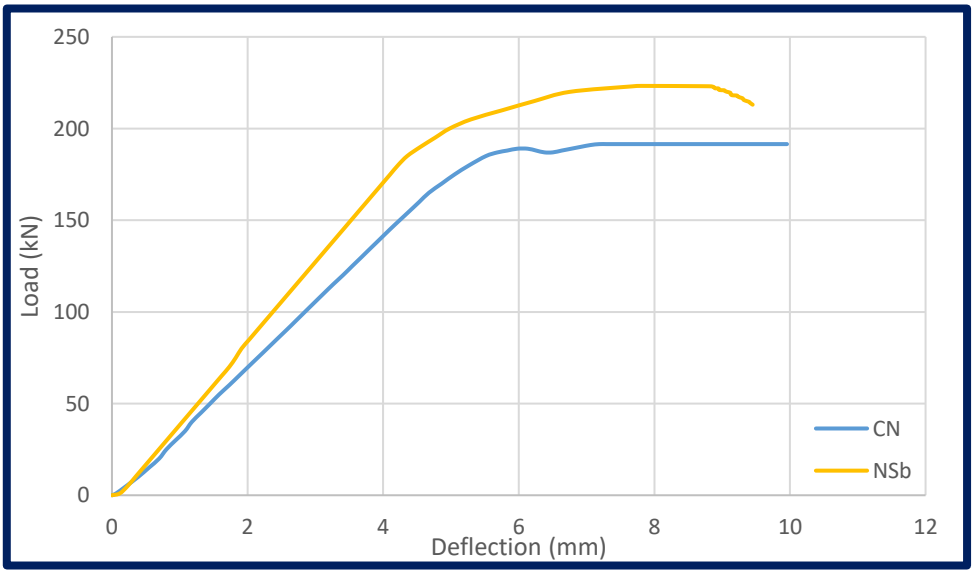

Figure (4-5): Load-Deflection curve for specimen NSb.

- ***Strengthened Beam Specimen (NSM-CFRP-EBR-CFRP Sheet (NCbT))***

To study the effect of the near surface mounted technique on the two types of strengthening that are used, the beam specimen **NSM-CFRP** is strengthened with one CFRP bar of length (1200mm) and diameter (6 mm) and an **EBR-CFRP** sheet of length (1200mm) and width (150mm). The first crack is observed at a load of (29kN).The cracks pattern as shown below in Plate(4-6). The first crack occurred at a lower load than that of the strengthened beam and unstrengthened beam specimens NCb and CN, respectively. As the load increased, new cracks formed along the beam specimen. The beam failed due to splitting in CFRP at load (275.9237kN), which is greater than the control beam (CN) by 44.08%. It is possible for the cover to delaminate or the FRP to deboned; either of these behaviors is referred to as debonding.

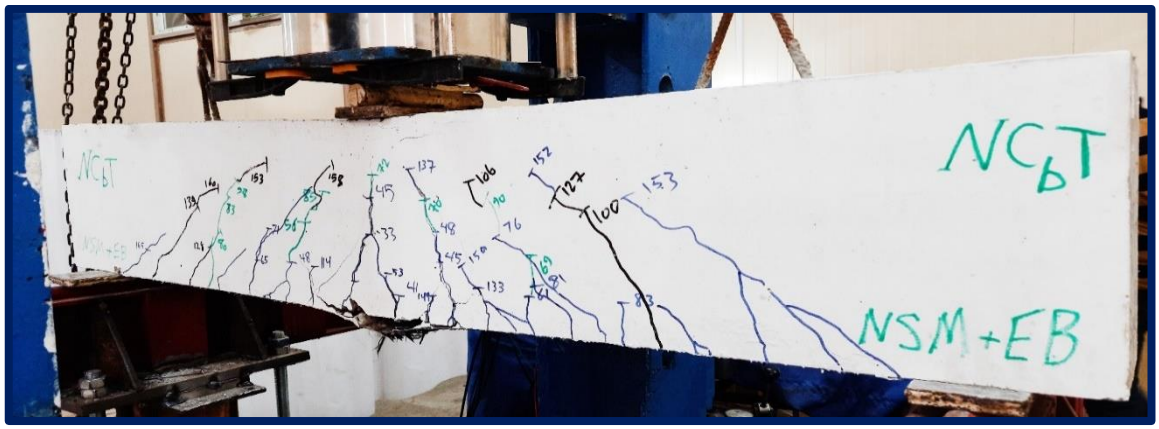

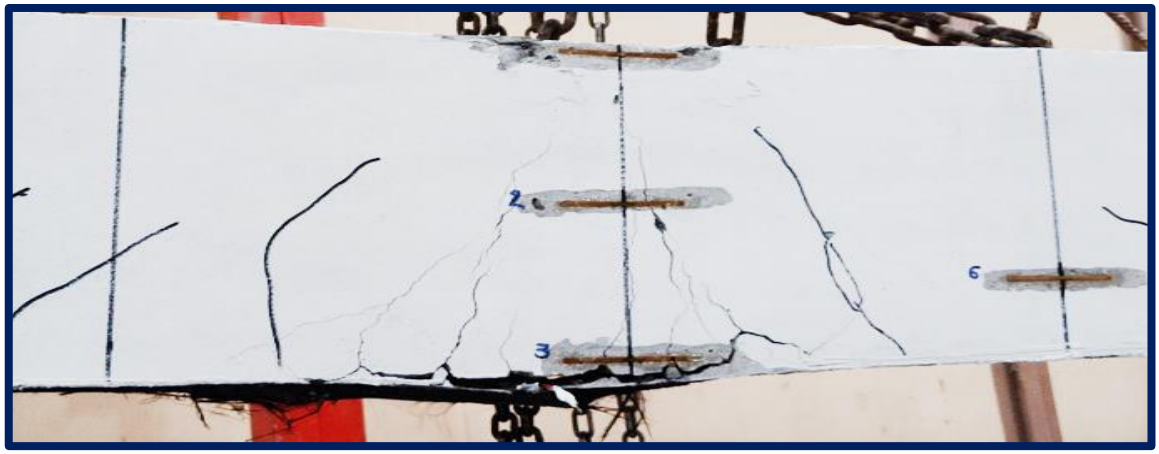

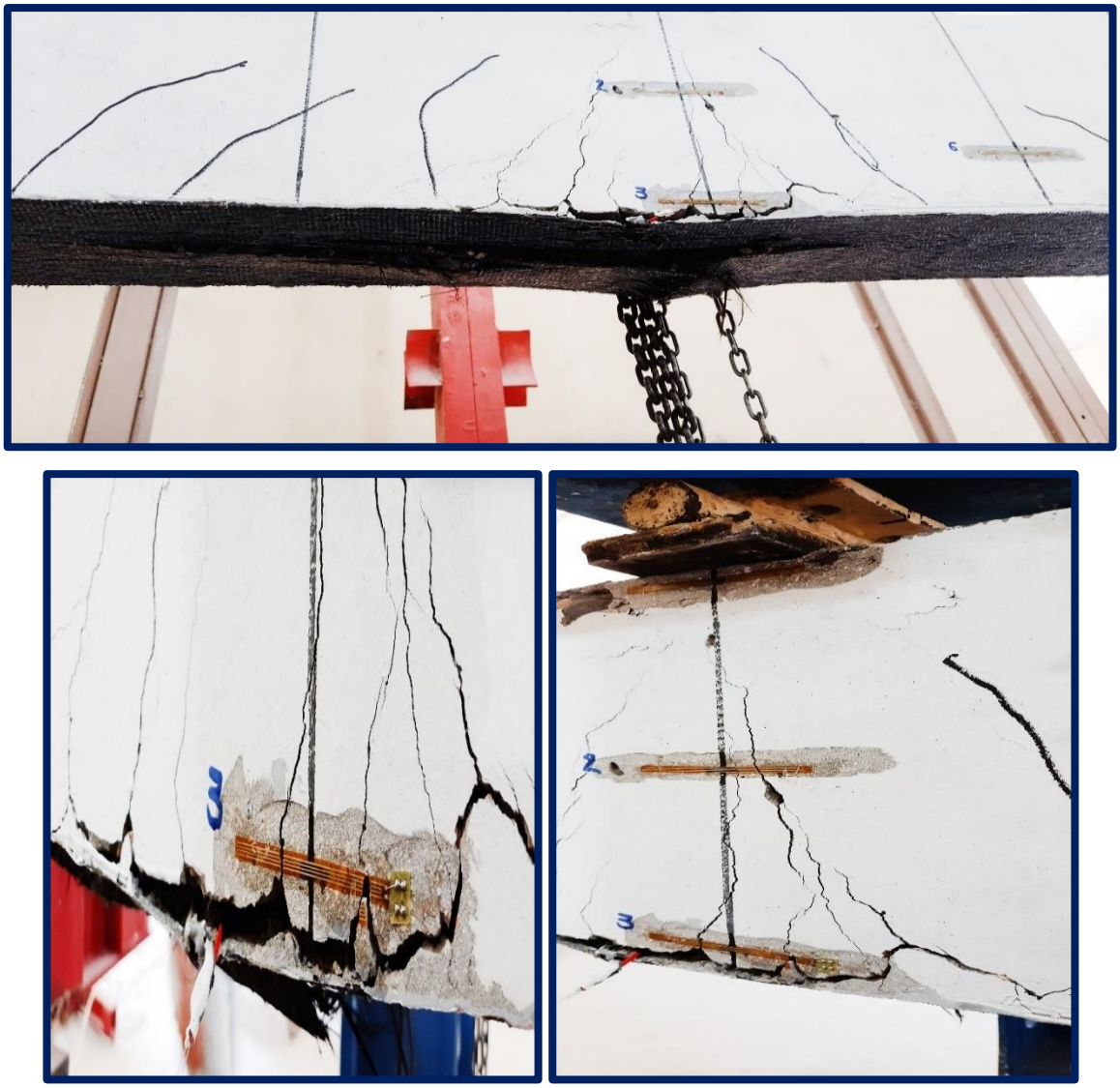

Plate (4-6): Crack pattern after failure for beam NCbT.

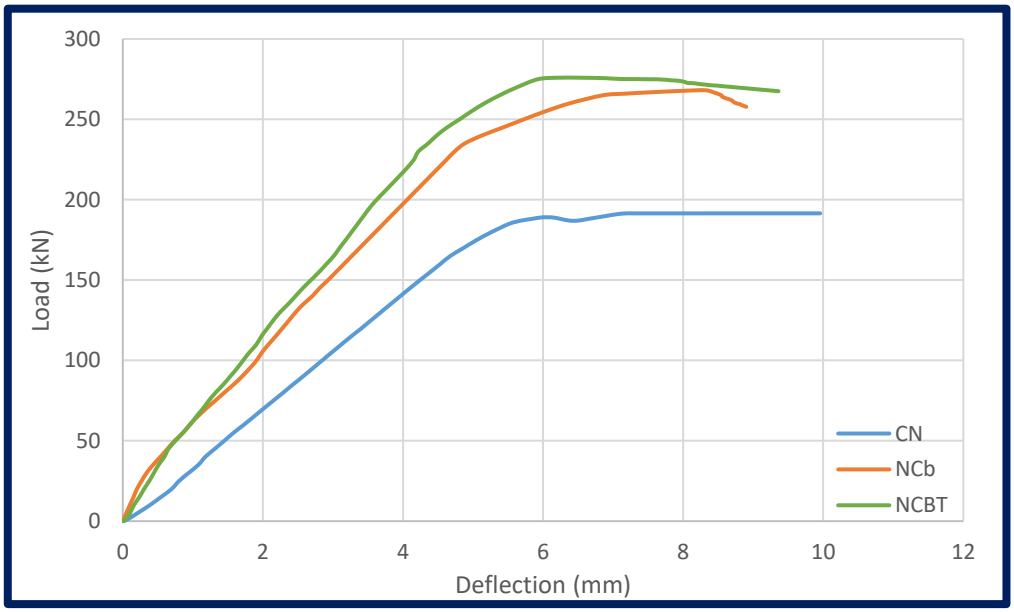

Figure (4-6): Load-Deflection curve for specimen NCbT.

- ***Strengthened Beam Specimen (NSM-GFRP-EBR-CFRP Sheet (NGbT))***

To study the effect of the near surface mounted technique on two types of strengthening that are used, the beam specimen **NSM-CFRP** is strengthened with one CFRP bar of length (1200mm) and a diameter of (6 mm) and an **EBR-GFRP** sheet that is length (1200mm) and width (150mm). The first crack is observed at a load of (20kN), with an initial crack forming in the constant moment region. The cracks pattern as shown below in Plate (4-7). First crack occurred at a lower load than of the strengthened beam and unstrengthen beam specimen NGb, CN respectively. As the load was increased, new cracks formed along the beam specimen. The beam failed due to splitting in CFRP at load (269.1589 kN), which is greater than the control beam (CN) by 40.55%. The cover delamination or FRP debonding can occur, this behavior is referred to as debonding.

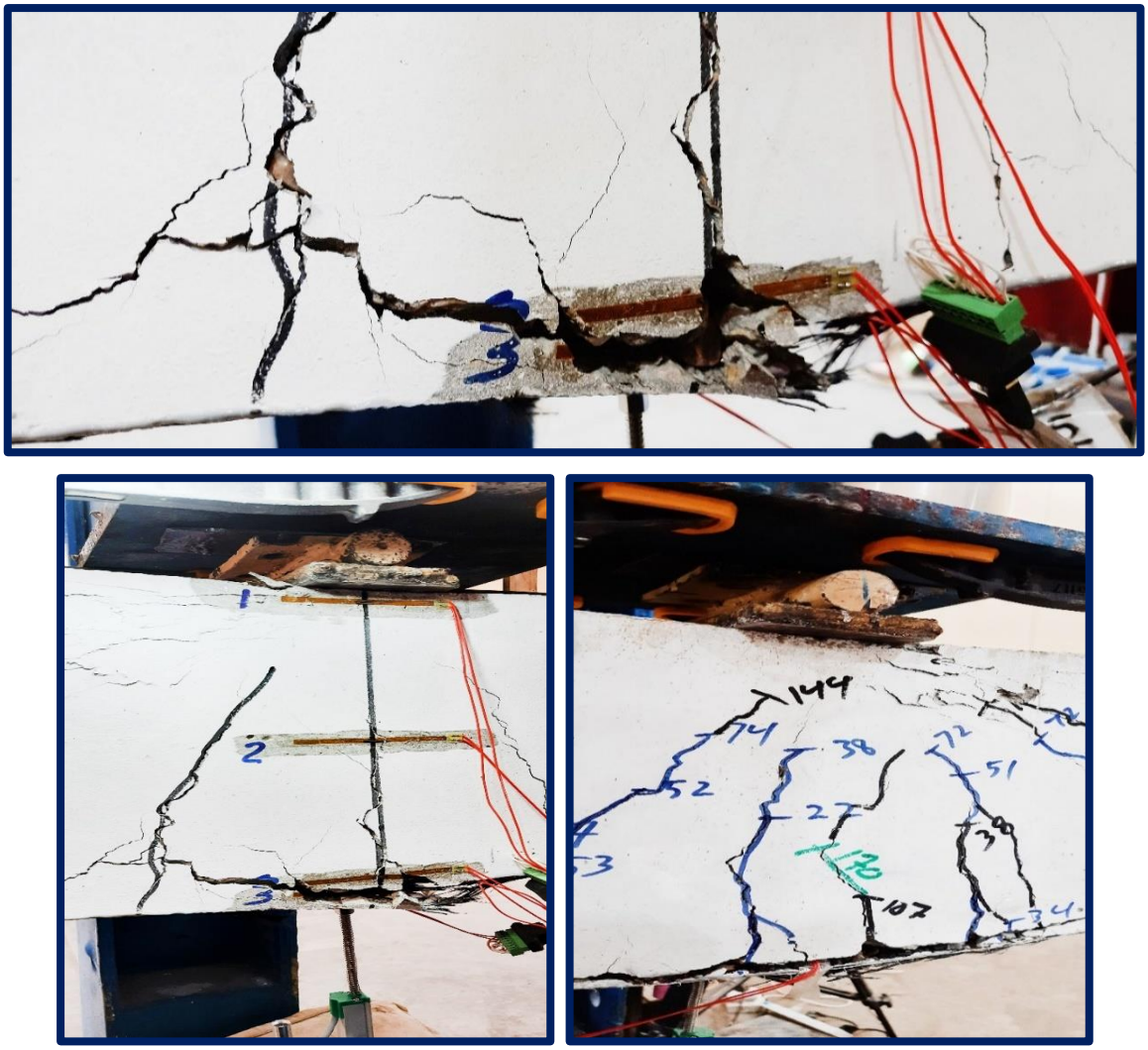

Plate (4-7): Crack pattern after failure for beam NGbT.

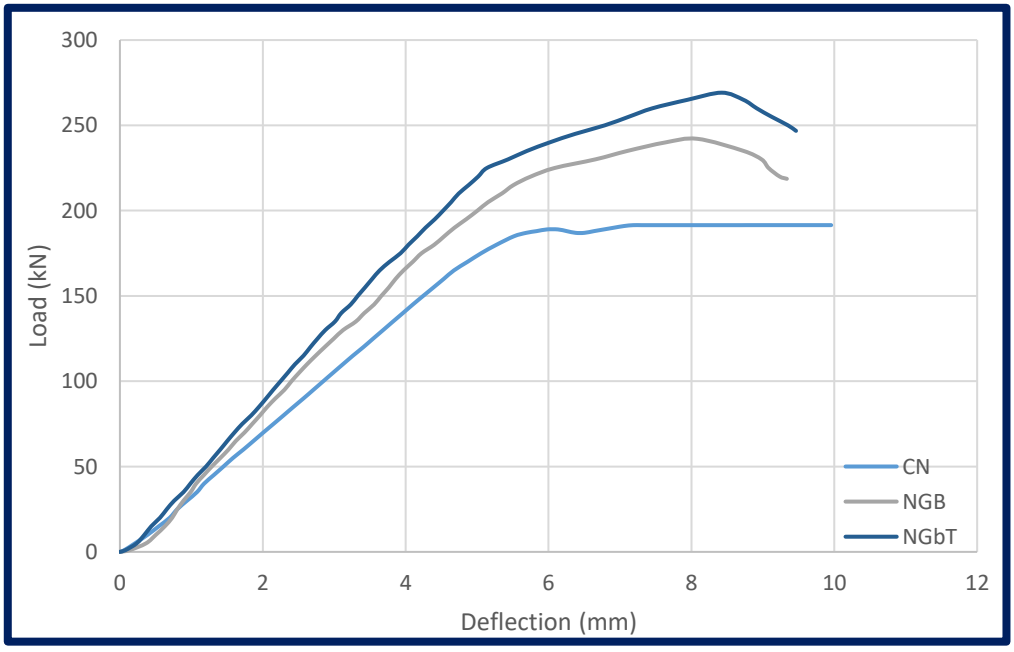

Figure(4-7): Load-Deflection curve for specimen NGbT.

- ***Strengthened Beam Specimen (NSM-Steel Reinforce bar -EBR-CFRP Sheet (NSbT))***

To study the effect of the near surface mounted technique on the two types of strengthening that are used, the beam specimen **NSM-CFRP** is strengthened with one CFRP bar of length (1200mm) and a diameter of (6 mm) and an **EBR-Steel Reinforce bar** sheet that is length (1200mm) and width (150mm). The first cracking was observed at a load of (20kN), with an initial crack forming in the constant moment region. The first crack, as shown below in Plate (4-8). The first crack occurs at a lower load than in the strengthened and unstrengthened beam specimens NSb, and CN. As the load is increased, new cracks form along the beam specimen. The beam failed due to splitting in CFRP at load (259.1761kN), which is greater than the control beam (CN) by 35.34%. The cover delamination or FRP debonding can occur, this behavior is referred to as debonding.

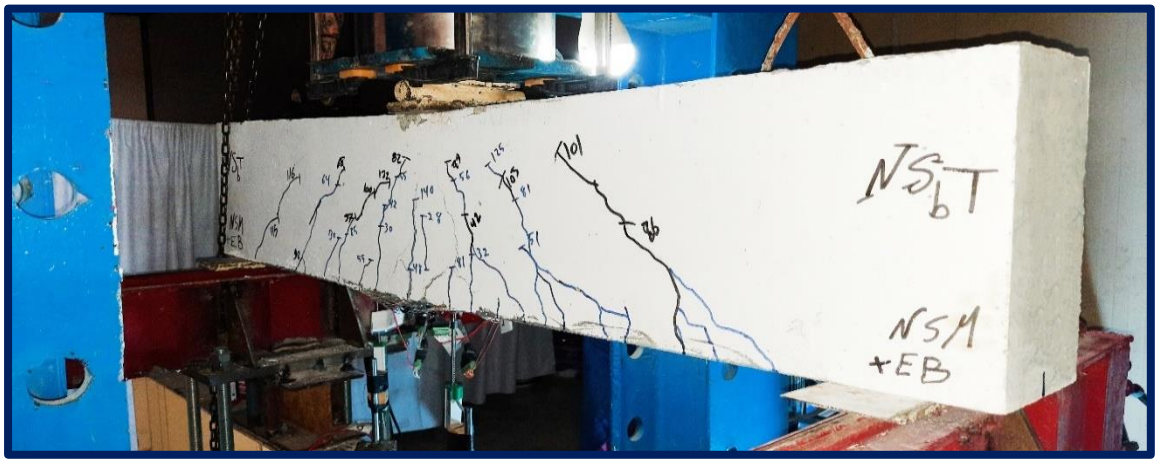

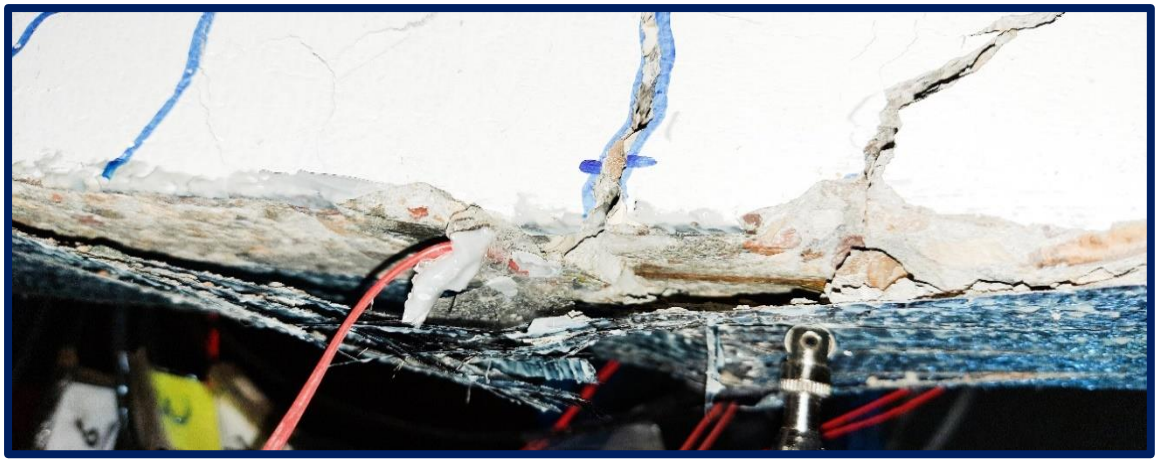

Plate (4-8): Crack pattern after failure for beam NSbT.

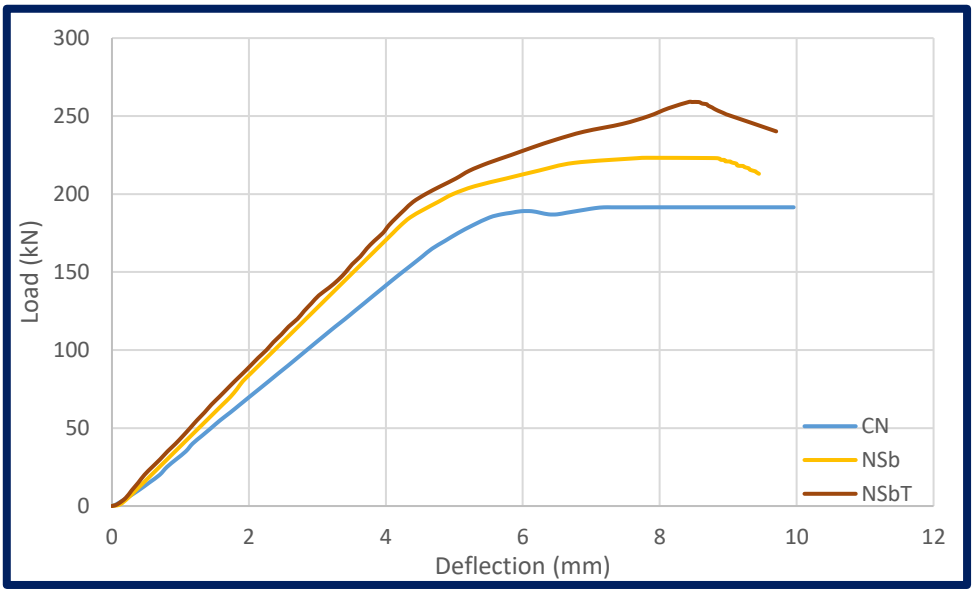

Figure(4-8): Load-Deflection curve for specimen NSbT.

Group Two

Group two consists of eight beams: CF, FCb, FGb, FSb, FT, FCbT, FGbT, and FSbT. In this group, the same mounting and strengthening process is used, but fiber is added at a rate of (1%). The fiber's effect may be seen by increasing the amount of resistance in general for all the model's groups. Details of these beams are shown below.

- ***Control Beam Specimen (CF)***

The main new feature in this beam, compared to the previous beams in group one, contained micro steel fiber with a ratio of 1%. The CF control beam is evaluated as an unstrengthen beam to compare to the strengthened beams.

Under flexural loading, the control beam responded as expected. It was gradually loaded until the initiation of cracking. The first flexural crack showed up in the constant moment zone of the beam load (26kN). As the load increased, flexural cracks occurred and expanded. The beam continued to cray additional applied load until flexural failure occurred at (220.1198kN). The crack width is measured at the value of the load (191.4kN) as the last value. Because the model is already loaded to its maximum capacity, accurately measuring the cracks' width is dangerously difficult. The mode of failure the typical flexure in Concrete shown in plate (4-9).

Plate (4-9): Crack pattern after failure for control beam CF.

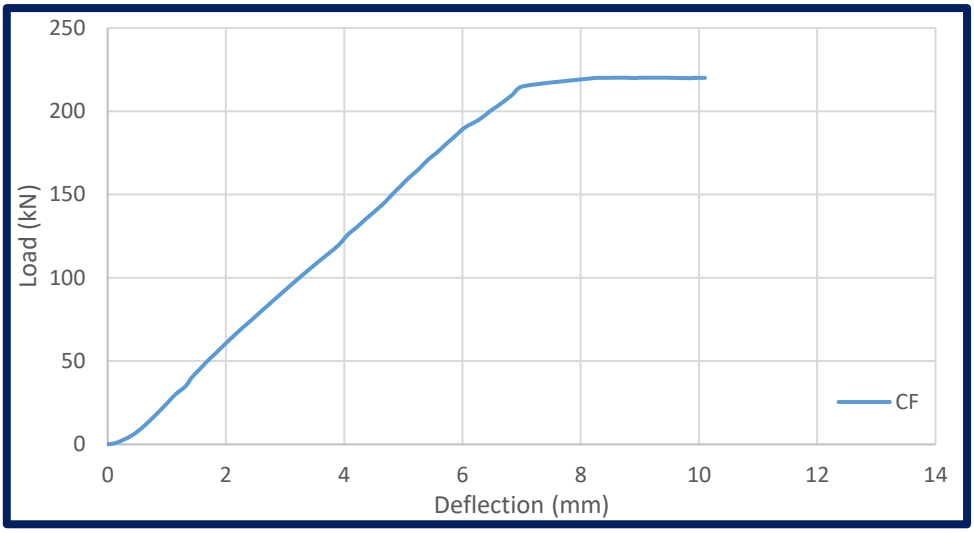

Figure (4-9): Load-Deflection curve for control beam specimen CF.

- ***strengthened Beam Specimen (EBR-CFRP Sheet (FT))***

For strengthened beam specimens FT, which are strengthened with only one CFRP sheet of length (1200mm) and width (150mm), the first cracking is observed at the load of (36kN) with an initial crack forming in the moment region. New cracks were observed along the beam specimen as the load was increased. Finally, debonding failure occurred at (288.844kN), which is greater than the control beam (CF) by 31.22%.

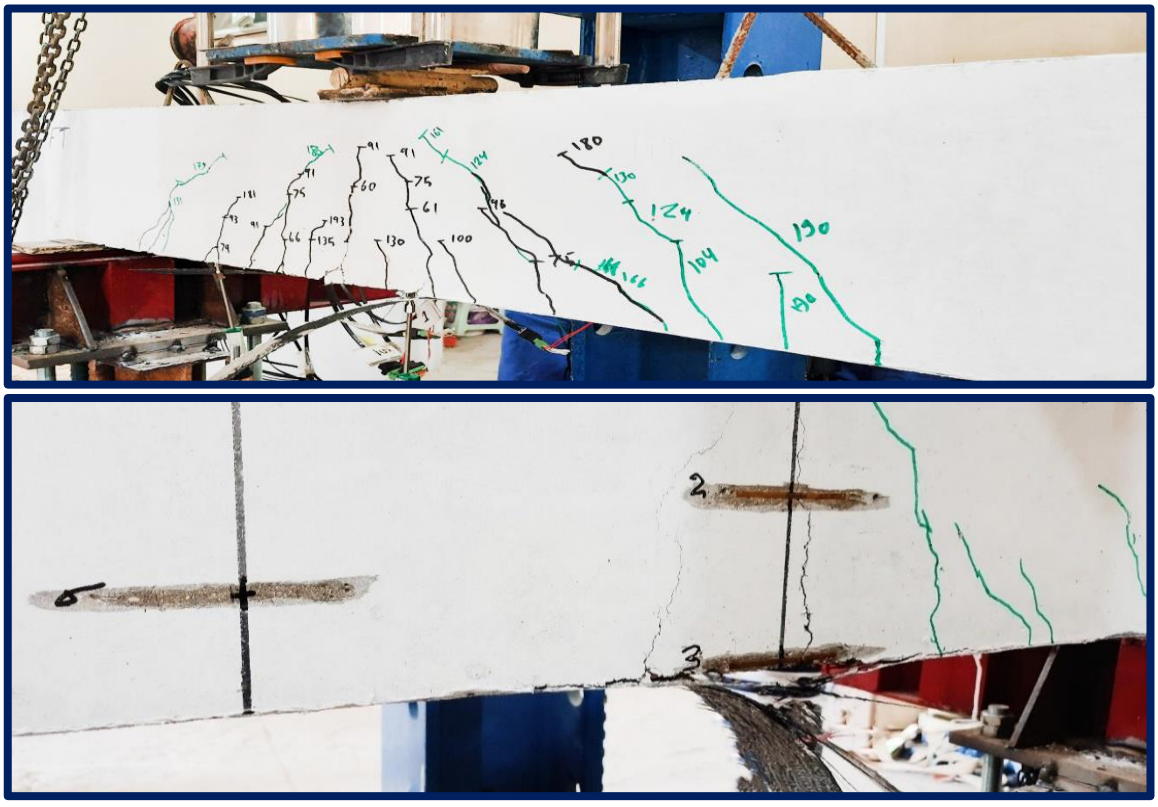

Plate (4-10): Crack pattern after failure for beam FT.

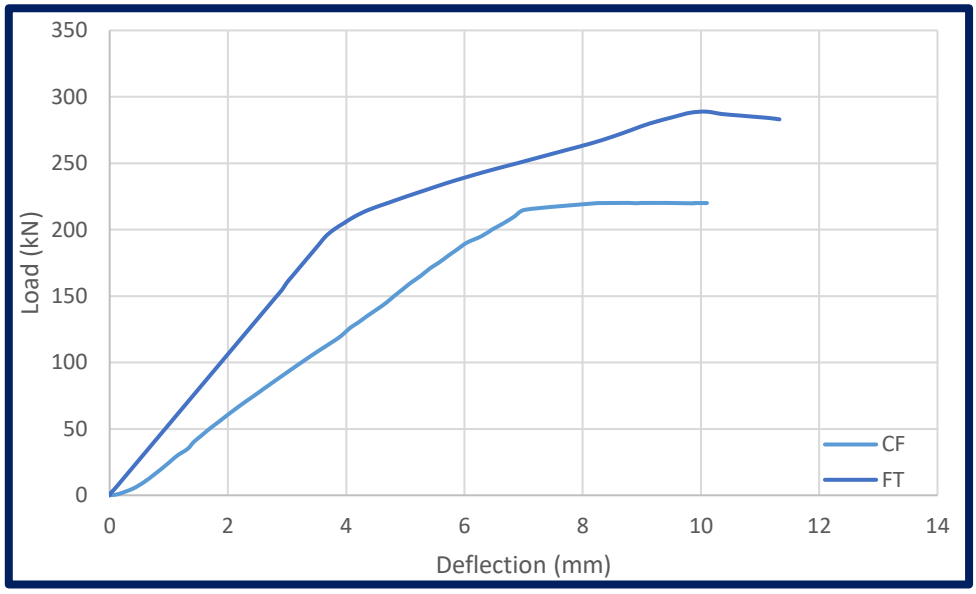

Figure(4-10): Load-Deflection curve for specimen FT.

- ***Strengthened Beam Specimen (NSM-CFRP(FCb))***

The beam specimen **NSM-CFRP** is strengthened with only one CFRP bar of length (1200 mm) and a diameter of(6mm). The first crack is observed with a load of about (39kN). As the load is increased, flexural cracks increase in number and depth. As the load is increased, new cracks formed along the beam specimen. The crack width was observed until the last value was reached (202kN). That's unable to assess the width of the cracks because the model is in late-stage loading, where it poses a risk to the reader. The beam failed due to splitting in CFRP at ultimate load failure occurred at load (293.854kN), which is greater than the control beam (CF) by 33.50%. when the load increases the crack development. as shown below in plate (4-11).

Plate (4-11): Crack pattern after failure for beam FCb.

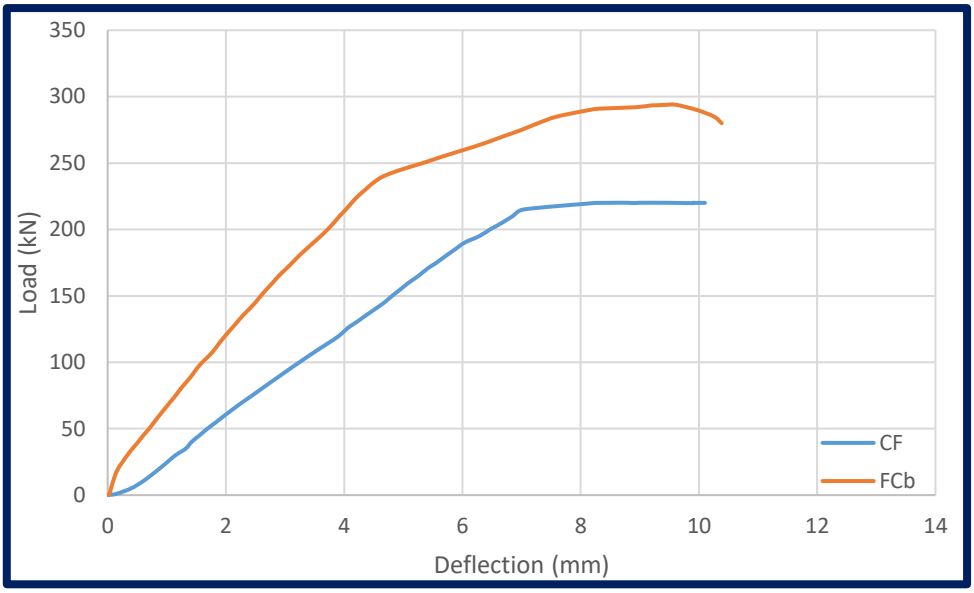

Figure (4-11): Load-Deflection curve for specimen FCb.

- ***strengthened Beam Specimen (NSM- GFRP(FGb))***

This beam comprises ***NSM-GFRP*** and is strengthened with GFRP bar of length (1200mm) and of a diameter of (6mm), which is installed on the tension bottom face of the reinforced concrete beam. The crack pattern of this beam specimen is shown in Plate (4-12). The first flexural crack appeared at load (38kN). The first crack occurred at a lower load than that of the unstrengthened beam specimen CF. The number, width, and depth of flexure cracks increased as the load was increased. Finally, the beam failed when it reached an ultimate load of (258.760kN), which is 17.55% larger than the control beam (CF).

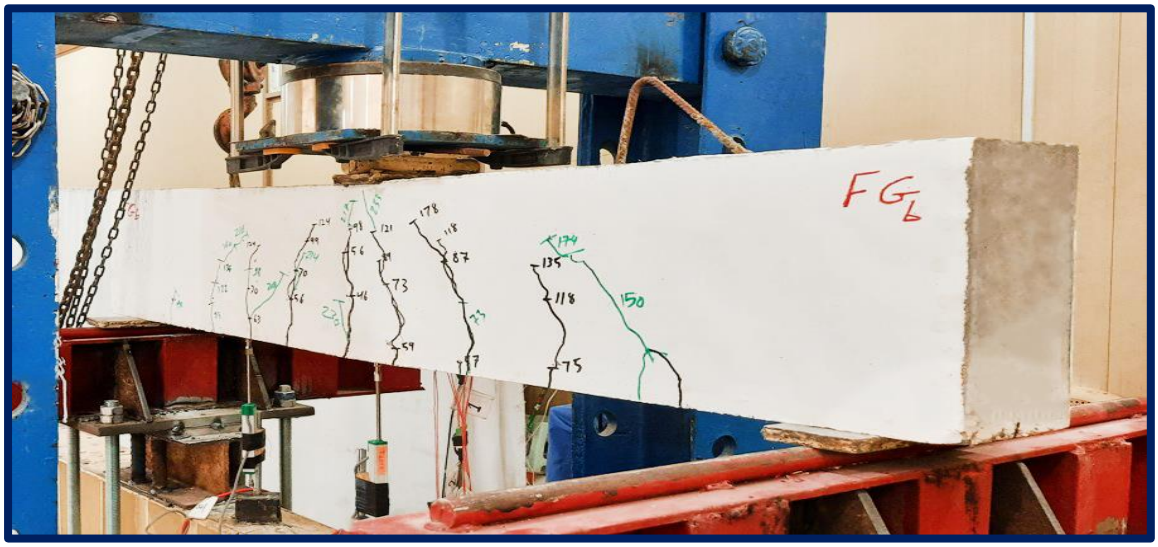

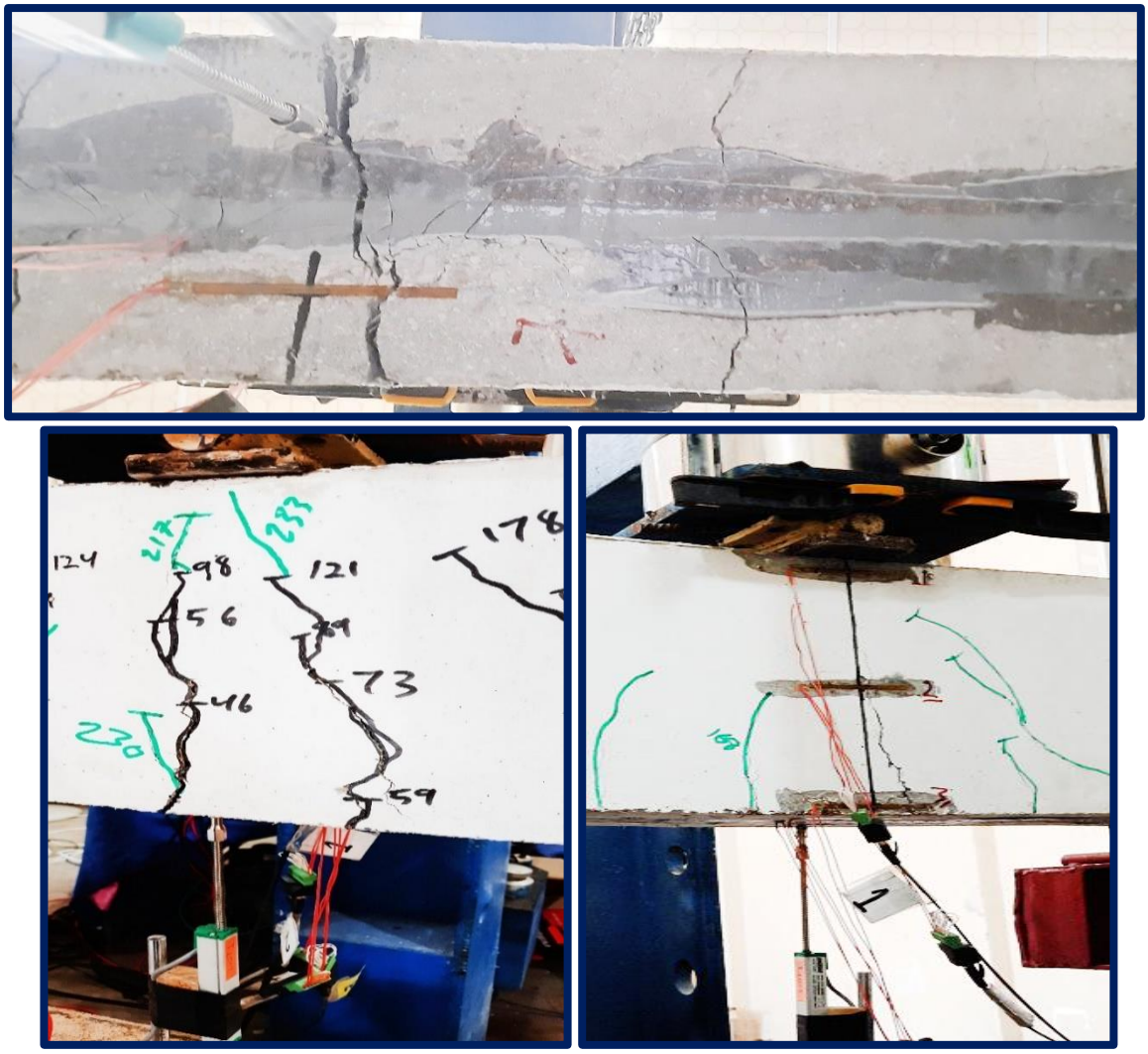

Plate (4-12): Crack pattern after failure for beam FGb.

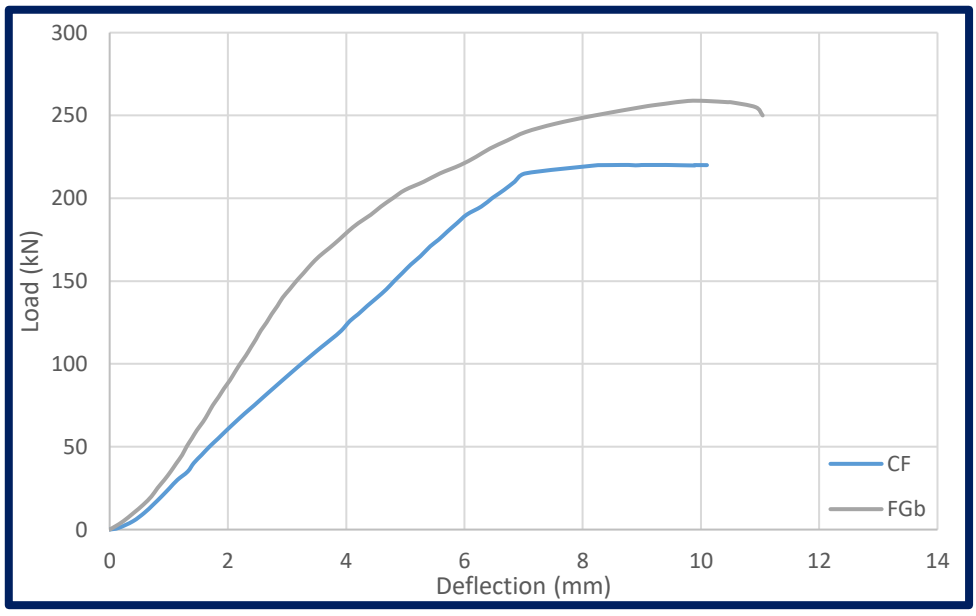

Figure(4-12): Load-Deflection curve for specimen FGb.

- ***Strengthened Beam Specimen (NSM-Steel Reinforce bar (FSb))***

The first flexural cracks appeared in this beam at a load of (36kN). When the load reaches (53kN), the first crack appears. The beam specimen **NSM-Steel Reinforce bar** is strengthened with steel reinforcement bar of length (1200mm) and diameter (6mm), which are installed on the tension bottom face of the reinforced concrete beam. The crack pattern of this beam specimen is shown in Plate (4-13). The beam finally collapses as typical flexural failure when it achieves an ultimate load of (223.256kN), which is 11.23% greater than the control beam (CF).

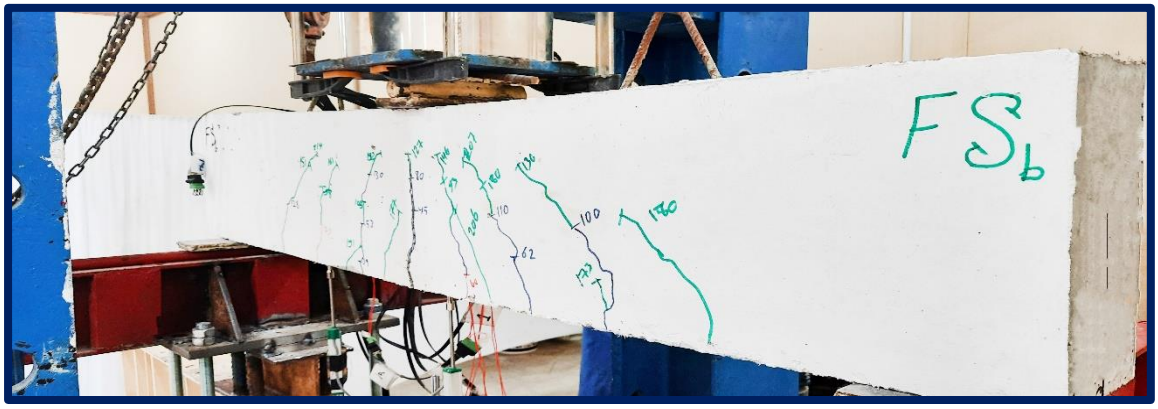

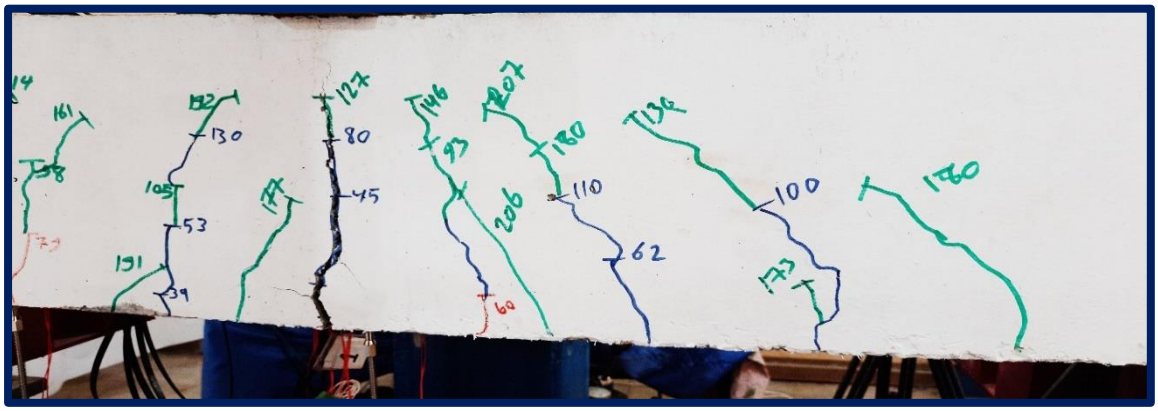

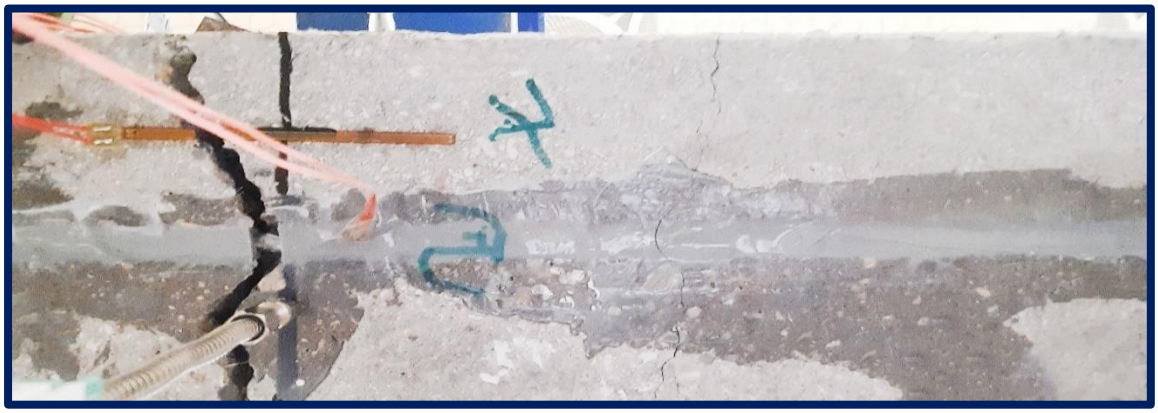

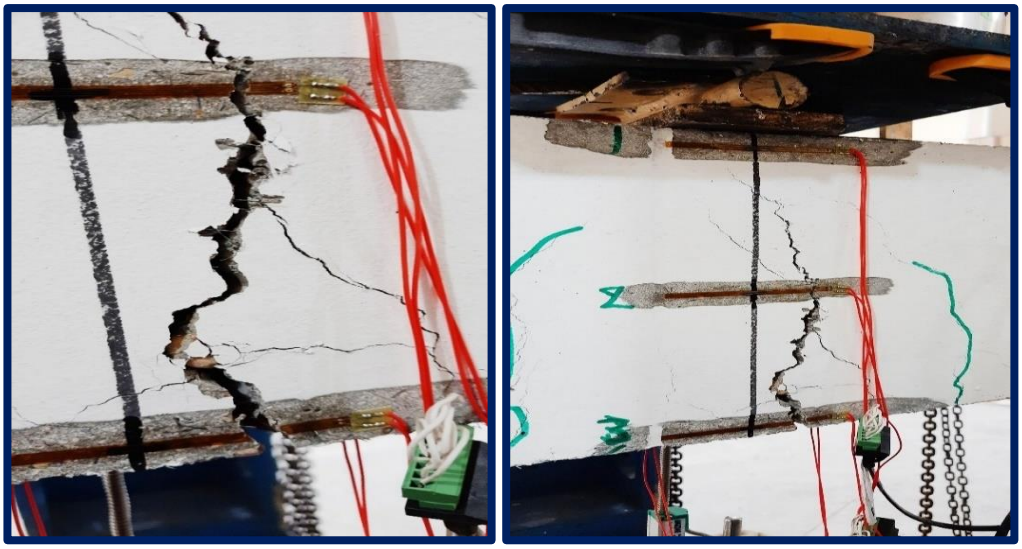

Plate (4-13): Crack pattern after failure for beam FSb.

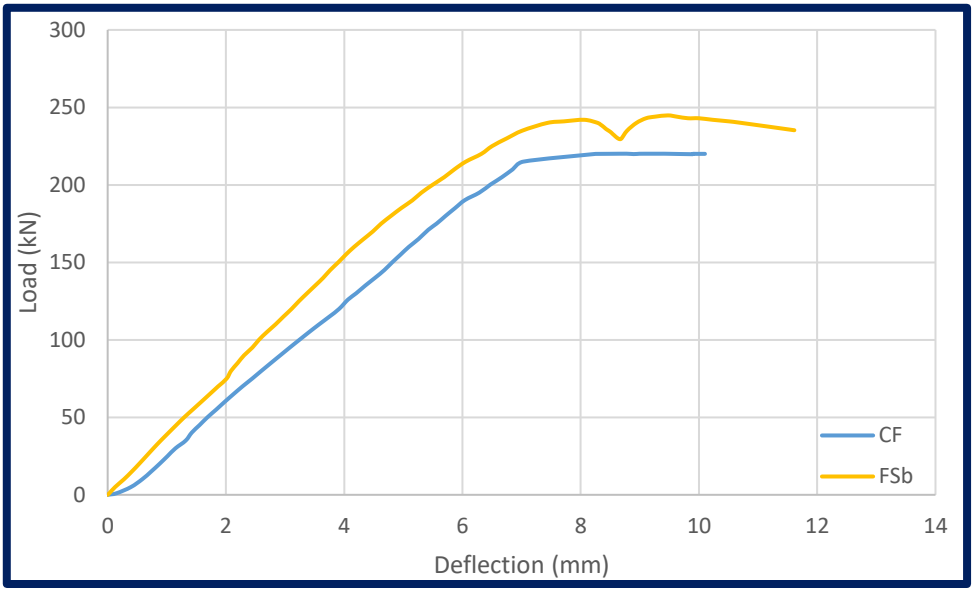

Figure(4-13): Load-Deflection curve for specimen FSb.

- ***Strengthened Beam Specimen (NSM-CFRP-EBR-CFRP Sheet (FCbT))***

The two types of strengthening are used in beam specimen **NSM-CFRP** is strengthened with one CFRP bar of length (1200mm) and a diameter (6mm) and an **EBR-CFRP** sheet of length (1200mm) and width (150mm). The first crack is observed at a load of (42kN). The pattern of cracks as shown below in Plate (4-14). The first crack appears when a load is higher than that of the strengthened and unstrengthened beam specimens FCb, and CF. The beam failed due to splitting in CFRP at load (304.588kN) which is greater than the

control beam (CF) by 38.37%. Cover delamination or FRP debonding can occur if the force in the FRP is not supplied by the substrate. This is referred to as debonding regardless of where the failure plane propagates throughout the FRP-adhesive-substrate region.

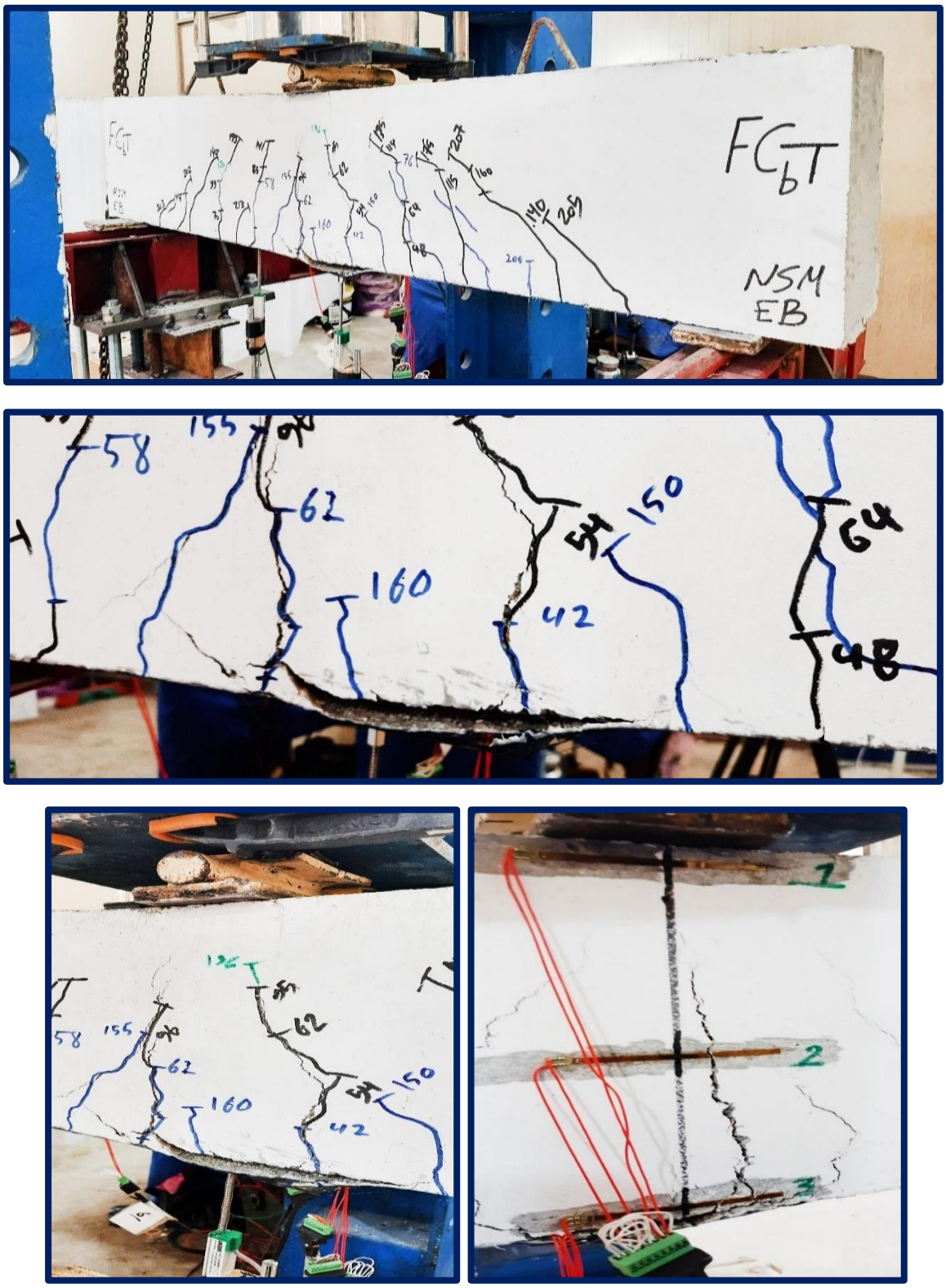

Plate (4-14): Crack pattern after failure for beam FCbT.

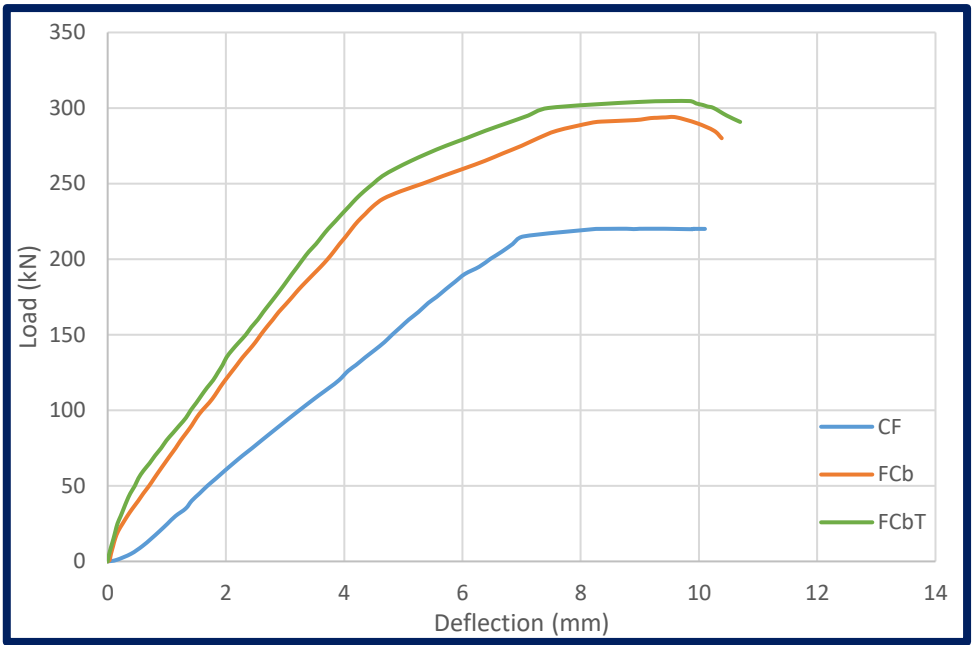

Figure (4-14): Load-Deflection curve for specimen FCbT.

- ***Strengthened Beam Specimen (NSM-GFRP-EBR-CFRP Sheet (FGbT))***

The technique is that two types of strengthening are used. The beam specimen **NSM-GFRP** is strengthened with one GFRP bar of length (1200mm) and a diameter of (6 mm), and an **EBR-CFRP** sheet that is length (1200mm) and width (150mm). The first cracking was observed at a load of (20kN). As the load was increased, flexural cracks increased. Further flexure-shear cracks appeared, and diagonal shear cracks appeared at a load of about (130kN). The failure mode in this beam is changed from shear failure to flexural failure due to the effect at the ultimate load (335kN). The cracks are shown below in Plate (4-15). The first crack occurred at a lower load than that of the strengthened beam and unstrengthened beam specimens NGb and NC, respectively. As the load is increased, new cracks form along the beam specimen. The beam failed at load (269.159kN), which is greater than the control beam (CF) by 40.55%.

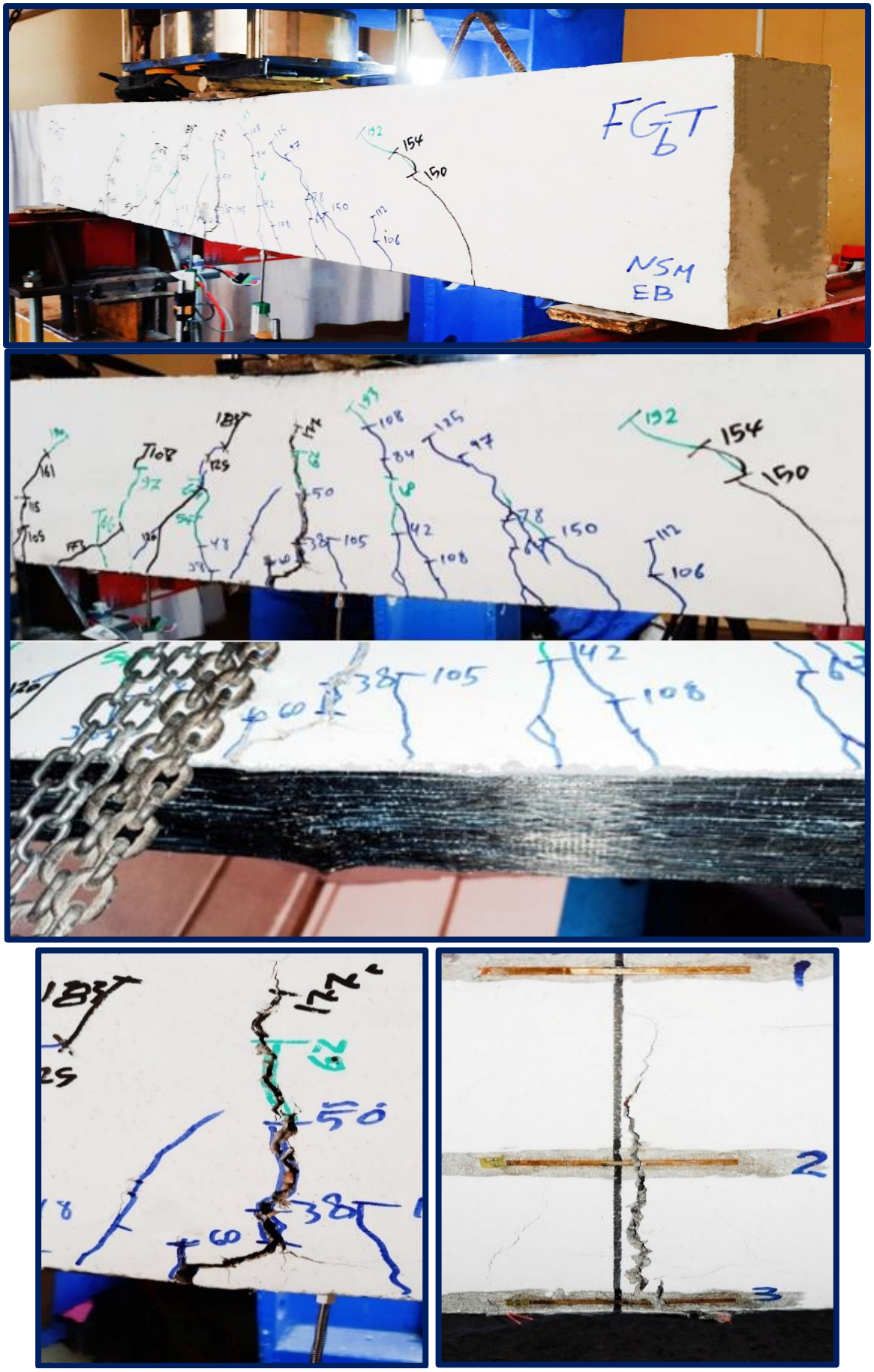

Plate (4-15): Crack pattern after failure for beam FGbT.

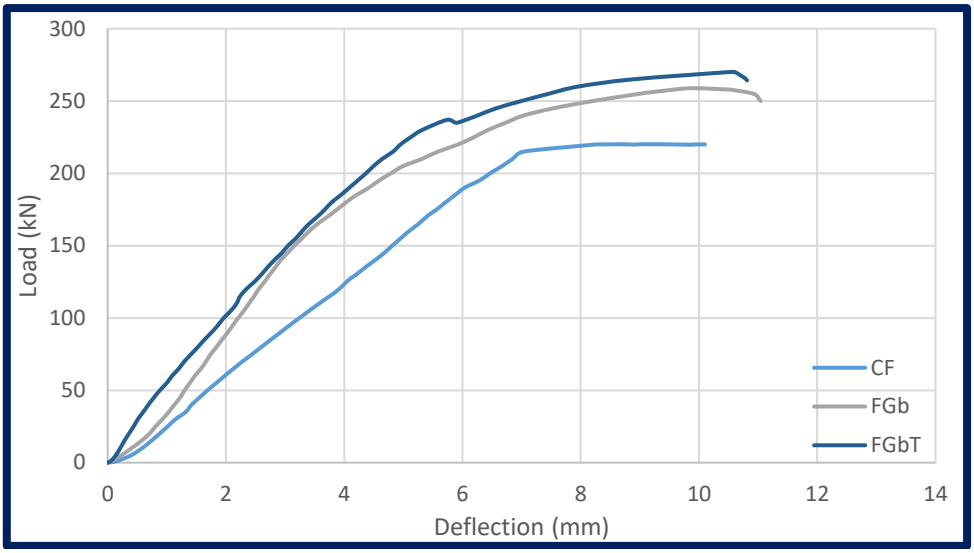

Figure (4-15): Load-Deflection curve for specimen FGbT.

- ***Strengthened Beam Specimen (NSM-Steel Reinforce bar -EBR-CFRP Sheet (FSbT))***

To study the effect of technique on two types of strengthening that are used, the beam specimen **NSM-SFRP** is strengthened with one steel reinforcement bar of length (1200mm) and a diameter of (6 mm) and an **EBR-CFRP** sheet of length (1200mm) and width (150mm). The first crack is observed at a load of (35kN). The cracks shown below in Plate (4-16). The first cracks occurred at a load lower than that of the strengthened beam FSb but higher than that of the unstrengthened beam specimen CF. As the load is increased, new cracks form along the beam specimen. The beam failed at load (265.8379kN), which is greater than the control beam (CF) by 20.77%.

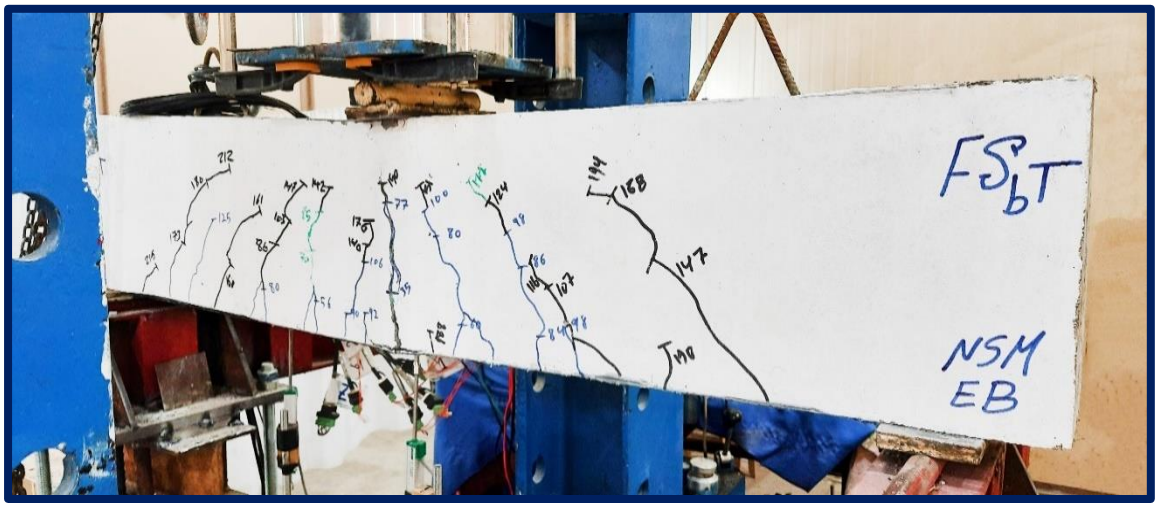

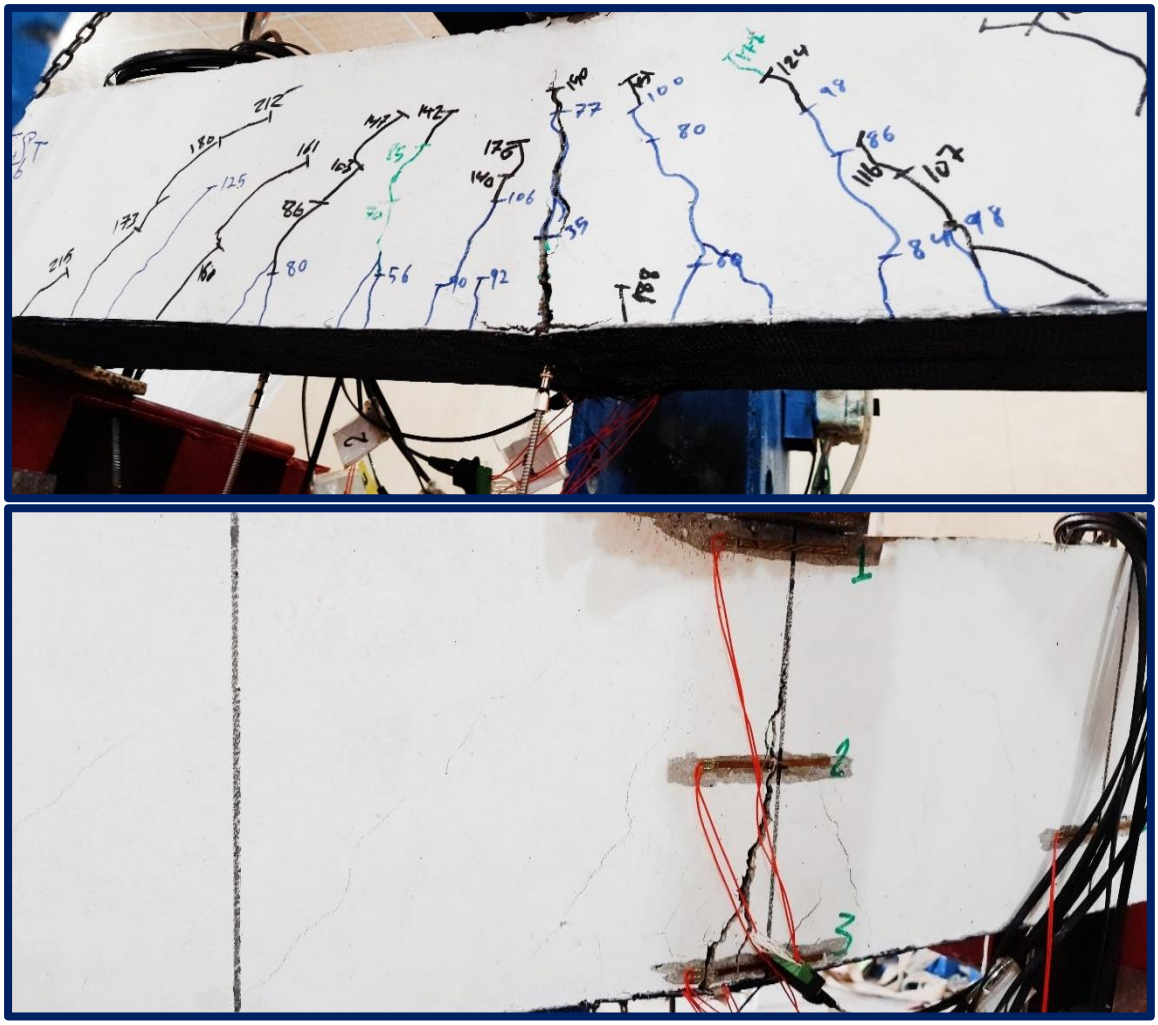

Plate (4-16): Crack pattern after failure for beam FSbT.

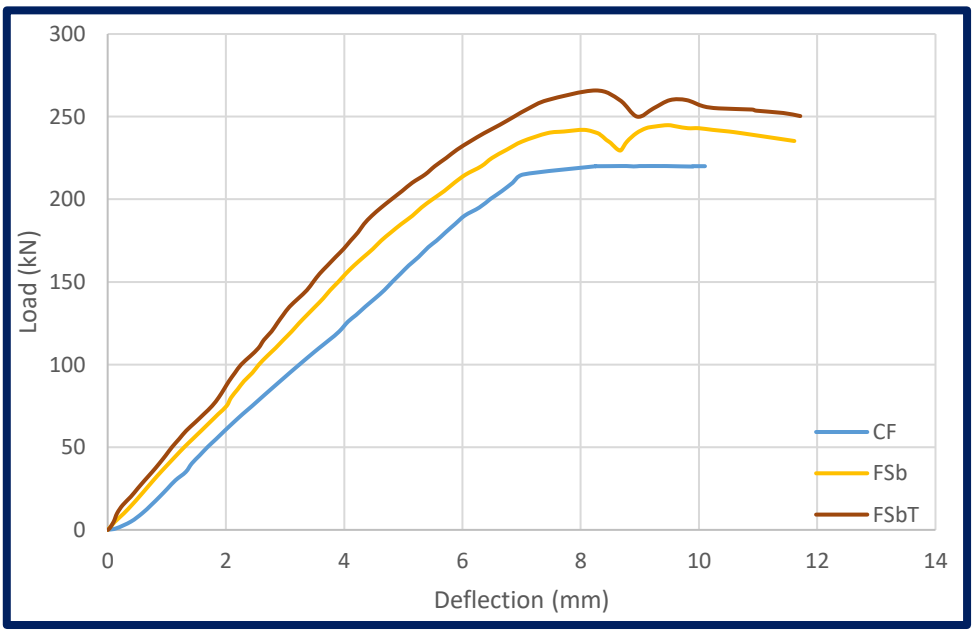

Figure(4-16): Load-Deflection curve for specimen FSbT.

4.2.1.3 Crack Width

Crack Width The cracks in the present study are measured with a crack-meter. The first crack's creation is observed throughout the test to record the crack's width as the load increases until the beam models are near failure. Plate (4-17) crack meter instrument. Figure (4-17), and Figure (4-18) demonstrate the relationship between load and crack width for the two groups.

Plate (4-17): Crack meter.

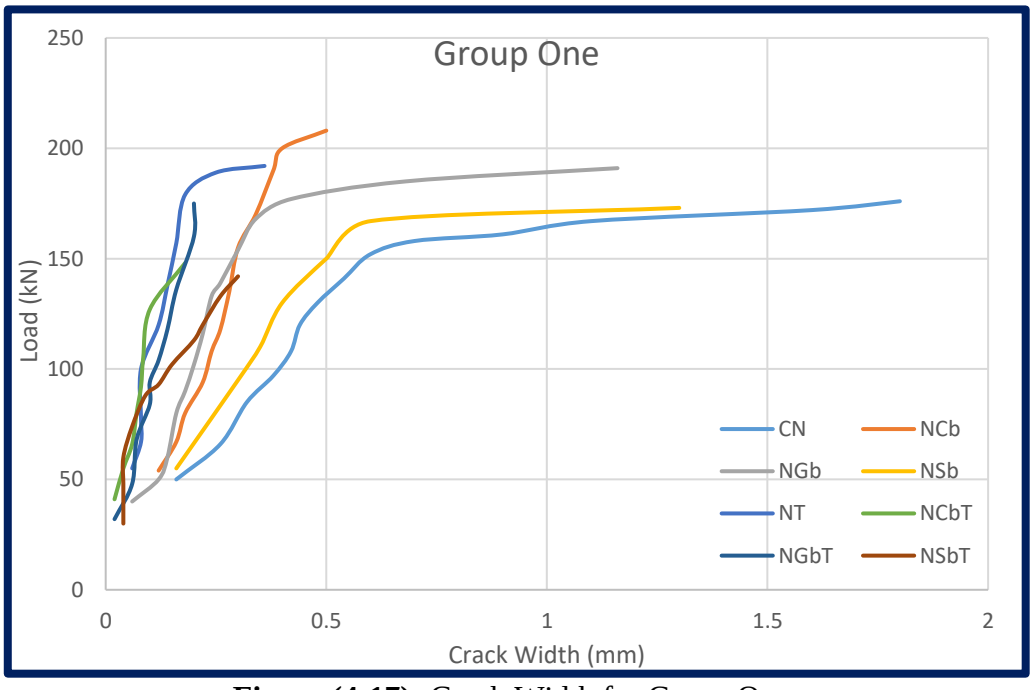

Figure (4-17): Crack Width for Group One.

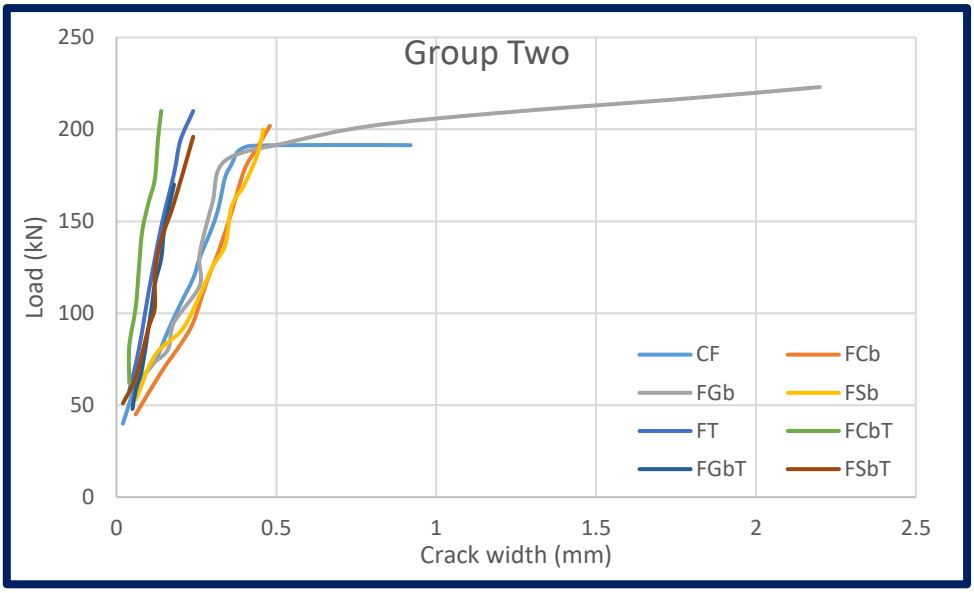

Figure (4-18): Crack Width for Group Two.

4.3 Instrumentation

The instrumentation on the beam specimens is selected to obtain the most data on local strains, deflections, and crack widths possible.

4.3.1 Concrete strains on the mid-span section surface

All specimens were instrumented with six concrete strain gauges bonded to the surface of the mid-span section. These strain gauges were positioned along the beam's height. (Three on the side face, one 10 mm from the top, one at midface 750 mm from the top, one 1490 mm from the top, one on the quarter beam 1125mm, one the bottom surface and one on the NSM bar), to quantify the evolution of the concrete strain with load. The concrete strain gauges that are utilized in the experiment with a resistance of 120Ω are made in China.

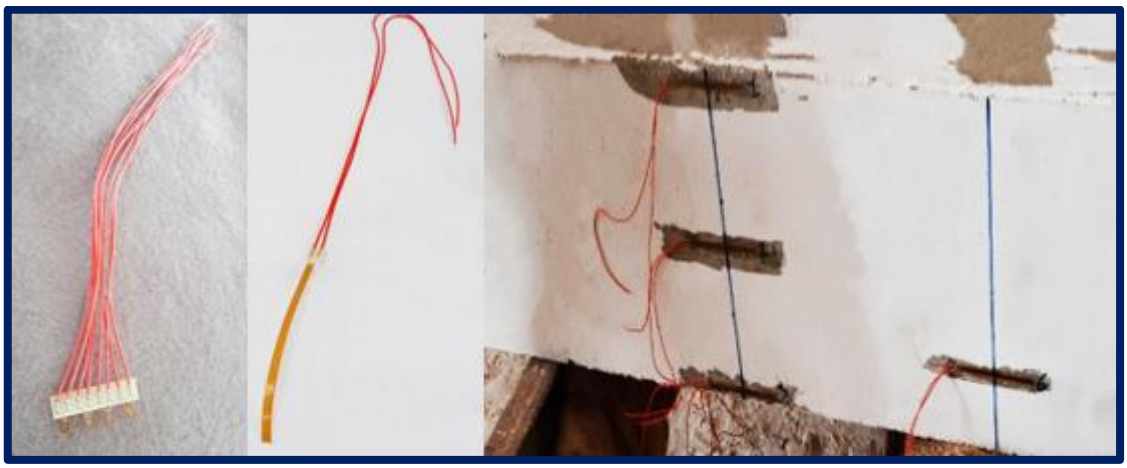

Figure(4-19): Strain gauge type, arrangement.

4.3.2 Strain of concrete

Three strain gages are used to measure the distribution of concrete strains in the midspan section of the tested beam specimens over the depth of each beam. In general, the strain distribution in the compression zone remained essentially linear throughout the loading range. The strain distribution in the tension zone is nearly linear at low loads and becomes nonlinear at higher loads due to cracking. Also, the presence of CFRP composites at the bottom tension zone surface reduced concrete strains, which was reflected in the strains in the bottom tension steel bar reinforcement (i.e., reducing the tension steel bar strains). This meant that the tension strength went up, and CFRP composites took on some of the tension stresses.

4.4 Effect of NSM bar type

The influence of NSM reinforcement on beam performance is represented in Figure(4-20). Using CFRP bars instead of GFRP steel bars resulted in improved performance. Load capacity of NCb beam 1.33 % ,1.17% and 1.11% more than NC respectively. This may be due to the higher tensile strength of CFRP bar and GFRP bar compared to steel bar. So, NSM CFRP bar is recommended when the ultimate strength of a reinforced concrete building needs to be increased.

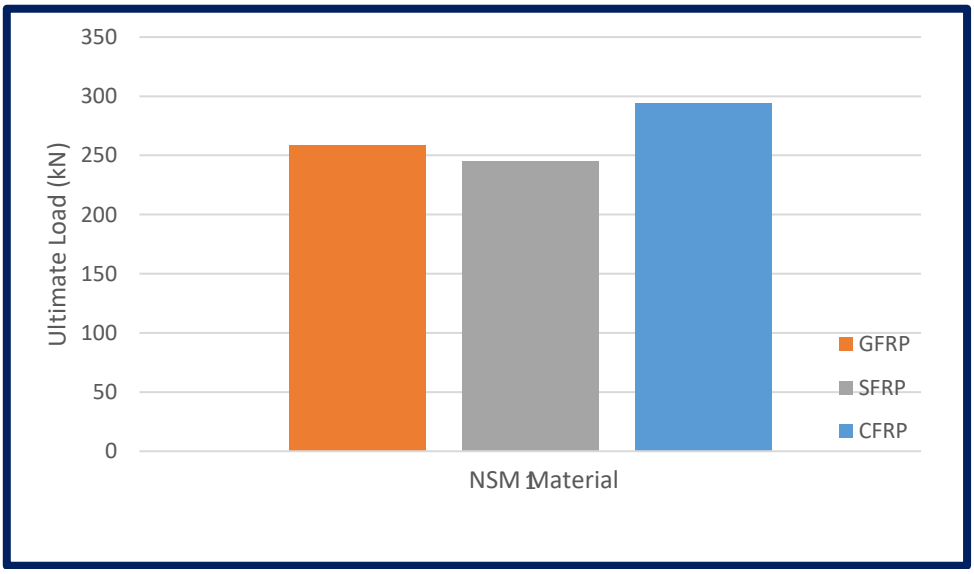

Figure(4-20): Effect of NSM bar type.

4.5 Load-Deflection Curves

To measure the deflection, three strain gages were used: one at the mid-span point and two LVDTs. In general, the load versus midspan deflection response can be separated into three stages. The load and the midspan deflection had an almost linear relationship in the first stage. The section was uncracked at this point, and both the concrete and steel, as well as the CFRP, behaved essentially elastically.

The second stage demonstrates the behavior of the composite section after initial cracking, when the stiffness of the beam is lowered, as seen by the decreasing slope of the load against the midspan deflection curve. This stage has come to an end when the main steel reinforcement begins to demonstrate inelastic behavior.

The third stage was distinguished by a decrease in the curve's slope after the tension steel reinforcement had reached the stage of strain hardening. For these models, the experimental load versus mid span deflection is shown in Figure(4-21) and Figure (4-22). Most of the time, the deflections of the CFRP-enhanced beams were less than those of the control beam.

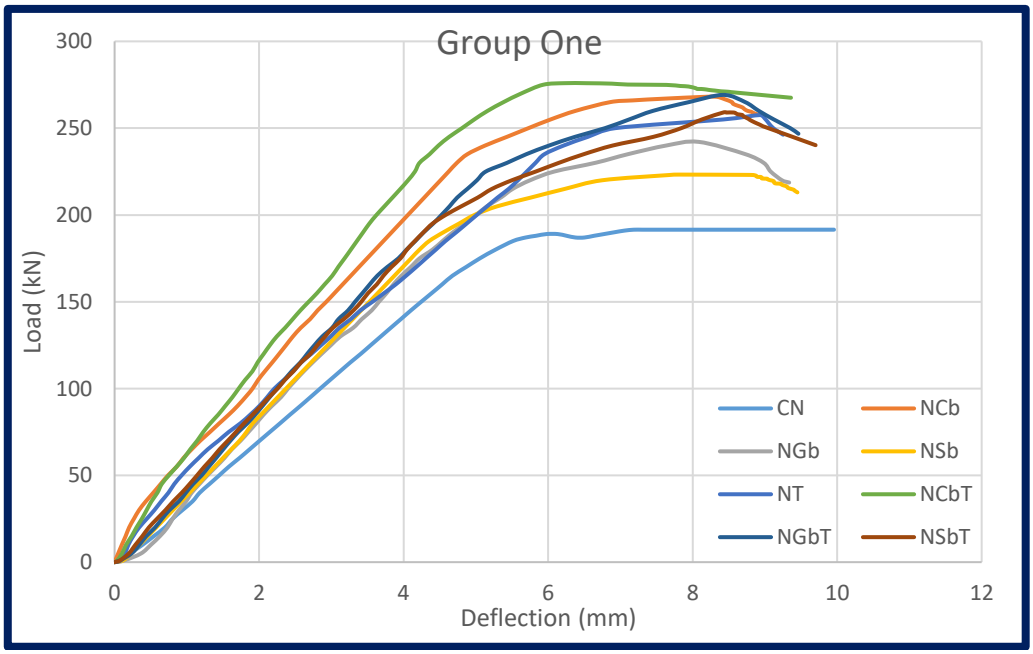

Figure(4-21): Load versus Deflection for all Beams of Group One.

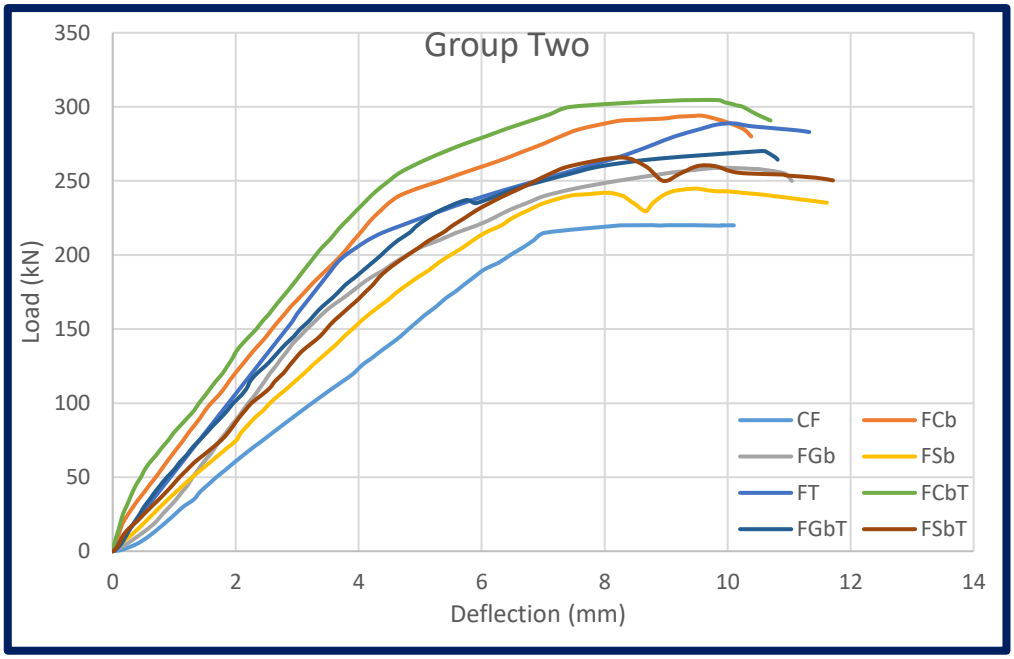

Figure(4-22): Load versus Deflection for all Beams of Group Two.

4.6 Ultimate Load and Failure Modes

All the RC beam specimens, both unstrengthened and strengthened, are tested to failure. Table (4-1) shows the documented ultimate loads and failure modes for these beam specimens.

Table (4-1): Ultimate load capacity and failure mode for tested beams.

Specimen	Ultimate load, kN	Increase in ultimate load, %	First Cracking Load (kN)	Failure mode
CN	**191.5051**	**N\A**	**30**	**Typical flexural failure**
NSM-NCb	**268.0787**	**39.98**	**45**	**Concrete cover separation**
NSM-NGb	**242.1188**	**26.43**	**28**	**Depending between epoxy and concrete**
NSM-NSb	**223.2563**	**16.58**	**32**	**Yielding of bar**
EBR-NT	**257.5615**	**34.49**	**38**	**Debonding**
NSM-NCb-EBR-NT	**275.9237**	**44.08**	**39**	**Rupture of CFRP sheet**
NSN-NGb-EBR-NT	**269.1589**	**40.55**	**30**	**Rupture of CFRP sheet**
NSN-NSb-EBR-NT	**259.1761**	**35.34**	**32**	**Rupture of CFRP sheet**
CF	**220.1198**	**N/A**	**35**	**Typical flexural failure**
NSM-FCb	**293.8543**	**33.50**	**39**	**Spalling of concrete cover**
NSM-FGb	**258.76**	**17.55**	**38**	**Concrete cover separation**
NSM-FSb	**244.8435**	**11.23**	**36**	**Typical flexural failure**
EBR-FT	**288.8442**	**31.22**	**36**	**Debonding**
NSM-FCb-EBR-FT	**304.588**	**38.37**	**42**	**Rupture of CFRP sheet**
NSM-FGb-EBR-FT	**270.7061**	**22.98**	**38**	**Rupture of CFRP sheet**
NSM-FSb-EBR-FT	**265.8379**	**20.77**	**35**	**Rupture of CFRP sheet**

For ***Group One***, the beam specimen ***NSM-CFRP***, which is strengthened with one CFRP bar at length (1200mm), the increase in ultimate load capacity was about 39.98% over the control beam ***CN***. Whereas the beam ***NSM-GFRP*** is strengthened with one GFRP bar at length (1200mm), it showed an increase of 26.43% in ultimate load capacity when compared with the control beam ***CN***. The beam specimen ***NSM-SFRP***, which was strengthened with one steel reinforcement bar at length (1200mm), the increase in ultimate load capacity was about 16.58% over the control beam ***CN***. The experimental results show that reinforced concrete beams strengthened with NSM-CFRP perform better than those strengthened with GFRP and SFRP, respectively. The beam specimen ***EBR-NT***, which was strengthened with CFRP sheet at length (1200mm) width (150mm), the increase in ultimate load capacity was about **34.49** percent when compared with the corresponding control beam specimen ***CN***. The experimental results show that reinforced concrete beams reinforced with NSM-CFRP are better than reinforced concrete beams reinforced with EBR, GFRP, and SFRP, respectively. This is due to the bond between the fiber and concrete in the NSM method compared to the EBR, GFRP, and SFRP.

For ***Group has two strengthening (NSM, EBR)***, the beam specimen ***NSM*-NCb-EBR-NT**, ***NSM*-NGb-EBR-NT**, and ***NSM*-NSb-EBR-NT**, which are strengthened with one bar at length (1200mm), with a (6mm) diameter and a CFRP sheet length (1200mm) and a width of (150mm). The effect of type NSM is observed in the results where the increase in ultimate load capacity is about 44.08%,40.55%, and 35.34%, respectively, over the control beam ***CN***.

For ***Group Two***, the beam specimen ***NSM-CFRP***, which was strengthened with one CFRP bar at length (1200mm), the increase in ultimate load capacity was about 33.50% over the control beam ***CF***. Whereas the beam ***NSM-GFRP***, which was strengthened with one GFRP bar at length (1200mm) to show an increase of 17.55% in ultimate load capacity when compared with the control beam ***CF***, the beam specimen ***NSM-Steel Reinforce bar***, which was

strengthened with one steel reinforcement bar at length (1200mm), the increase in ultimate load capacity was about 11.23% over the control beam ***CF***. The experimental results show that reinforced concrete beams strengthened with NSM-CFRP perform better than those strengthened with GFRP and SFRP, respectively.

The beam specimen ***EBR-FT***, which was strengthened with CFRP sheet at length (1200mm) and width (150mm), has an increase in ultimate load capacity of about **31.22** percent when compared with the corresponding control beam specimen ***CF***. The experimental results show that reinforced concrete beams reinforced with NSM-CFRP are better than reinforced concrete beams reinforced with EBR, GFRP, and Steel Reinforce bar, respectively. This is due to the bond between the fiber and concrete in the NSM method compared to the EBR, GFRP, and Steel Reinforce bar.

Other beams have two strengthenings (NSM, EBR), the beam specimen ***NSM*-NCb-EBR-FT**, ***NSM*-NGb-EBR-FT,** and ***NSM*-NSb-EBR-FT**, which are strengthened with one bar at length (1200mm), with a (9mm) diameter and a CFRP sheet length (1200mm) width (150mm). The effect of type NSM observed in the result is that the increase in the ultimate load capacity is about 38.37%, 22.98%, and 20.77%, respectively, over the control beam ***CF***.

The experimental results above show that the reinforced concrete beams strengthened with the NSM method are better than the reinforced concrete beams strengthened with the EBR method. This is due to the bond between the fiber and concrete in the NSM method compared with the EBR.

4.7 Strain of concrete

The distribution of concrete strains at midspan section of the tested beam specimens were measured using three strain gages over the depth of each beam. The concrete strain distribution over the depth of all the tested beams at different load levels is shown in Figure (4-23) and Figure (4-24). Generally,

the strain distribution remained approximately linear in compression zone throughout loading range. While in the tension zone, the strain distribution is approximately linear at low loads and becomes nonlinear at higher loads due to cracking. The same result can be seen in the second test group. In addition to that, the presence of CFRP composites at the bottom tension zone surface reduced the concrete strains, and this reduction was reflected to strains in the bottom tension steel bar reinforcement (i.e., reducing the tension steel bar strains), and that means increasing the tension strength and some tensile stresses were carried by CFRP composites.

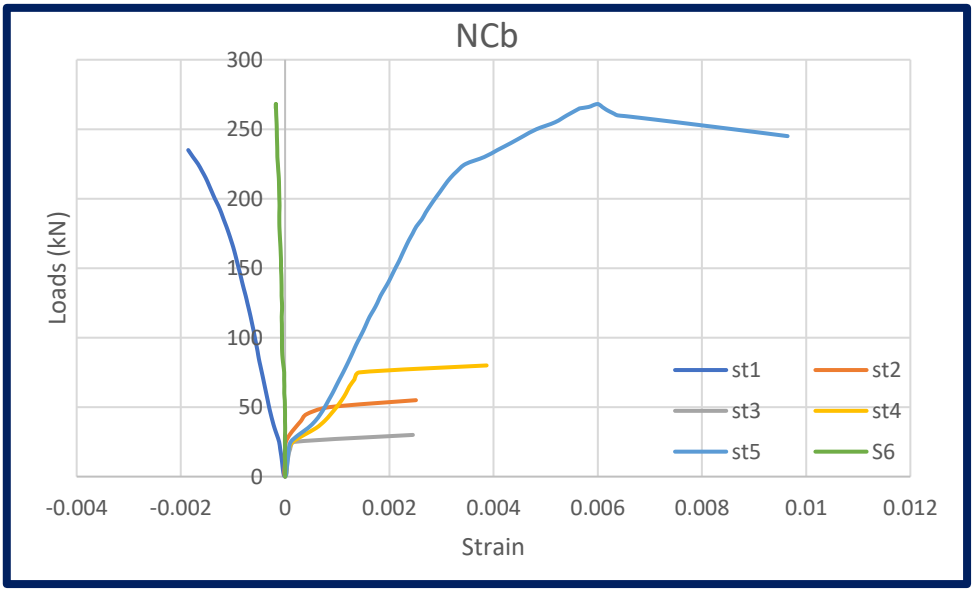

Figure (4-23): strain gage at beam NCb.

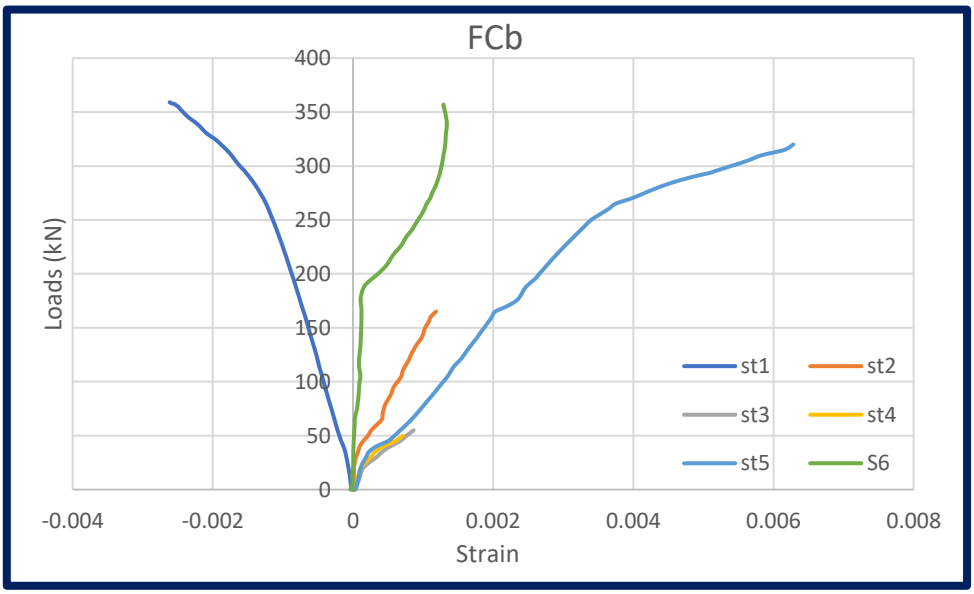

Figure (4-24): Strain gage at beam FCb.

4.8 Ductility Index

Ductility of RC elements is defined as its ability to resist inelastic deformation without any decreasing in its load-carrying capacity up to failure. In other words, the ductility can be considered as the ratio between the deformations at ultimate stage to yield deformation. The deformation can be strains, curvatures, or deflections. In this study, ductility index is taken as the ratio of the deflection at ultimate load to the yield deflection of the equivalent elastoplastic system as presented in Figure (4-25), the notional yield displacement (Δy) is defined as the intersection of the two straight tangent lines associated with the load-displacement curves at the elastic and post-elastic stages respectively [57].

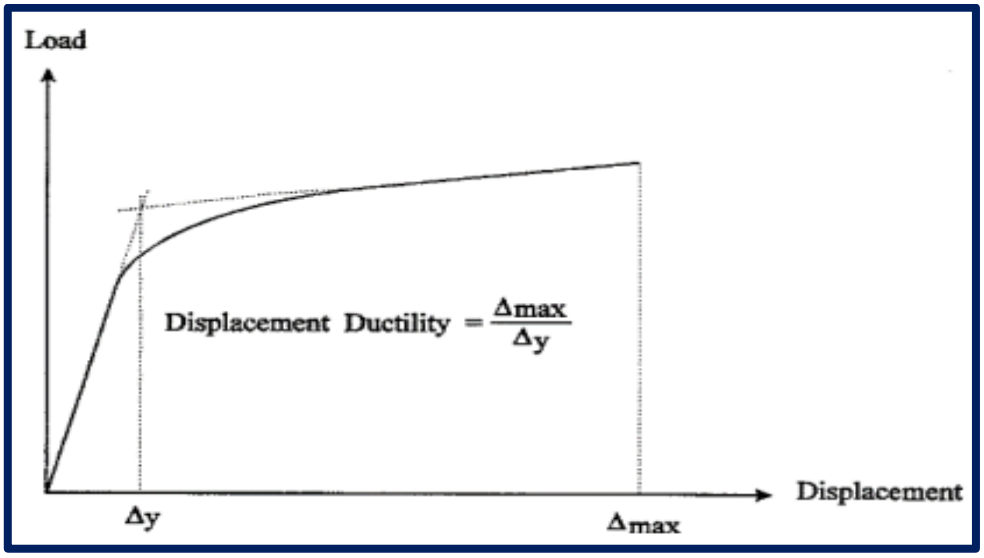

Figure(4-25): Definition of displacement ductility [57].

The results of ductility index for beams of this group are presented in Table (4-2). To clarify the calculation procedures of the ductility results, the determination of the displacement ductility by the mentioned approach adopted for reference beam are depicted in Figure (4-26).

In general, all tested beams have low ductility due to the double strengthened also note the beams strengthen with NSM in carbon bar is higher than other. From Table (4-2), it can be noticed that the presence of group two decrease in the ductility when compared with the group one.

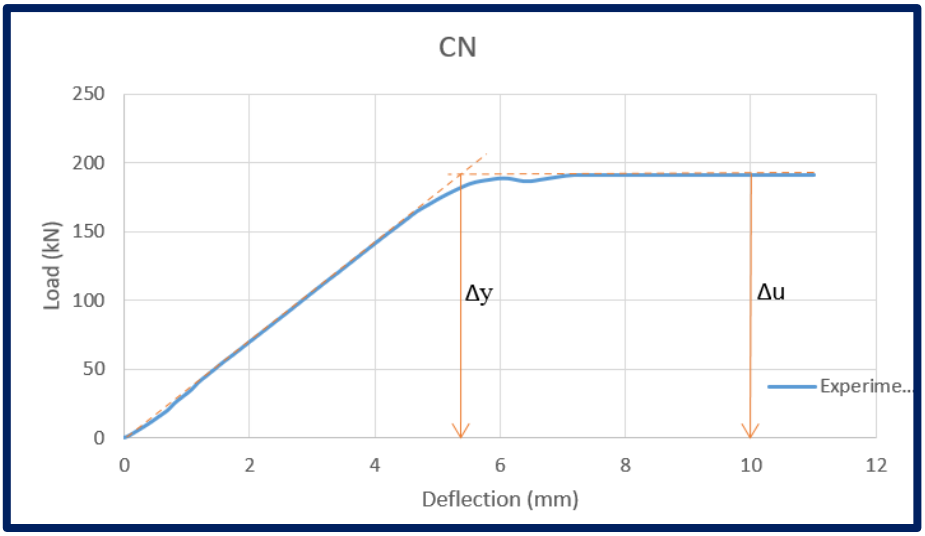

Figure (4-26): Typical diagram for determining the ductility index of RC beams (CN).

Table(4-2): Ductility index for beams.

Specimen	Yield deflection (mm)Δy	Ultimate deflection (mm)Δu	Ductility index=Δu/Δy	Reduction in ductility (%)
CN	**3.122**	**10.089**	**3.231**	------
NSM-NCb	**3.156**	**6.857**	**2.173**	**48.725**
NSM-NGb	**3.421**	**8.082**	**2.362**	**36.774**
NSM-NSb	**3.065**	**7.81**	**2.548**	**26.824**
EBR-NT	**3.569**	**8.930**	**2.502**	**29.149**
NSM-NCb-EBR-NT	**2.907**	**6.226**	**2.142**	**50.853**
NSN-NGb-EBR-NT	**3.531**	**9.327**	**2.641**	**22.328**
NSN-NSb-EBR-NT	**3.414**	**8.435**	**2.470**	**30.796**
CF	**4.201**	**8.774**	**2.089**	------
NSM-FCb	**3.009**	**9.435**	**3.135**	**33.389**
NSM-FGb	**3.156**	**9.780**	**3.098**	**32.597**
NSM-FSb	**3.763**	**9.475**	**2.518**	**17.061**
EBR-FT	**3.183**	**10.086**	**3.169**	**34.097**
NSM-FCb-EBR-FT	**2.927**	**9.841**	**3.362**	**37.883**
NSM-FGb-EBR-FT	**3.288**	**10.571**	**3.215**	**35.05**
NSM-FSb-EBR-FT	**3.585**	**8.250**	**2.301**	**9.255**

4.9 Stiffness Criteria

Stiffness is defined as load required for producing unit deformation in the member. the stiffness criteria of any member can be determined as the slope of the secant which drawn in the load deflection curve at 0.75 of the ultimate loads. The stiffness criteria of the beams are given in Table (4-3).

$$\boldsymbol{Stiffness\ (K) = 0.75 * Pu/075 * \delta u}$$

Table (4-3): Stiffness criteria of the tested beams.

Specimen	Ultimate load, kN	0.75 Pu kN	Deflection at 0.75 Pu. (mm)	Stiffness, K (kN/mm)
CN	**191.5051**	**143.6288**	**4.197039**	**34.22146**
NSM-NCb	**268.0787**	**201.059**	**4.12575**	**48.73272**
NSM-NGb	**242.1188**	**181.5891**	**4.493434**	**40.4121**
NSM-NSb	**223.2563**	**167.4422**	**4.038057**	**41.46603**
EBR-NT	**257.5615**	**193.1711**	**4.924835**	**39.22387**
NSM-NCb-EBR-NT	**275.9237**	**206.9428**	**3.802917**	**54.41686**
NSN-NGb-EBR-NT	**269.1589**	**201.8692**	**4.629293**	**43.60692**
NSN-NSb-EBR-NT	**259.1761**	**194.3821**	**4.537825**	**42.83596**
CF	**220.1198**	**165.0899**	**5.260829**	**31.38097**
NSM-FCb	**29.8543**	**220.3907**	**4.154839**	**53.04434**
NSM-FGb	**258.76**	**194.07**	**4.732164**	**41.01084**
NSM-FSb	**244.8435**	**183.6326**	**5.053964**	**36.33437**
EBR-FT	**288.8442**	**216.6332**	**4.510269**	**48.0311**
NSM-FCb-EBR-FT	**304.588**	**228.441**	**4.107272**	**55.61867**
NSM-FGb-EBR-FT	**270.7061**	**203.0296**	**4.629042**	**43.85996**
NSM-FSb-EBR-FT	**265.8379**	**199.3784**	**4.85029**	**41.10649**

All the stiffnesses of the tested beams with NSM bar increase about (15% to 45%) compared to the reference specimen beams. While in group two the stiffnesses of the tested beams with NSM bar increase about (15% to 70%). For beams with CFRP sheet (14%) in group one noticed increased with fiber up to (50%). The stiffness of the beams with two strengthened (25% to 60%) in group one while (30% to77%) in group two.

Chapter Five
NUMERICAL APPLICATION

5.1 Introduction

Although classical empirical methodologies are still adequate for conventional reinforced concrete member design, the widespread availability of computers and the development of the finite element method have enabled more complex systems to be analyzed in a more realistic manner.

The finite element analysis approach is widely used to solve a wide range of engineering problems. The present finite element analysis method may be traced all the way back to the early 1900s. The early 1900s were the birthplace of the contemporary finite element analysis method.

As part of the research, there are sixteen FE models in all, and the numerical solutions are compared to the experimental results. ANSYS 19.2, a finite element (FE) code, is used to construct the FE models. The models have the same geometry, dimensions, and boundary conditions as the tested simply supported beam specimen. The objective of this chapter is to discuss the possibilities of finding the best method of near-surface mounted reinforced concrete model in practical use. It gives the results of some analyses done with the ANSYS general-purpose finite element code and its reinforced concrete models.

This chapter compares the experimental data with the results of the ANSYS finite element analyses for the sixteen tested beams. The following comparisons are made load-strain diagrams at selected locations; load-deflection plots at midspan; first cracking loads; loads at failure; and crack patterns at failure. For the finite element models, the development of crack

patterns for each beam and summaries of the maximum bond stresses occurring in the FRP rebars are also discussed. The load tests for the tested beams are conduct at the same locations as the data from the finite element analyses.

5.2 Finite Element Material Modeling

5.2.1 Real Constants

The two forms of concrete (NC and CF) are represented in the ANSYS program using the solid element (SOLID65). The SOLID65 element is composed of eight nodes. Each of these nodes has three translational degrees of freedom. This node has the ability to crack under tension and crush under compression [58]. This type of element's geometry, node position, and coordinate system were presented in Figure (5-1). Three-dimensional brick elements (SOLID185) are also selected to represent the model steel plates used at loading and supporting points. This component is utilized to spread the load and avoid stress concentration issues. Figure (5-2) shows a schematic of the element.

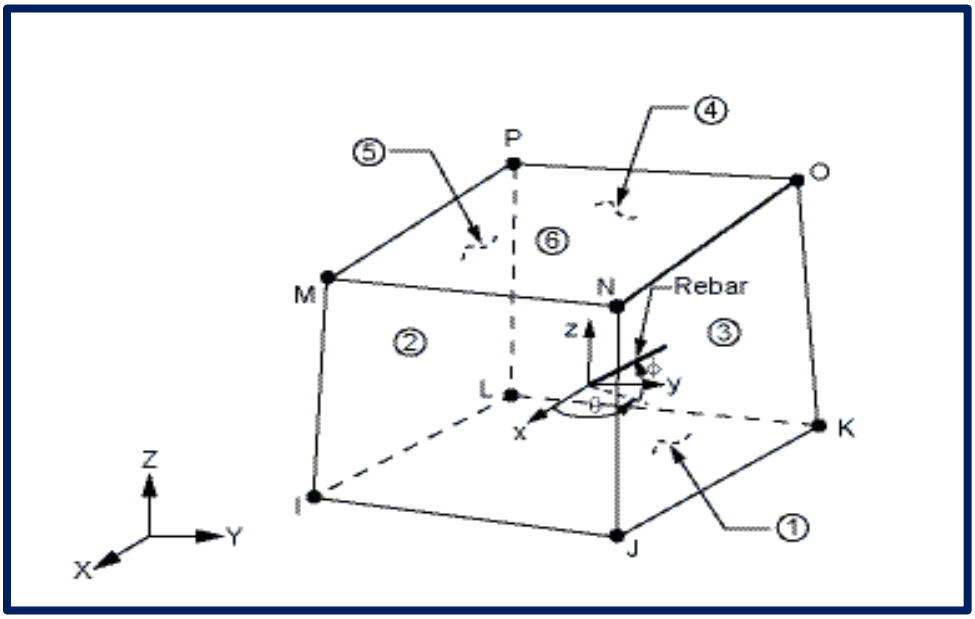

Figure(5-1): Geometry of Element SOLID65[58].

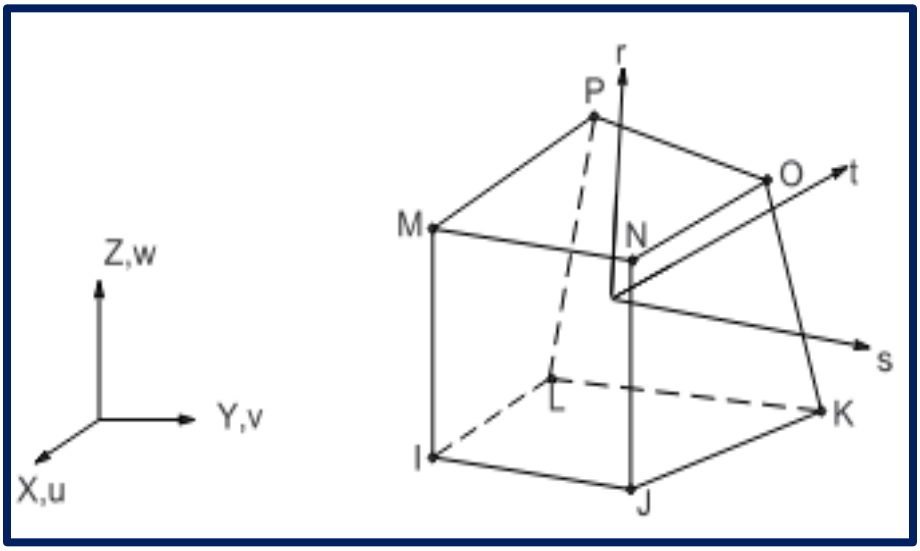

Figure (5-2): Geometry of Element SOLID185 [58].

Steel reinforcement bars were modelled using a three-dimensional bar element (LINK180) with three degrees of freedom. The geometry and location of nodes for this type of element are shown in Figure (5-3).

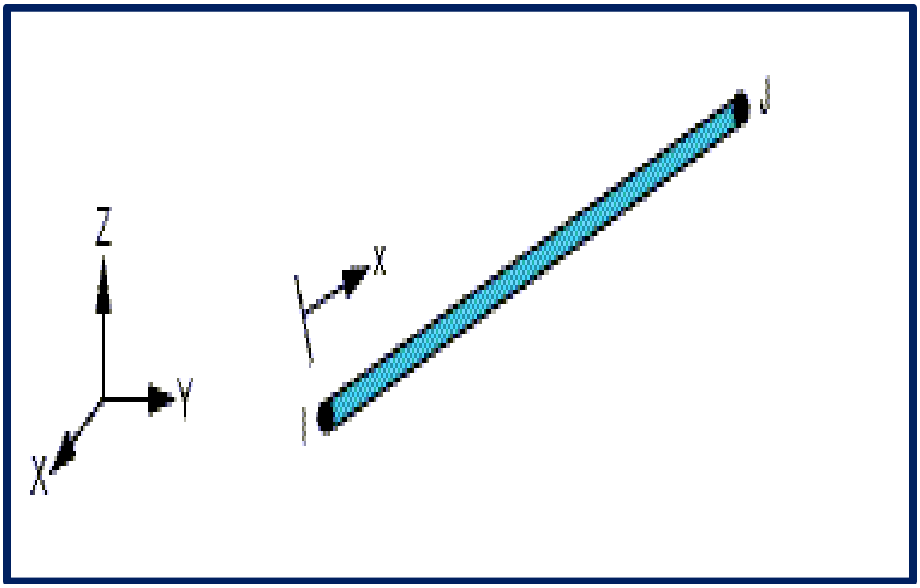

Figure (5-3): Geometry of Element LINK 180[58].

The interface element was utilized to depict the relative motion and associated deformation caused by the discontinuity in the structural element between precast concrete and cast-in-place concrete. Table (5-1) summarizes the major types of elements applied in modeling reinforced concrete girders.

Table(5-1): Types of the Elements used in ANSYS.

Type of Material	**Element in ANSYS**
Concrete	Solid 65
Steel Plate	Solid 185
Steel Reinforcement	Link 180
CFRP, GFRP bar	Beam188
EB-CFRP sheet	Shell 181

5.2.2 Concrete

The internal structure of concrete is extremely heterogeneous. It is made up of inert aggregate particles embedded in a cement and water binding paste. Prior to any load application, the presence of bond micro-cracks at interfaces between the cement paste (and mortar) and notably the coarse aggregate might be seen as a cause of concrete structural weakness. Segregation, shrinkage, and thermal motions in the mortar cause many of these micro-cracks. Because of the stiffness differential between the aggregate and the mortar, certain microcracks may form during loading. The steady propagation of these microcracks with increasing loading adds to the concrete's nonlinear behavior[59] . Depending on the nature and magnitude of the produced stresses, concrete can act as a linear or nonlinear material. There have been several experimental studies of concrete's behavior under uniaxial and multiaxial loading conditions. The goals of these studies were to better understand concrete's complicated reaction to various imposed stress situations and to provide the data needed to construct accurate numerical models for nonlinear finite element analysis of concrete structures [13].

5.2.2.1 Uniaxial compressive stress-strain relationship for normal concrete

In this study, numerical expressions are used along with equations to construct the uniaxial compressive stress-strain curve of normal concrete for use in finite element analysis [59][13]:-

$$Ec = \frac{fc}{\varepsilon_{\circ}} \qquad 5\text{-}1$$

$$\varepsilon_{\circ} = \frac{2 * f'c}{Ec} \qquad 5\text{-}2$$

$$fc = \frac{\varepsilon * Ec}{1 + \left(\frac{\varepsilon}{\varepsilon_{\circ}}\right) 2} \qquad 5\text{-}3$$

where:
fc= stress at any strain ε
ε = strain at stress fc
f'c = ultimate compressive strength
$\varepsilon_{\circ}$ = strain at the ultimate compressive strength f'c
Figure (5-4) shows the simplified uniaxial compressive stress-strain relationship employed in this research.

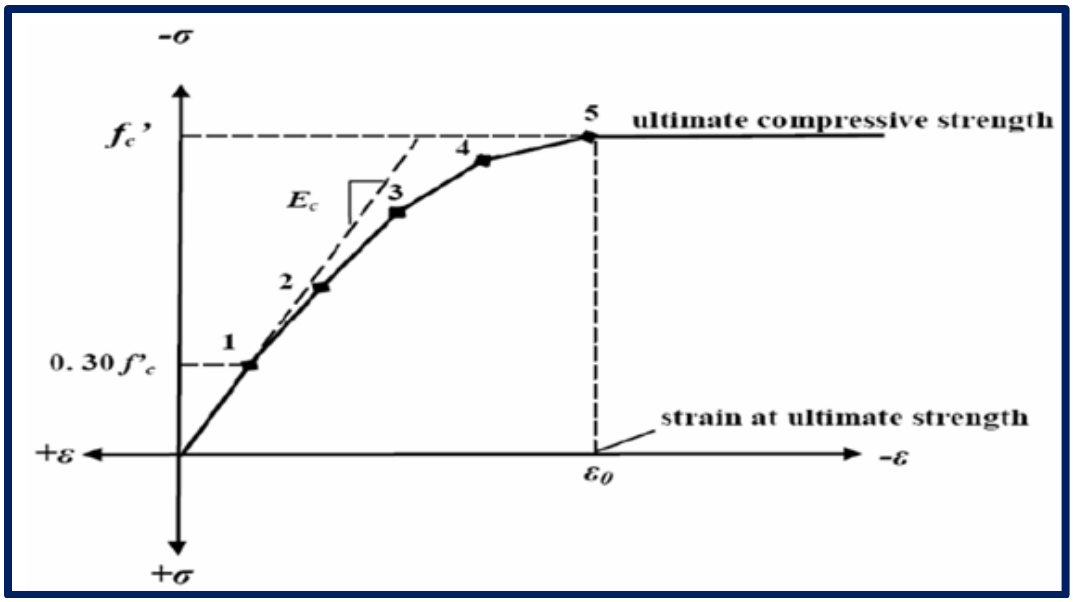

Figure (5-4): Simplified compressive uniaxial stress-strain curve for concrete [59].

5.2.2.2 Modeling of Crack

Three different approaches to crack modeling have been used in finite element analysis of concrete structures:

- Smeared cracking model.
- Discrete cracking model.
- Fracture mechanic's model.

The cracked concrete is supposed to be continuous in this approach, meaning that the cracks are smeared out in a continuous pattern. After the first breaking, the concrete is thought to become orthotropic or transversely isotropic, with one of the material axes orientated along the cracking path. In the smeared cracking model, a crack is not a single fissure but a sign of an infinite number of parallel cracks across the finite element Figure (5-5).

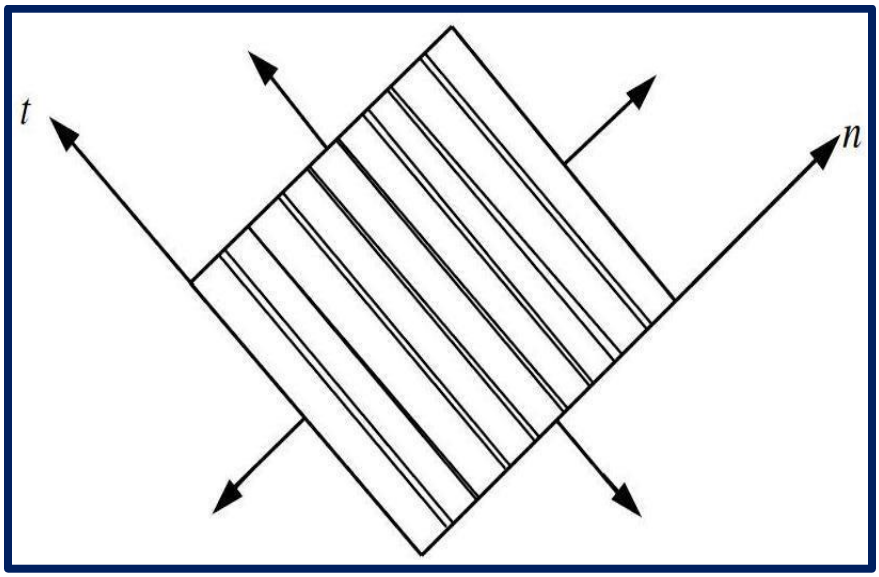

Figure (5-5): Smeared cracking model [13].

The displacement at nodal points for neighboring elements is disconnected in this model. The location and orientation of the cracks are not known in advance, which is an obvious difficulty in such an approach. This can be mitigated to some extent by redefining element nodes. However, such solutions are both difficult and time-consuming.

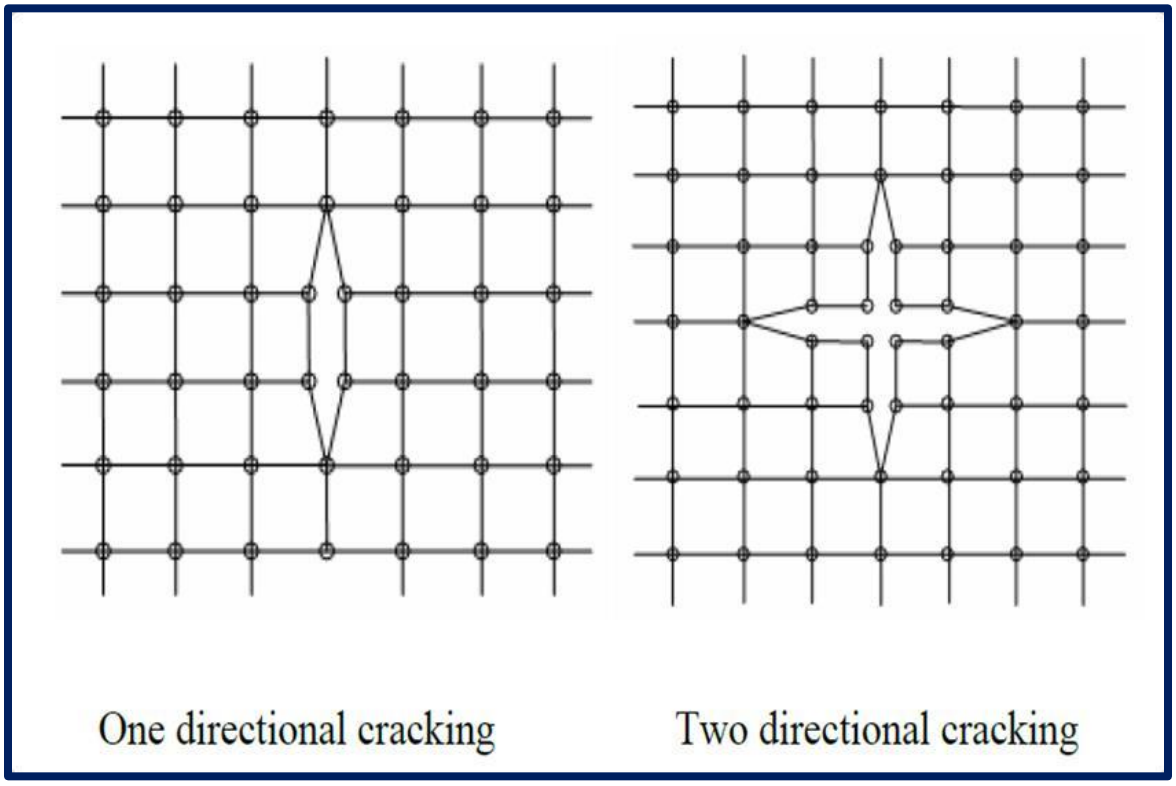

Figure (5-6): Cracking Representation Using Discrete Cracking Modeling [13].

5.2.2.3 Modeling of Concrete Crushing

If the material fails in uniaxial, biaxial, or triaxial compression at an integration point, the material is assumed to crush at that point. Crushing is described in SOLID65 as the full destruction of the materials' structural integrity. Material strength is thought to have decreased to the point where the contribution of an element's integration point to its stiffness can be ignored when it's being crushed [60].

5.2.3 Steel Plate Idealization

Steel plates are inserted at loading and support sites in finite element models to prevent stress concentration concerns and provide stress distribution over the loading areas (as in the experimental test). Steel plates were represented using a solid element (SOLID185). It is assumed that the steel plates are linear elastic materials [60].

5.3 Finite Element Modeling of Steel Reinforcement Bars

Steel reinforcement bars are modeled in this study using a 2-node discrete representation (LINK180 in ANSYS) and are included in the properties of 8-node brick elements (SOLID65 element). This component can be used to create trusses, sagging cables, linkages, and springs, among other things. The three-dimensional spar element is a uniaxial tension-compression element having three degrees of freedom at each node: nodal x, y, and z-direction translations [60].

5.4 Steel Modeling

Steel is a homogeneous material whose strain-stress behavior can be assumed to be identical in tension and compression, and its properties are well characterized, making it a lot easier to describe than concrete. A typical uniaxial stress-strain curve is given for a steel specimen loaded monotonically under tension as shown in Figure (5-7).

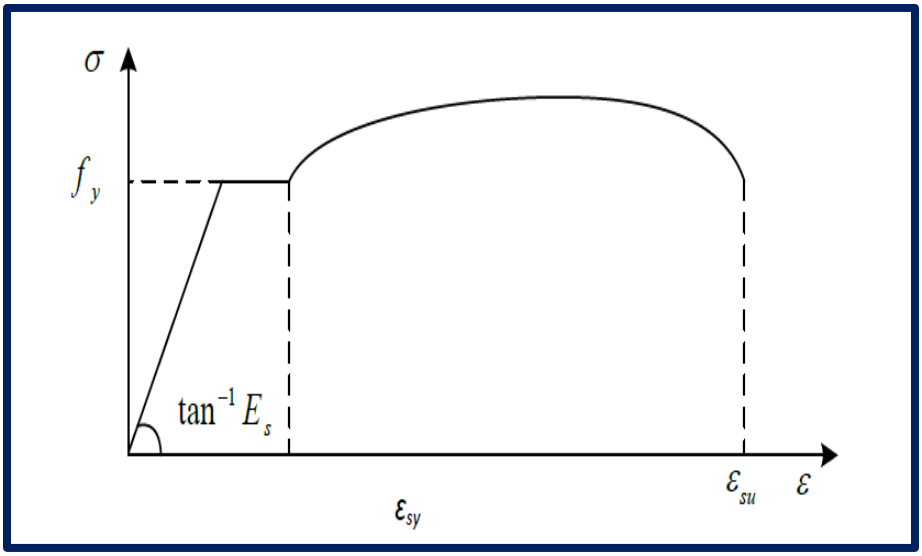

Figure (5-7): Typical stress-strain curve for steel.[13].

For clarity, the stress-strain diagram could have two branches:

The first branch starts from the origin with a slope equal to *Es*, up to *fy*.

The second branch is horizontal, or is supposed to have a very modest slope, such as 0.001E, for practical computer use, and this last instance is limited to the strain of 0.01 according to [13]. As a result, the following two scenarios can be applied:

- For design calculations, the relationship between stress and strain in structural steel can be thought of as if it were elastic and perfectly plastic. as shown in Figure(***5-8***).
- The alternative bilinear stress-strain relationship shown in Figure(5-9) might be used to avoid possible computational issues when utilizing a computer.

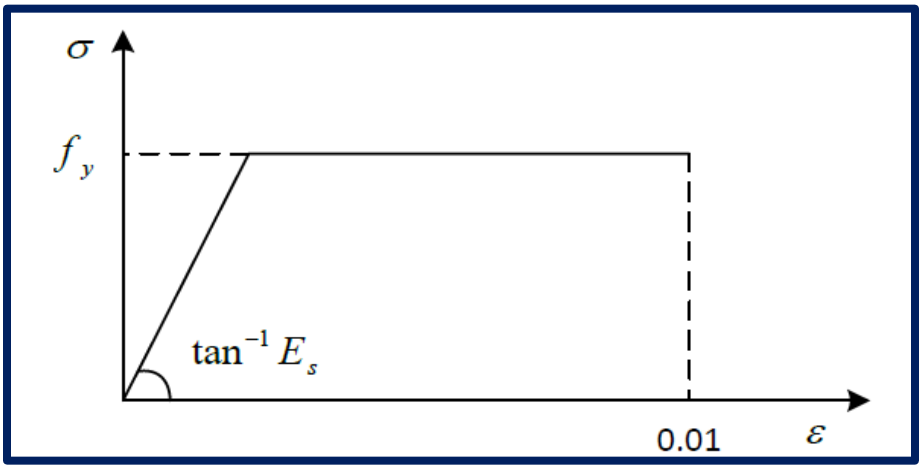

Figure(5-8): Elastic-perfect plastic stress-strain relationships[61].

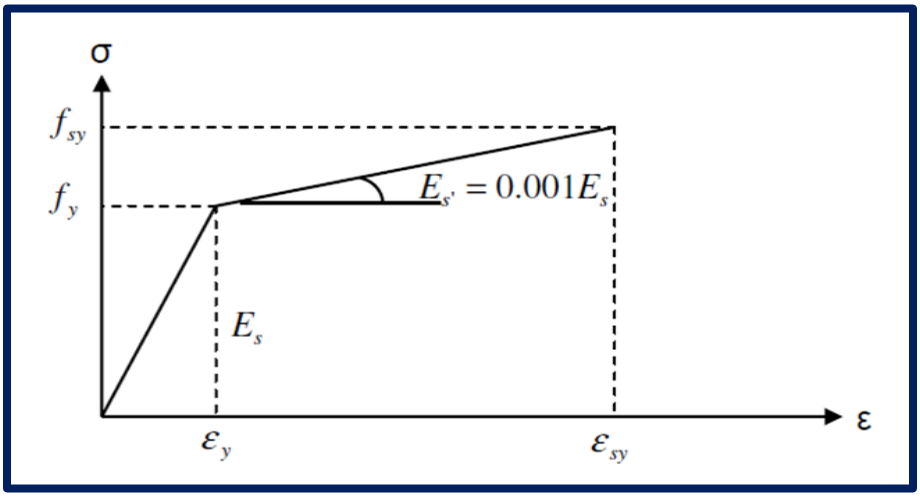

Figure(5-9): Idealization for computer calculations[13].

The following material coefficients will be used in calculations for the steels covered by this study (according to ACI-318-08) [62]:

The modulus of elasticity, Es = 200000 MPa.

Vs = 0.3 Poisson's ratio

The value of steel yield strength (fy), which corresponds to steel, is calculated as revealed in chapter three's tensile test. In finite element concrete with reinforcement, there are three ways to model steel reinforcement [61].

5.5 Modeling of CFRP, GFRP Composites

FRP composites are materials made up of two different components. The elements are macroscopically mixed and are not soluble in one another. The reinforcement is one of the constituents, and it is incorporated into the matrix, which is a continuous polymer. Fibers are used as reinforcing materials because they are stiffer and stronger than the matrix.

FRP composites are anisotropic materials, which means their properties differ in different directions. The FRP composite's linear elastic orthotropic characteristics are assumed throughout this investigation.

5.6 Criteria for Convergence

Iteration continues for each incremental load until convergence is achieved. Therefore, a convergence criterion is required to end the iterative process when the solution is deemed sufficiently precise. The nonlinear analysis of structural issues convergence criterion can be classified as follows:

- Force criterion
- Displacement criterion
- Stress criterion

In this investigation, the displacement criterion was applied. The incremental displacements at iteration I and the total displacement are defined by the

displacement criterion. When the norm of the incremental displacements is within 0.01 of the norms of the total displacement, the solution is regarded as being converged.

5.7 Modeling of Beams Reinforced Concrete

In order to assess the ANSYS program's accuracy in representing the behavior of reinforced concrete girders, in the finite element modeling, the identical details of the tested girders were used as in the experimental program in chapter three. Simply supported girder (control) mesh modeling of concrete, steel plates, and steel reinforcement is exhibited in Figure (5-10) and Figure (5-11).

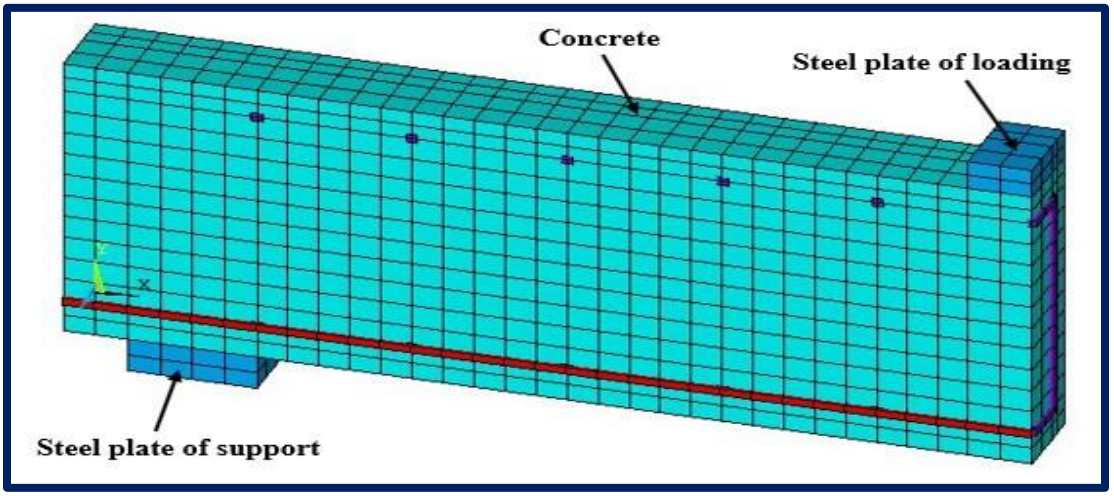

Figure (5-10): Mesh Modeling of Concrete and Steel Plates for control beam.

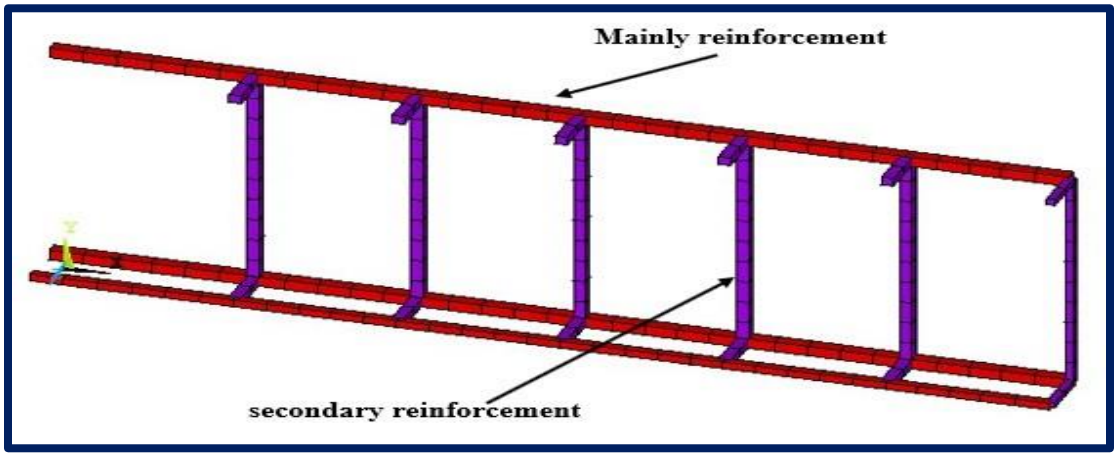

Figure(5-11): Mesh Modeling of Steel Reinforcement of beams.

5.8 Loading and Boundary Conditions

As in the experimental work, the load was applied to each tested beam by one points, these loads have been represented by steel plates of dimensions (100 mm) located at the top face which transforms the load to the beam. The total load has been distributed on nodes. Only one-quarter of the beam was modeled, with the benefit of two symmetry planes. This method significantly reduces the time it takes to analyze. Representation of a representative specimen with the imposed boundary conditions (reinforced concrete, original and NSM bars, CFRP sheet) (applied load, support), as shown in Figure (5-12).

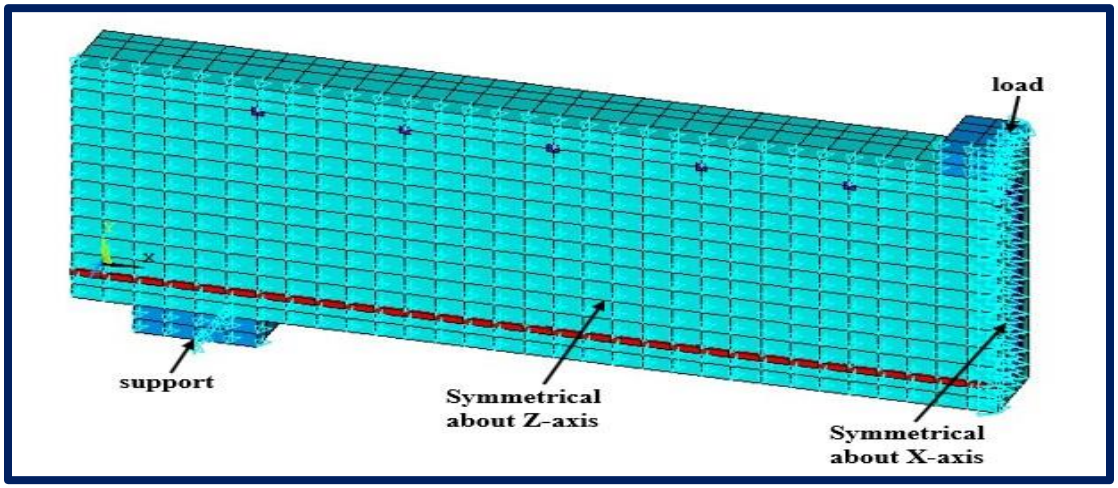

Figure (5-12): Boundary Conditions for the Quarter Beam.

To obtain a solution, displacement boundary conditions must be applied to each model. Steel plates were used to represent the supports, just as they were for the point load. The nodes representing a pin support were confined in both the X and Y directions (Ux=0 and Uy=0), whereas the nodes representing a roller support were only bound in the Y direction (Uy=0).

5.9 Comparison Between Experimental Results and Finite Element Analysis

Table(5-1) includes numerical results, of cracking load, ultimate load and ultimate deflection. To find and clarify the amount of difference between experimental and numerical results.

5.9.1 Load-Deflection Behavior

One of the best features of the ANSYS program is the ability to provide the deflected shape at each step of the load increments as well as the deflection at each node. The deflected shape at the failure stages for each strengthened and unstrengthen simply supported beam for each group were presented in Figure (5-13) to Figure (5-28).

- **Group One**

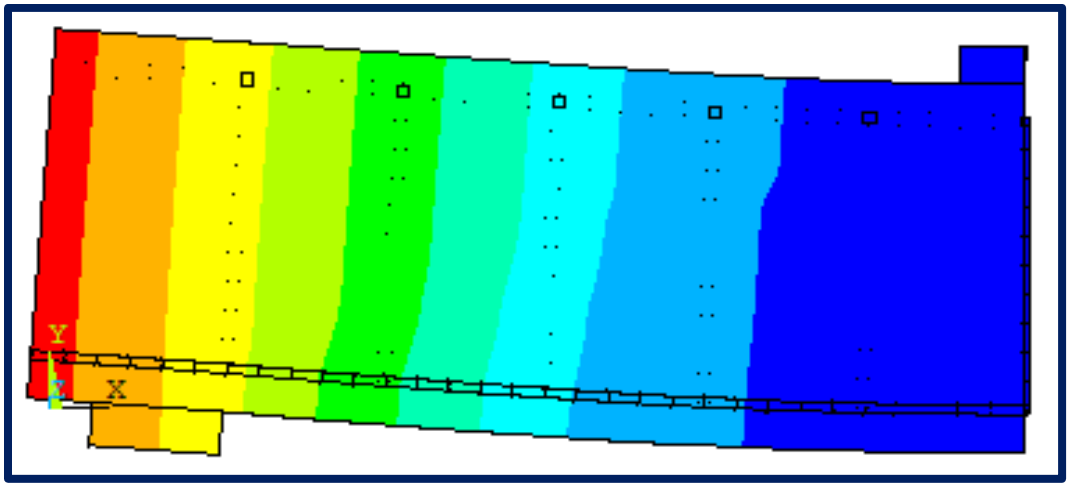

Figure (5-13): Deflection shape for unstrengthen beam (CN).

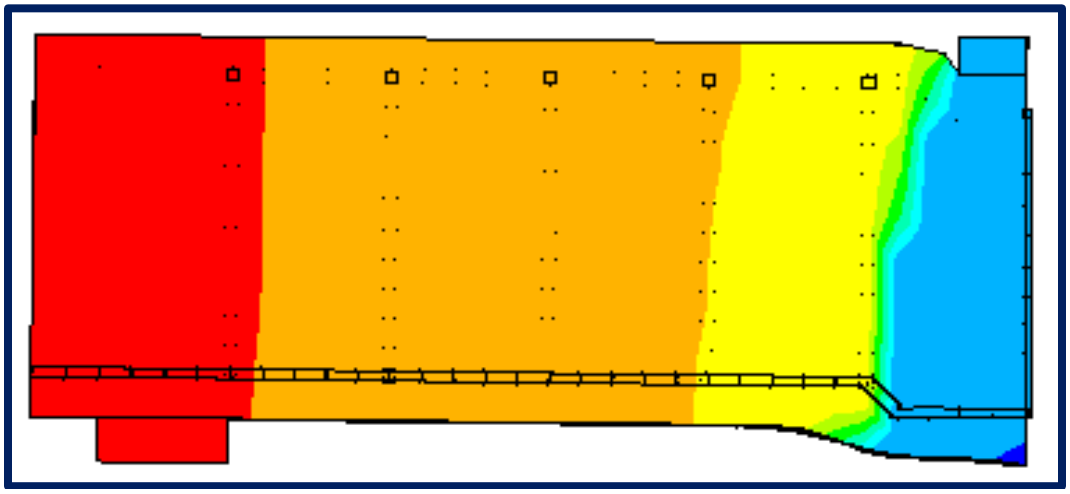

Figure (5-14): Deflection shape for strengthen beam with FRP sheet (NT).

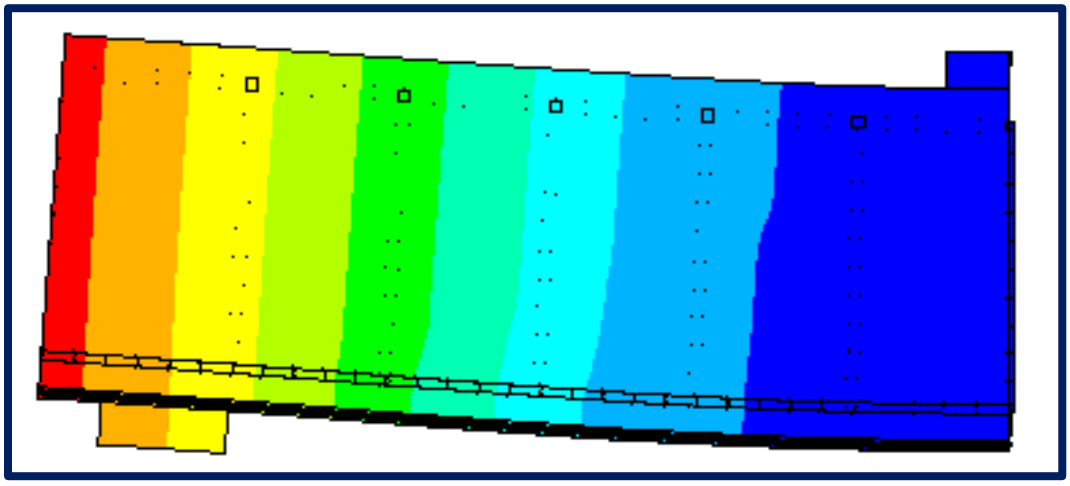

Figure (5-15): Deflection shape for strengthen beam with carbon bar (NCb).

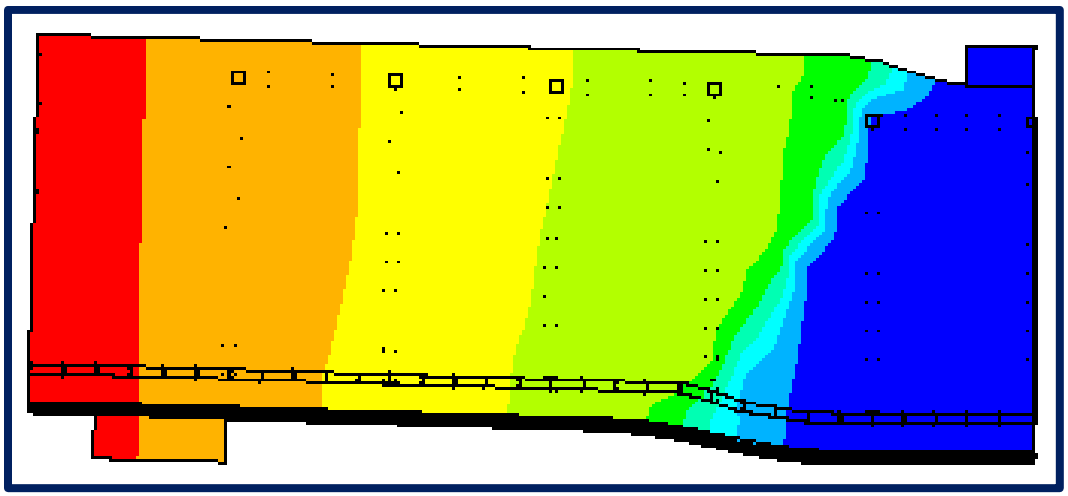

Figure (5-16): Deflection shape for strengthen beam with carbon bar and FRP sheet (NCbT).

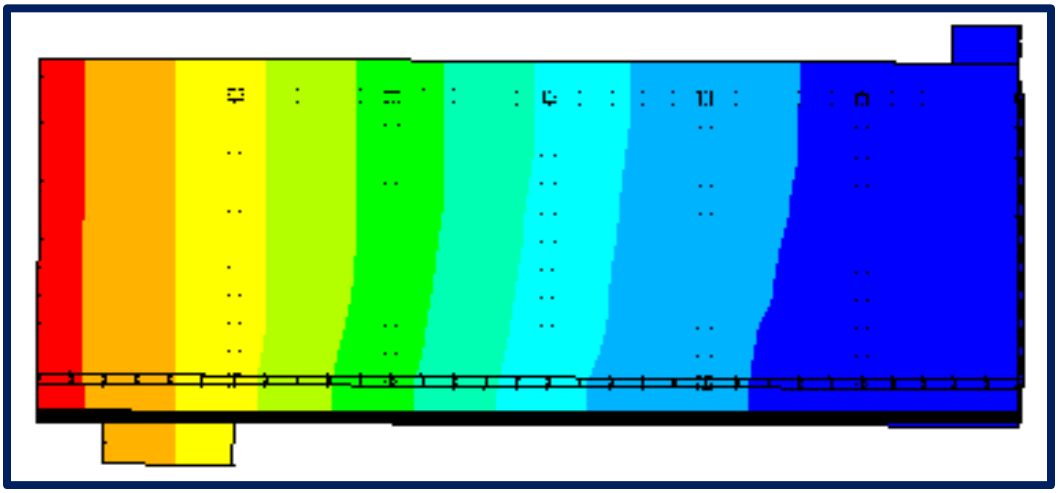

Figure (5-17): Deflection shape for strengthen beam with glass bar (NGb).

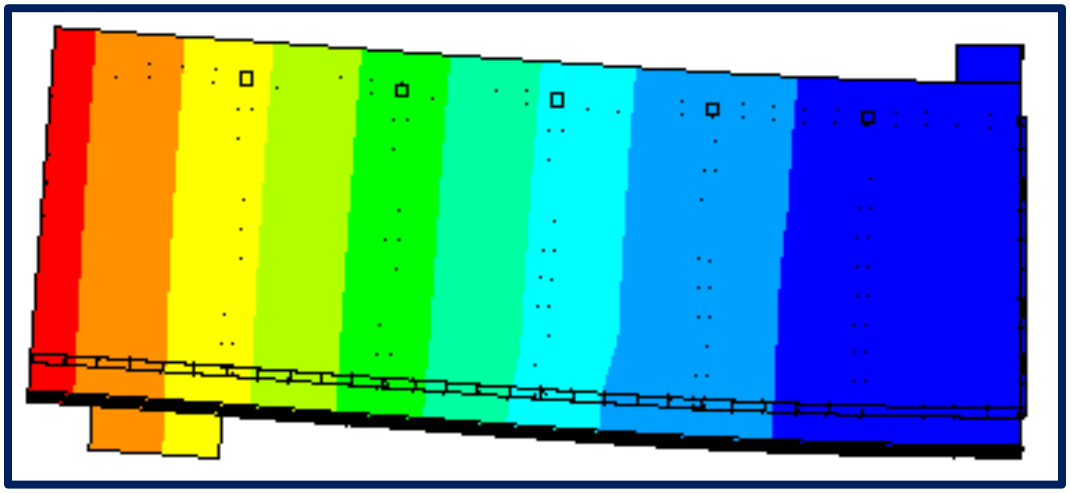

Figure (5-18): Deflection shape for strengthen beam with glass bar and FRP sheet (NGbT).

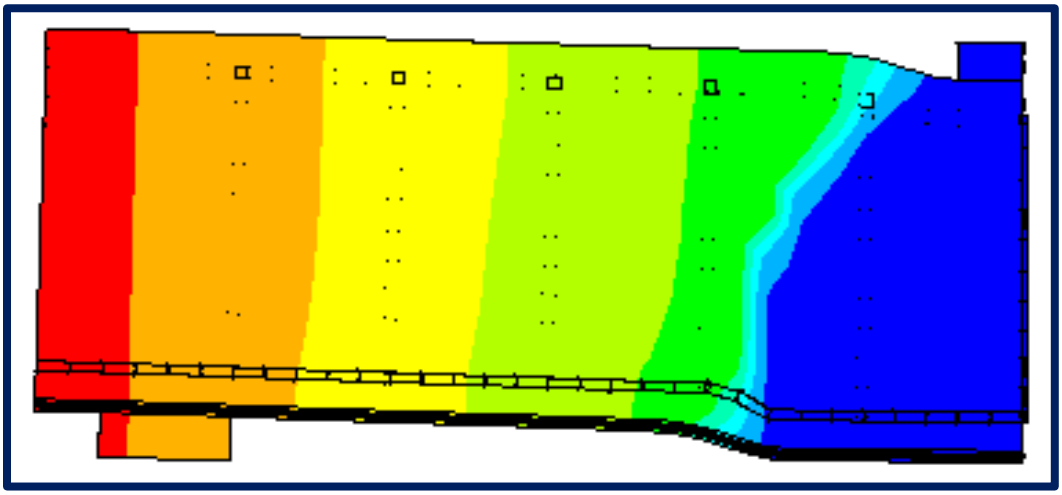

Figure (5-19): Deflection shape for strengthen beam with glass bar (NSb).

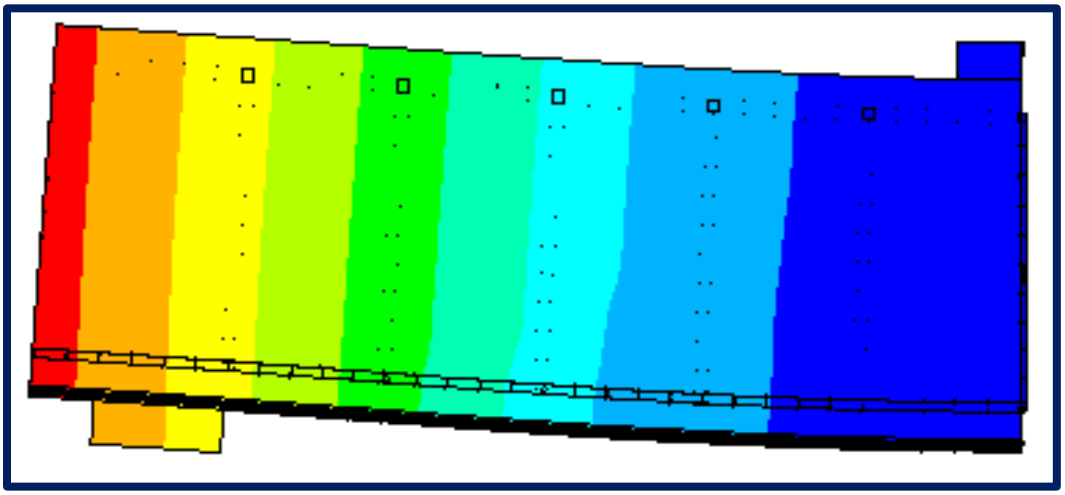

Figure (5-20): Deflection shape for strengthen beam with glass bar and FRP sheet (NSbT).

- **Group Two**

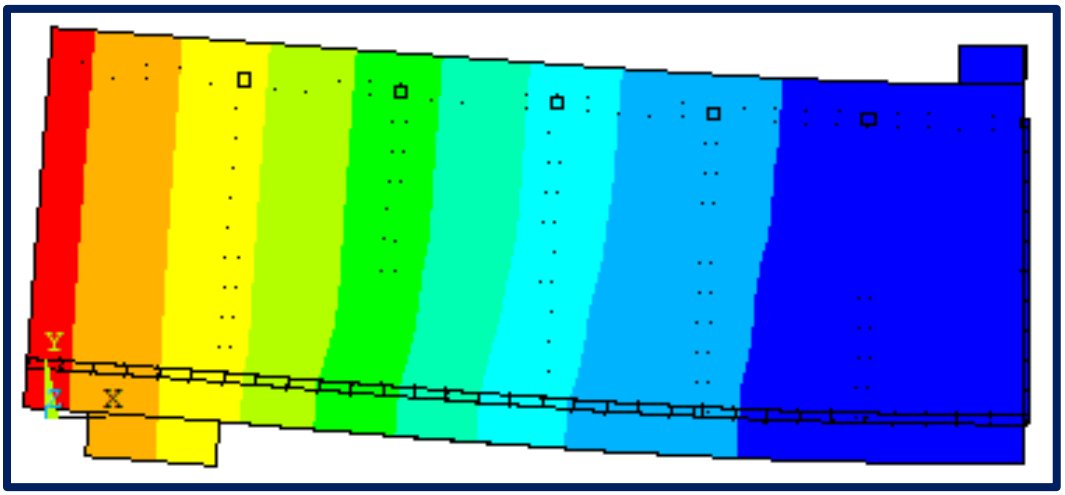

Figure (5-21): Deflection shape for unstrengthen control beam (CF).

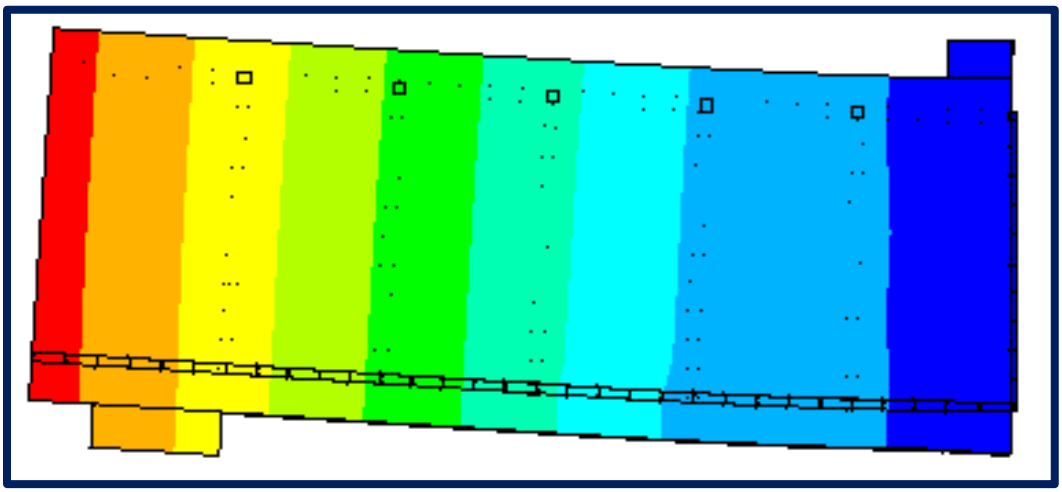

Figure(5-22): Deflection shape for strengthen beam with FRP sheet (FT).

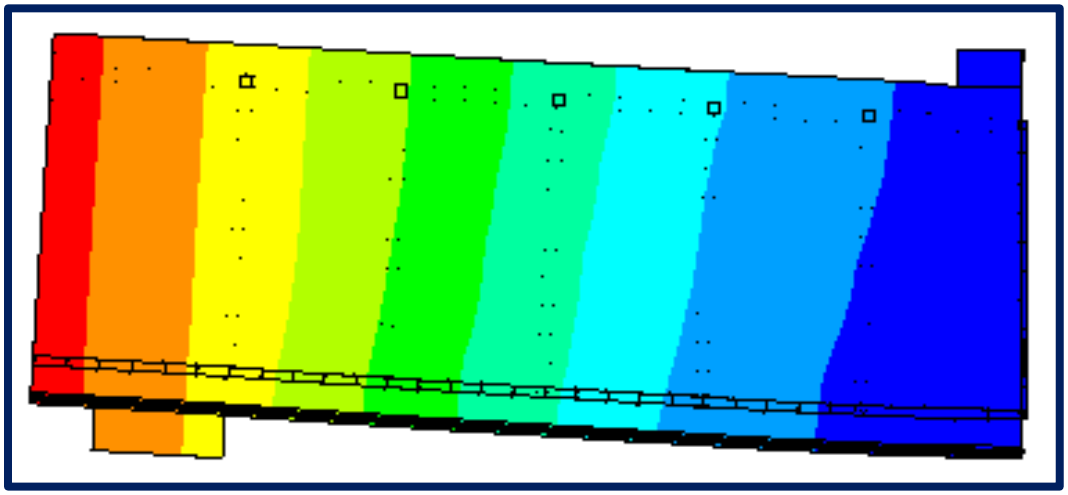

Figure (5-23): Deflection shape for strengthen beam with CFRP bar (FCb).

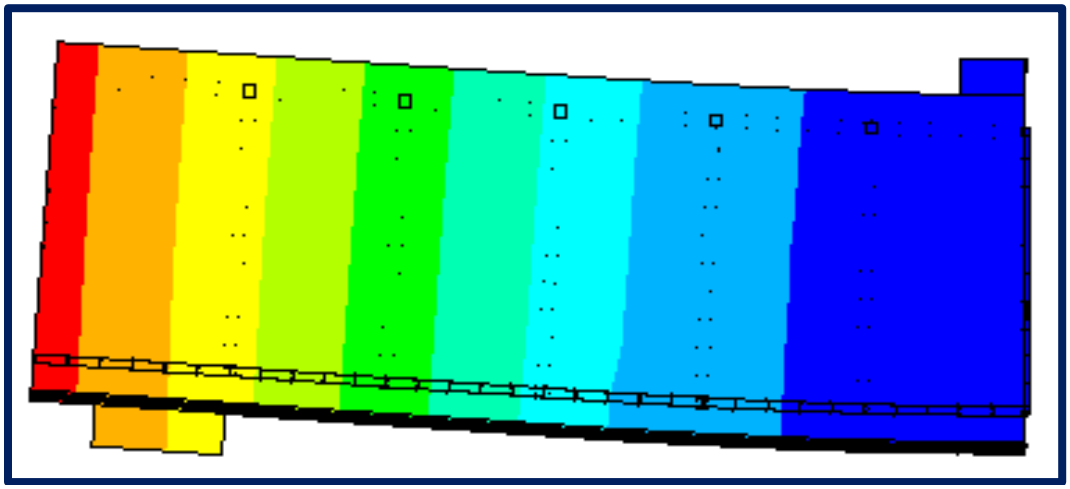

Figure (5-24): Deflection shape for strengthen beam with carbon bar and FRP sheet (FCbT).

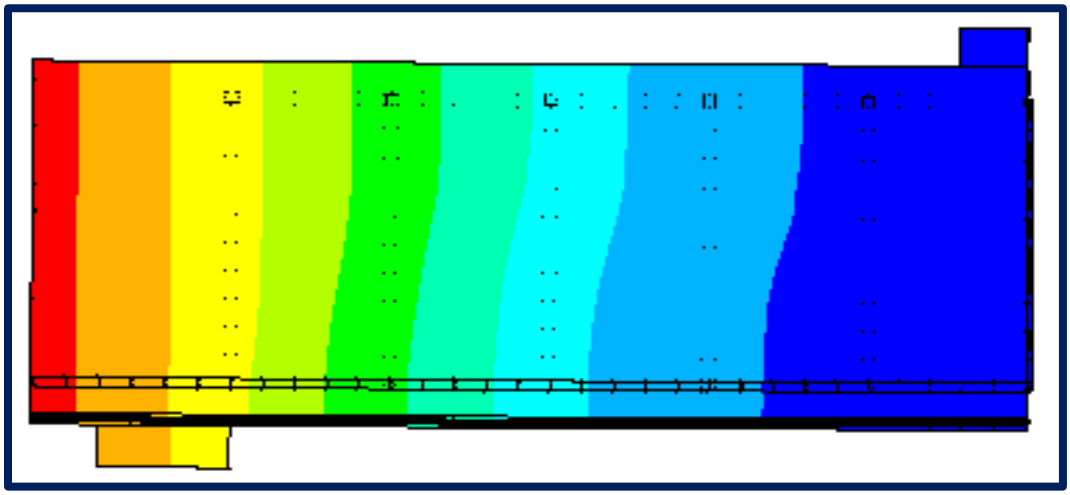

Figure (5-25): Deflection shape for strengthen beam with glass bar (FGb).

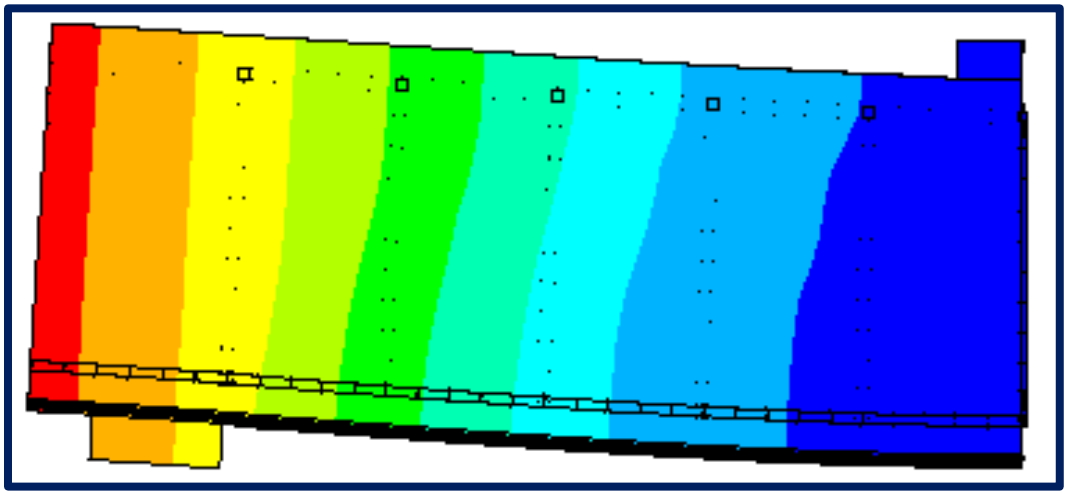

Figure (5-26): Deflection shape for strengthen beam with glass bar and FRP sheet (FGbT).

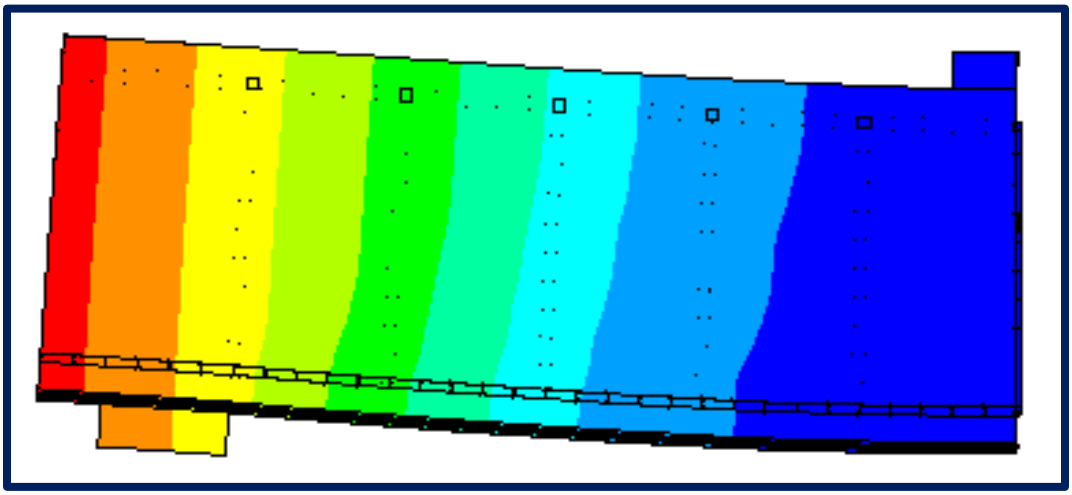

Figure (5-27): Deflection shape for strengthen beam with steel reinforcement (FSb).

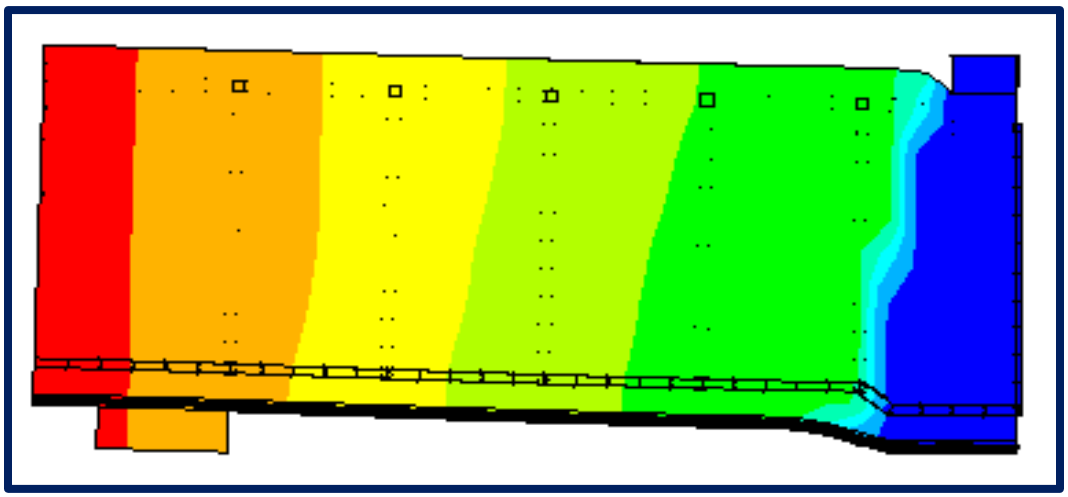

Figure (5-28): Deflection shape for strengthen beam with steel reinforcement and FRP sheet (FSbT).

The deflection for each of the tested beams was evaluated as an experimental test. The deflection was evaluated at mid-span. The load-deflection curve has been calculated for each increment of load. Figures (5.13) to (5.18). In term of the load-deflection relationship, there was a comparison of numerical and experimental results. It can be seen from these figures that the numerical and experimental results are in reasonable agreement.

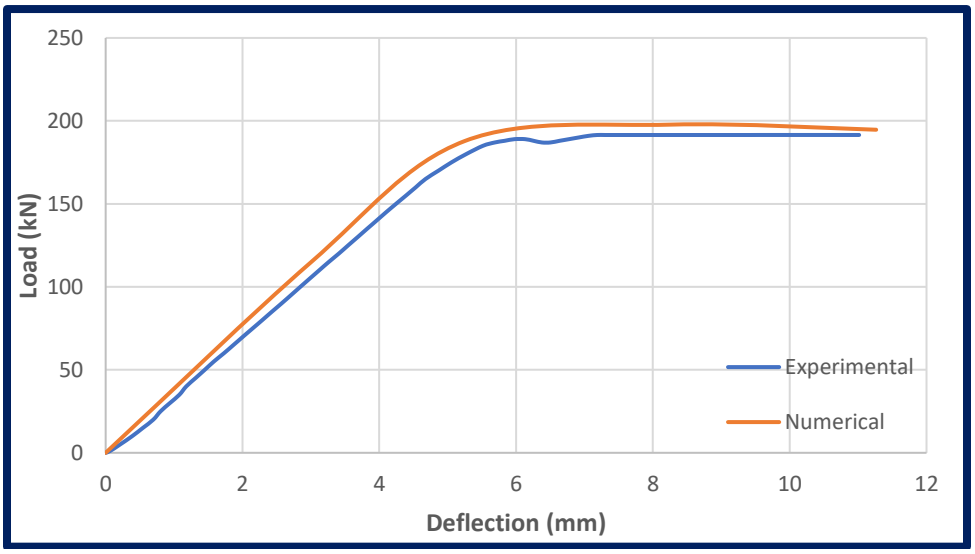

Figure(5-29): Experimental and Numerical Load-Deflection Curves of beam (CN).

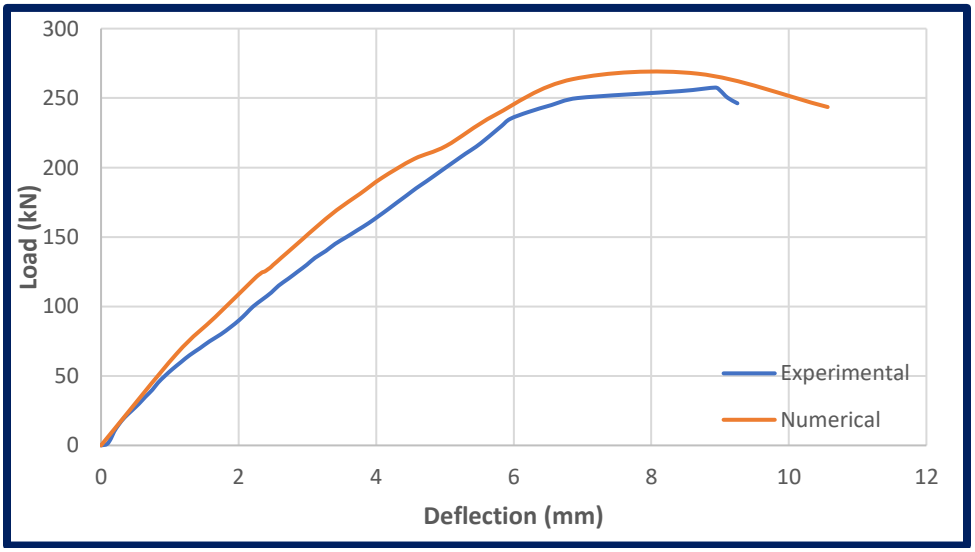

Figure (5-30): Experimental and Numerical Load-Deflection Curves of beam (NT).

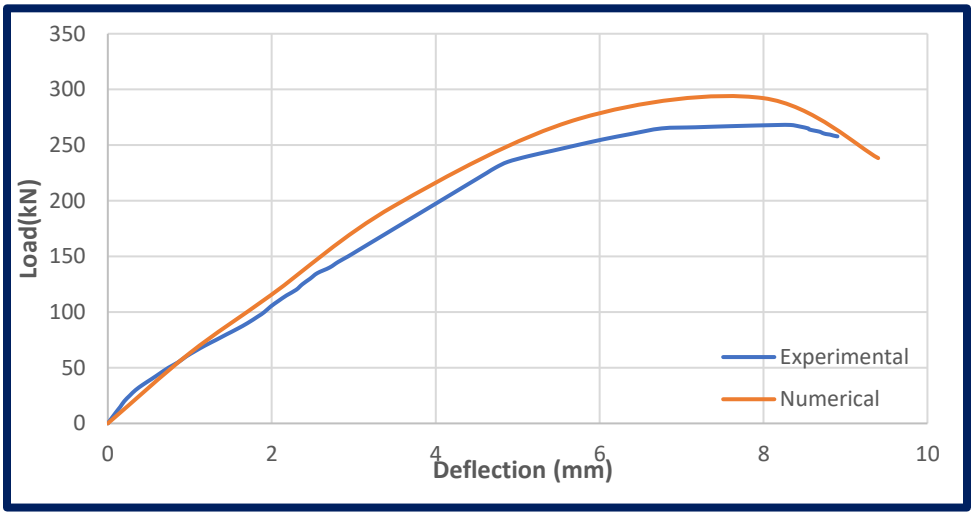

Figure(5-31): Experimental and Numerical Load-Deflection Curves of beam (NCb).

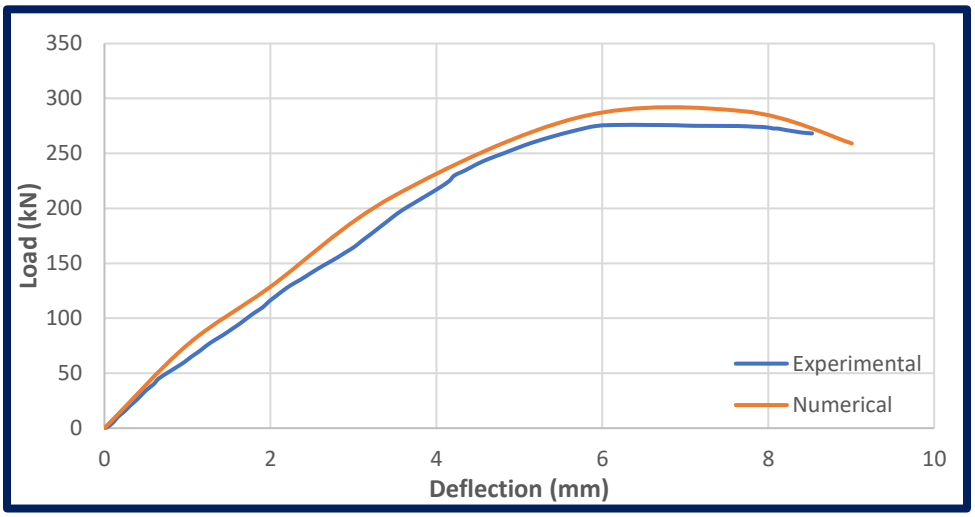

Figure (5-32): Experimental and Numerical Load-Deflection Curves of beam (NCbT).

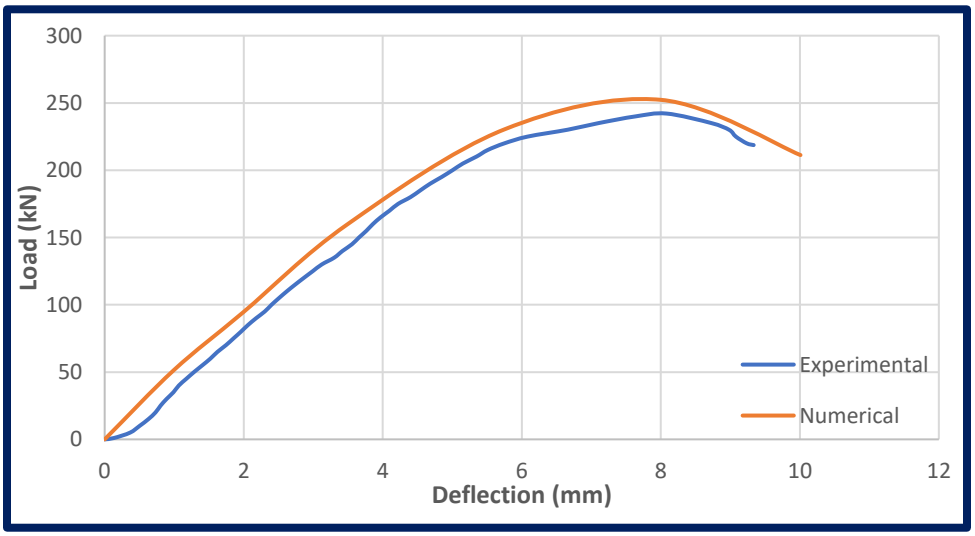

Figure(5-33): Experimental and Numerical Load-Deflection Curves of beam (NGb).

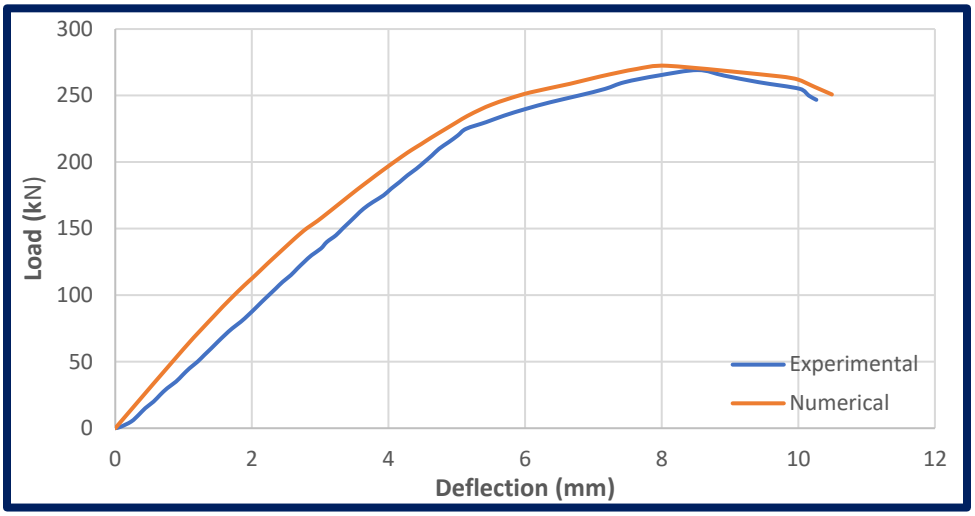

Figure(5-34): Experimental and Numerical Load-Deflection Curves of beam (NGbT).

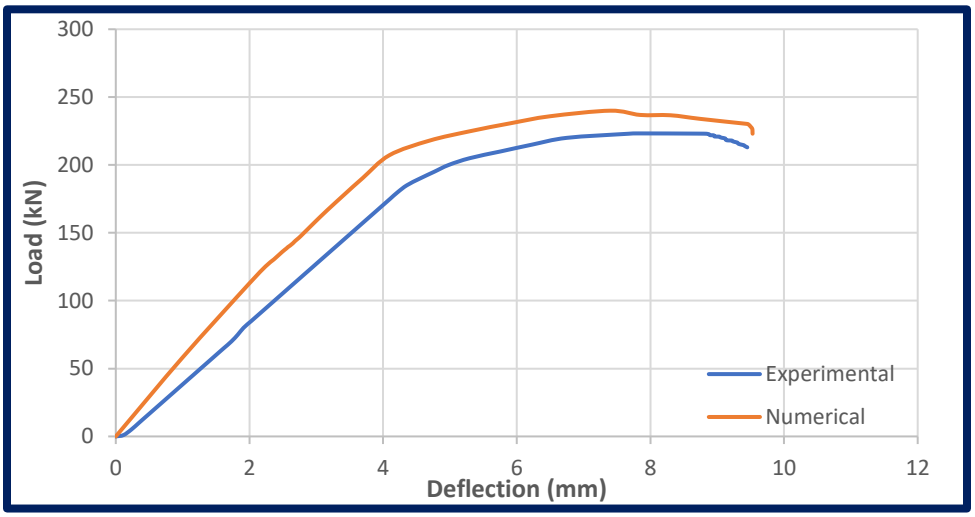

Figure(5-35): Experimental and Numerical Load-Deflection Curves of beam (NSb).

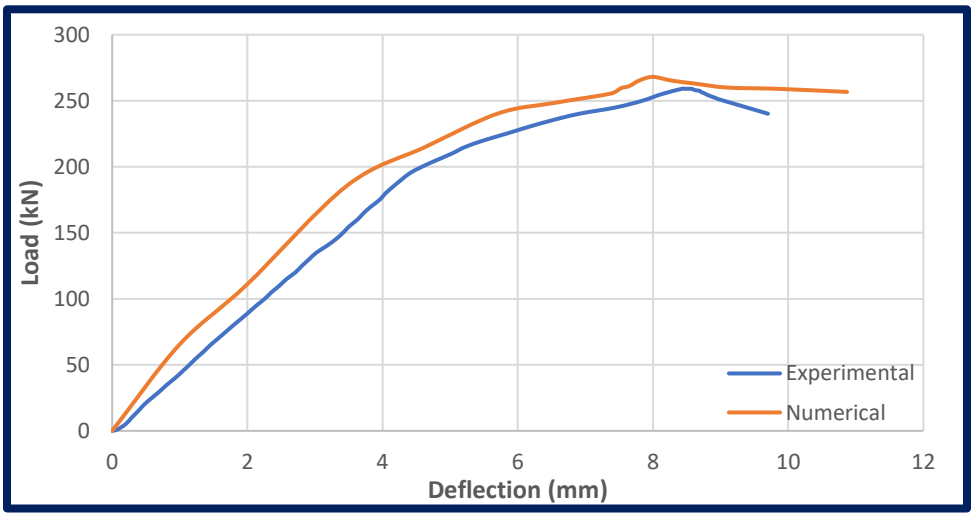

Figure(5-36): Experimental and Numerical Load-Deflection Curves of beam (NSbT).

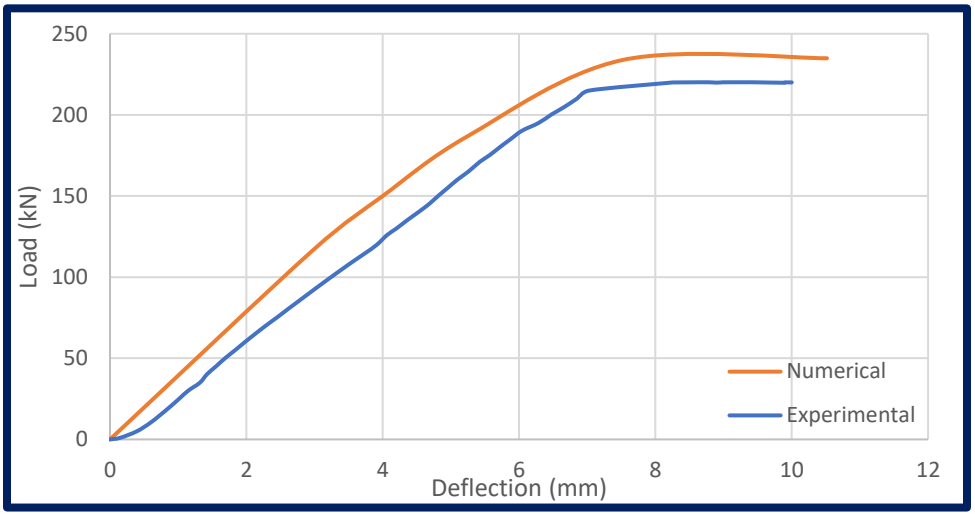

Figure(5-37): Experimental and Numerical Load-Deflection Curves of beam (CF).

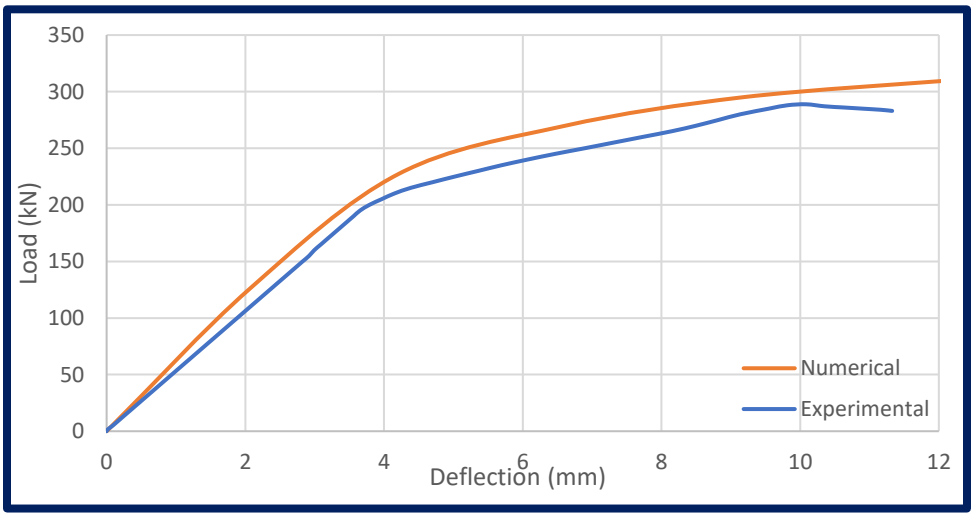

Figure(5-38): Experimental and Numerical Load-Deflection Curves of beam (FT).

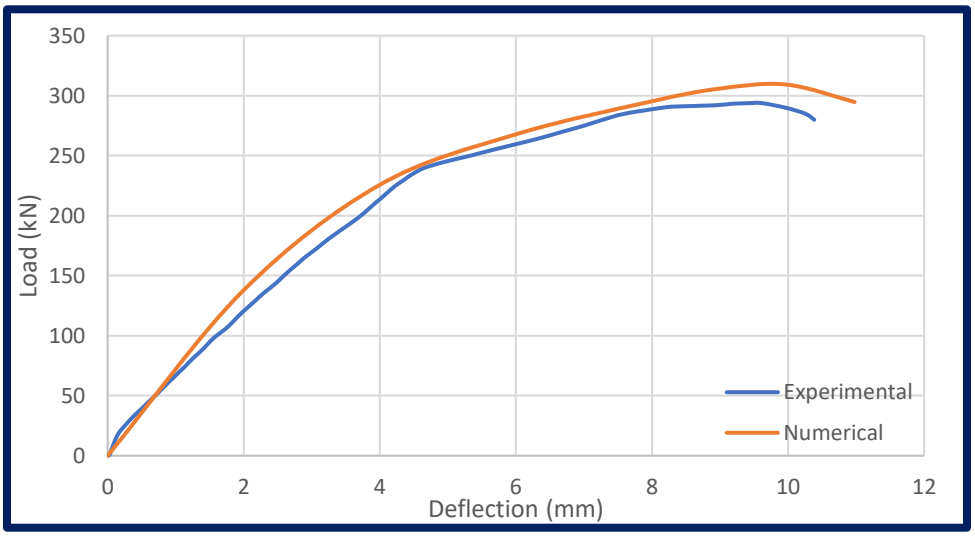

Figure(5-39): Experimental and Numerical Load-Deflection Curves of beam (FCb).

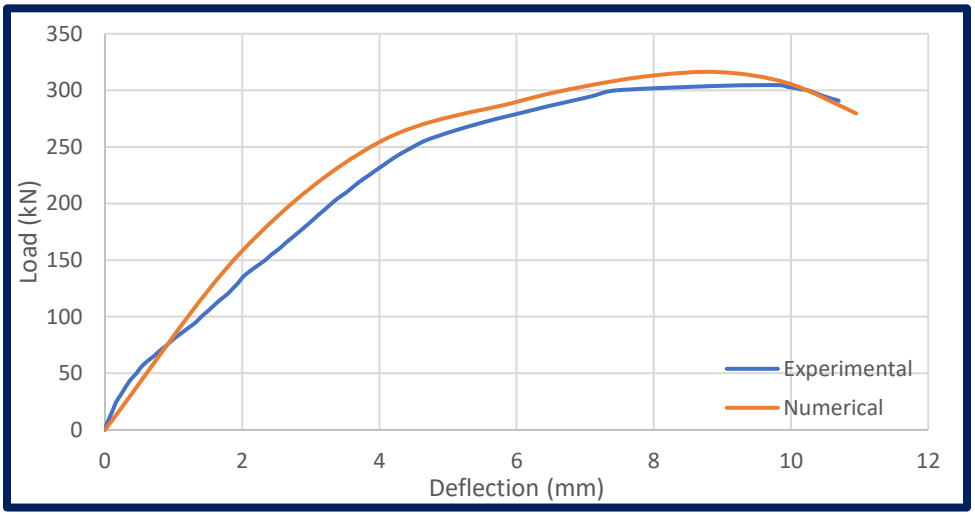

Figure(5-40): Experimental and Numerical Load-Deflection Curves of beam (FCbT).

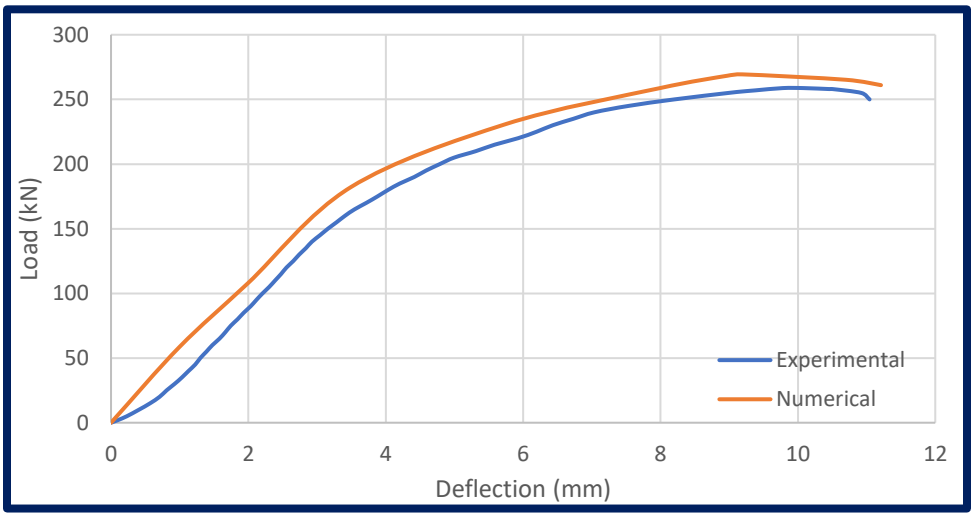

Figure (5-41): Experimental and Numerical Load-Deflection Curves of beam (FGb).

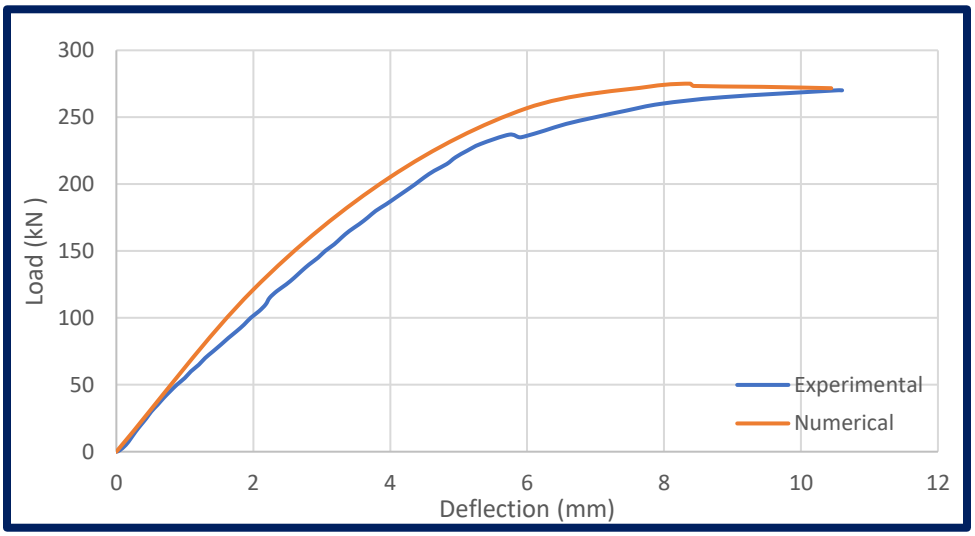

Figure (5-42): Experimental and Numerical Load-Deflection Curves of beam (FGbT).

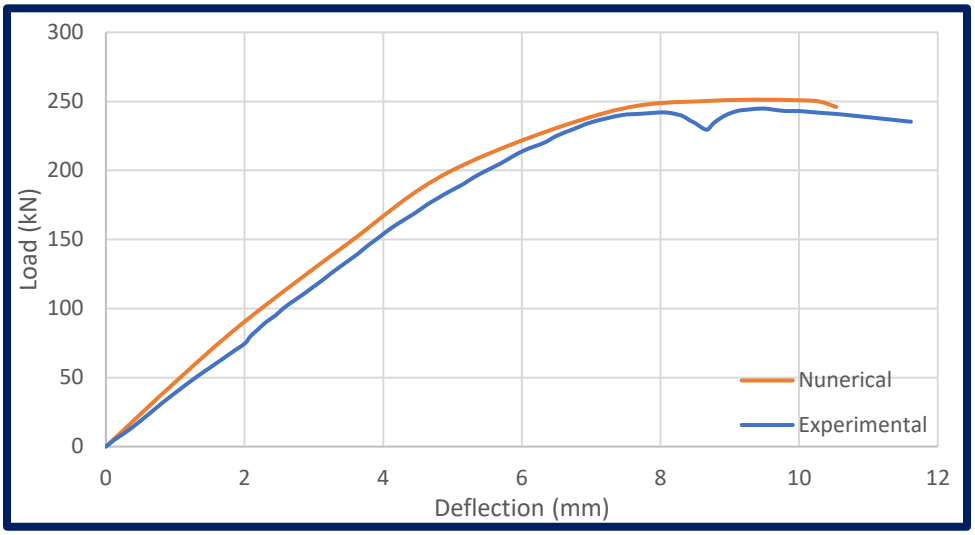

Figure (5-43): Experimental and Numerical Load-Deflection Curves of beam (FSb).

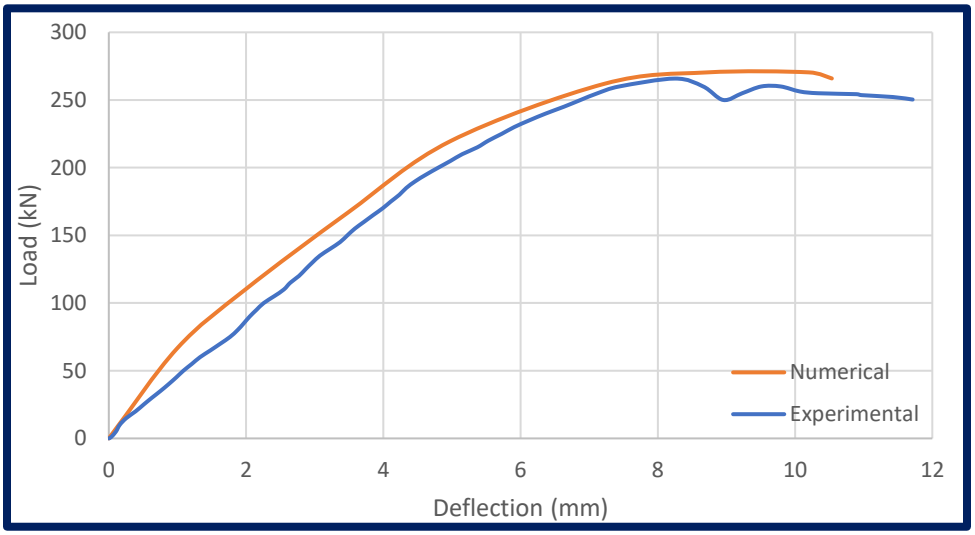

Figure (5-44): Experimental and Numerical Load-Deflection Curves of beam (FSbT).

5.9.2 Ultimate Load Deflection

A comparison of the numerical ultimate load produced by the ANSYS software, and the experimental ultimate load is presented in Table (5-2). The maximum differences in ultimate load for the two groups were (44.08%) and (59.05%), respectively. After the solution was completed, the numerical ultimate load was recorded when convergence between the two subsequent values could not be achieved since the stress in steel had reached the yield stress.

Table(5-2): Experimental and Numerical results of ultimate load.

Beams		Num. (kN)	Exp. (kN)	Δ%= (Num-Exp)/ Exp	Increase in numerical ultimate load, % %=x-control/control
Group (1)	NC	197.7572	191.50509	3.2647	N/A
	NSb	239.9936	223.256	7.4970	16.58%
	NCb	292.171	268.0787	8.9870	39.98%
	NGb	252.3295	242.1188	4.2172	26.43%
	NT	267.5452	257.5602	3.8768	34.49%
	NSbT	268.074	259.1761	3.4331	35.34%
	NCbT	288.3179	275.9237	4.4919	44.08%
	NGbT	272.3836	269.1589	2.3126	40.55%
Group (2)	CF	234.906	220.1197	6.7174	N/A
	FSb	250.438	244.8435	2.2849	27.85%
	FCb	309.3412	293.8543	5.2703	53.44%
	FGb	269.3572	258.7599	4.0954	35.12%
	FT	309.9644	288.8442	7.3119	50.83%
	FSbT	270.438	265.8379	1.7304	38.82%
	FCbT	316.1144	304.588	3.7843	59.05%
	FGbT	275.0884	270.174	1.8189	41.08%

Chapter Six
CONCLUSIONS AND RECOMMENDATIONS

6.1 Overview

The main objective of this research is to compare and contrast the flexural behavior of two different types of concrete when used as simply supported beams and strengthened with (EBR & NSM) composites. This study employs both an experimental program and a nonlinear finite element model to predict the flexural behavior of the tested beams.

In this chapter, the experimental and analytical results are used to form conclusions. There are also recommendations for future work.

6.2 Conclusions

The following conclusions can be drawn based on the findings of the experimental work as well as the finite element analysis for beam strengthening: -

1) The near-surface mounted (NSM) technique gives good performance with a higher ultimate load in comparison with the external bonded reinforcement (EBR) technique.
2) For the same amount of NSM of the same type (like rods), the use of CFRP is better than GFRP and Steel Reinforce bar. Also, all types are the same (length of 1200mm with a diameter of 6mm). The maximum difference is about (2.41%).
3) In group one, when using normal concrete, the use of NSM CFRP with CFRP sheet (EBR) technique strengthening is better than using CFRP (NSM) only, and the increase in the ultimate load is about (5.49%).

4) In group one, when using normal concrete, NSM GFRP with CFRP sheet (EBR) technique strengthening is less than using GFRP (NSM) only and the decrease in the ultimate load is about (5.99%).
5) In group one, when using normal concrete, NSM Steel Reinforce bar with CFRP sheet (EBR) technique strengthening is less than using Steel Reinforce bar (NSM) only and the decrease in the ultimate load is about (13.32%).
6) Using micro steel fiber in group two in reinforcement in RC beams has a significant effect on the flexural strength and deflection of tested beams about (14.94%) better than in group one.
7) The strengthening by CFRP composites decreases the crack width and increases the number of cracks. This is one of the several advantages of using CFRP composites.
8) The strengthening of beams by CFRP composites reduces the maximum deflection under the same load. The mid-span deflection is reduced by 55.92% for the beams with NSM CFRP of length (1200mm). On the other hand, the maximum deflection is reduced by 60.02% for beams with EBR CFRP of length (1200mm).
9) When comparing failure modes, R/C beams without any strengthening, typical flexure failure and concrete crushing at the compression zone are recorded, while beams strengthened with EBR CFRP sheets and plate at the length (1200mm) fail due to debonding of CFRP sheets with flexure failure as expected. No crushing of concrete is noticed at ultimate load. On the other hand, beams strengthened with EBR CFRP sheets at the length (1200mm) fail with splitting in concrete cover with concrete crushing occurring at ultimate load. Beams strengthened with NSM CFRP sheets failed due to rupture of CFRP in the flexure zone. While beams reinforced

with NSM CFRP bar failed due to concrete cover splitting. No concrete crushing is noticed at ultimate load.

10) The use of CFRP bars as tensile reinforcement in RC beams significantly improved the flexural strength and deflection of the beams evaluated. The CFRP rebars' low modulus of elasticity was discovered to be a critical factor in increasing the deflection of reinforced concrete beams at the same loads.
11) results showed that carbon fibers have a good ability to repair damaged beams, with an improvement in the bearing capacity of the beam. The optimum rehabilitation method is to use a CFRP bar with a CFRP sheet about (44.08% -38.37%).
12) Fiber concrete has a good response when using different types of strengthening.
13) finite element model used in this study is able to model reinforced concrete beams with various types of strengthening. The anticipated cracking loads, crack patterns, and ultimate loads are very similar to those seen during experimental testing. The ultimate load differential might be as high as (8.09%).
14) The finite element model's crack patterns at the final load match the experimental results' observed failure very well.

6.3 Suggestions for Future Work

Further work is required to understand the flexural behavior of reinforced concrete beams strengthened with various types of strengthening. More investigation is required. The following are recommended factors that will be important:

1) The behavior of FRP-strengthened reinforced concrete beams under other loading methods like two-point load, dynamic and impact loading is also determined.
2) The effects of various concrete compressive strengths can be studied using the same experimental program.
3) The same experimental program can be applied to reinforced concrete in other shapes, such as T-shaped or I-shaped simply supported beams.
4) The structural behavior of continuous R.C beams or deep beams enhanced with (NSM, EBR) can be investigated using the same experimental program.
5) Investigate the structural behavior of reinforced concrete beams with various types of strengthening under the combined effects of bending, shear, and torsion.
6) Experimental investigation into the structural behavior of hybrid or restressed reinforced concrete beams strengthened with various types of strengthening reinforced concrete under a one-point load.
7) Studying the effect of using round gravel instead of crushed gravel was used in the research.
8) The same proportions can be used for the materials included in the research with the possibility of adding some materials such as plasticizers to increase the operability, and it is possible to use other proportions of the fiber added in the concrete containing the fiber.

References

[1] E. Kern and H. Schorn, "Steel Fiber Reinforced Concrete," *Beton- und Stahlbetonbau*, vol. 86, no. 9, pp. 205–208, 1991, doi: 10.1002/best.199100380.

[2] J. M. Sena-Cruz, J. A. O. Barros, M. R. F. Coelho, and L. F. F. T. Silva, "Efficiency of different techniques in flexural strengthening of RC beams under monotonic and fatigue loading," *Constr. Build. Mater.*, vol. 29, pp. 175–182, 2012, doi: 10.1016/j.conbuildmat.2011.10.044.

[3] "Concrete - Designing Buildings Wiki," *Designing Buildings Ltd*. 2017, [Online]. Available: https://www.designingbuildings.co.uk/wiki/Concrete.

[4] C. Facilitator, "Fiber-reinforced concrete - Advantages, types and applications," Accessed: Jul. 24, 2020. [Online]. Available: https://www.constrofacilitator.com/fiber-reinforced-concrete-advantages-types-and-applications/.

[5] Concrete Information, "What is Concrete ? Advantages." p. 22, 2020, [Online]. Available: https://www.concrete-info.com/concrete-beams/.

[6] C. Engineerin, "Advantages and Disadvantages of Concrete - Civil Engineering." [Online]. Available: https://civiltoday.com/civil-engineering-materials/concrete/15-advantages-and-disadvantages-of-concrete.

[7] F. R. Concrete, "Fiber-reinforced concrete – Advantages , types and applications." 2020.

[8] D. Mostofinejad and E. Mahmoudabadi, "Grooving as Alternative Method of Surface Preparation to Postpone Debonding of FRP Laminates in Concrete Beams," *J. Compos. Constr.*, vol. 14, no. 6, pp. 804–811, 2010, doi: 10.1061/(asce)cc.1943-5614.0000117.

[9] D. Mostofinejad and S. M. Shameli, "Externally bonded reinforcement in grooves (EBRIG) technique to postpone debonding of FRP sheets in strengthened concrete beams," *Constr. Build. Mater.*, vol. 38, pp. 751–758, 2013, doi: 10.1016/j.conbuildmat.2012.09.030.

[10] D. G. Novidis, "Beam Tests of Nsm – Frp Laminates in Concrete Frprcs-8," pp. 1–10, 2007.

[11] H. Nordin, *Fibre reinforced polymers in civil engineering*. 2003.

[12] A. Carolin, *Carbon Fibre Reinforced Polymers for Strengthening of Structural Elements*, vol. 1992, no. 10. 2003.

[13] M. W. F. Al-Joubory, "Behavior of Self-Compacting R/C Simply Supported Beams Strengthened With NSM CFRP Composites," University of Babylon, 2013.

[14] X. G. Wang and X. L. Gu, "Strengthening of corroding reinforced concrete beams by means of CFRP laminates," vol. 16, no. 1, pp. 47--56--, 2010.

[15] A. L. I. S. Resheq, "STRENGTHENING OF CONTINUOUS REINFORCED CONCRETE BEAMS BY CFRP LAMINATES," University of Technology Building, 2010.

[16] A. M. Ibrahim, A. A. Mansor, and M. Hameed, "Structural Behavior of Strengthened RC Beams in Shear using CFRP Strips," *Open Civ. Eng. J.*, vol. 11, no. 1, pp. 205–215, 2017, doi: 10.2174/1874149501711010205.

[17] "Revolutionary Materials_ Technology and Economics - Sampe - Google Books." .

[18] K. Soudki and T. Alkhrdaji, *Guide for the Design and Construction of Externally*

Bonded FRP Systems for Strengthening Concrete Structures (ACI 440.2R-02). 2005.

[19] P. A. La Tegola and L. De Lorenzis, "STRENGTHENING OF RC STRUCTURES WITH NEAR-SURFACE MOUNTED FRP RODS," civil engineering, Lecce, Italy.

[20] H. M. ABDZAID and Asst. Prof. Dr. Hayder Hussain Kamonna, "Flexural Strengthening of Continuous Reinforced Concrete Beams with Near-Surface-Mounted Reinforcement," University of Kufa, 2018.

[21] L. De Lorenzis, A. Nanni, and A. La Tegola, "Strengthening of Reinforced Concrete Structures with Near Surface Mounted FRP Rods," *ACI Struct. J.*, vol. 1948, pp. 1–8, 2000, [Online]. Available: http://www.concrete.org/Publications/InternationalConcreteAbstractsPortal.aspx?m=details&i=11534.

[22] S. Y. Kim, C. H. Park, and S. Yeol, "FRACTURE ANALYSIS OF FRP REINFORCED CONCRETE BEAMS," *J. Eng. Mech.*, vol. 127, no. June, pp. 448–451, 2001.

[23] L. De Lorenzis and A. Nanni, "Bond between near-surface mounted fiber-reinforced polymer rods and concrete in structural strengthening," *ACI Struct. J.*, vol. 99, no. 2, pp. 123–132, 2002, doi: 10.14359/11534.

[24] J. S. Cruz and J. Barros, "Modeling of bond between near-surface mounted CFRP laminate strips and concrete," *Comput. Struct.*, vol. 82, no. 17–19, pp. 1513–1521, 2004, doi: 10.1016/j.compstruc.2004.03.047.

[25] R. Gussenhoven and S. Brena, "Fatigue behavior of reinforced concrete beams strengthened with different FRP laminate configurations," *ACI Spec. Publ.*, pp. 613–630, 2005, [Online]. Available: http://www.concrete.org/publications/internationalconcreteabstractsportal.aspx?m=details&i=14857.

[26] J. A. O. Barros and A. S. Fortes, "Flexural strengthening of concrete beams with CFRP laminates bonded into slits," *Cem. Concr. Compos.*, vol. 27, no. 4, pp. 471–480, 2005, doi: 10.1016/j.cemconcomp.2004.07.004.

[27] L. Vasseur, S. Matthys, and L. Taerwe, "Analytical study of a 2-span reinforced concrete beam strengthened with fibre reinforced polymer," no. 1, pp. 39–46, 2006.

[28] Q. L. Ma and L. P. Ye, "Study on the Fatigue Behavior of Rc Beams Strengthened With Prestressed Cfrp Sheets Frprcs-8," pp. 1–11, 2007.

[29] R. J. Gravina and S. T. Smith, "Flexural behaviour of indeterminate concrete beams reinforced with FRP bars," *Eng. Struct.*, vol. 30, no. 9, pp. 2370–2380, 2008, doi: 10.1016/j.engstruct.2007.12.019.

[30] M. M. Önal, "Reinforcement of beams by using carbon fiber reinforced polimer in concrete buildings," *Sci. Res. Essays*, vol. 4, no. 10, pp. 1136–1145, 2009.

[31] S. Rankovic, R. Folic, and M. Mijalkovic, "Effects of RC beams reinforcement using near surface mounted reinforced FRP composites," *Facta Univ. - Ser. Archit. Civ. Eng.*, vol. 8, no. 2, pp. 177–185, 2010, doi: 10.2298/fuace1002177r.

[32] R. Kotynia *et al.*, "Repairing corroded RC beam with Near-Surface Mounted CFRP rods," *ACI Struct. J.*, vol. 04, no. 5, pp. 795–806, 2011, doi:

10.1016/j.conbuildmat.2018.06.065.

[33] S. H. Ahmad, A. Bin Najm, and A. Naani, "Flexural behavior of near surface mounted CFRP bars strengthened reinforced concrete beams," *Adv. Mater. Res.*, vol. 535–537, pp. 1702–1710, 2012, doi: 10.4028/www.scientific.net/AMR.535-537.1702.

[34] J. A. O. O. Barros *et al.*, "Application of artificial intelligence techniques to predict the performance of RC beams shear strengthened with NSM FRP rods. Formulation of design equations," *Constr. Build. Mater.*, vol. 43, no. 2, pp. 51–62, 2013, doi: 10.1016/j.compositesb.2017.01.028.

[35] R. A. Hawileh, H. A. Rasheed, J. A. Abdalla, and A. K. Al-Tamimi, "Behavior of reinforced concrete beams strengthened with externally bonded hybrid fiber reinforced polymer systems," *Mater. Des.*, vol. 53, pp. 972–982, 2014, doi: 10.1016/j.matdes.2013.07.087.

[36] I. A. Sharaky, L. Torres, and H. E. M. Sallam, "Experimental and analytical investigation into the flexural performance of RC beams with partially and fully bonded NSM FRP bars/strips," *Compos. Struct.*, vol. 122, pp. 113–126, 2015, doi: 10.1016/j.compstruct.2014.11.057.

[37] A. H. Abdullah, M. Raouf, and A. Kadir, "NSM FRP Reinforcement for Strengthening Reinforced Concrete Beams- Overview ZANCO Journal of Pure and Applied Sciences NSM FRP Reinforcement for Strengthening Reinforced Concrete Beams," *ZANCO J. Pure Appl. Sci.*, vol. 28, no. 2, pp. 178–200, 2016.

[38] S. S. Zhang and T. Yu, "Effect of groove spacing on bond strength of near-surface mounted (NSM) bonded joints with multiple FRP strips," *Constr. Build. Mater.*, vol. 155, pp. 103–113, 2017, doi: 10.1016/j.conbuildmat.2017.08.064.

[39] M. Coelho, L. Neves, and J. Sena-Cruz, "Designing NSM FRP systems in concrete using partial safety factors," *Composites Part B: Engineering*, vol. 139, pp. 12–23, 2018.

[40] F. A. Tarek Hassan1 and Sami Rizkalla, "Investigation of Bond in Concrete Structures Strengthened with Near Surface Mounted Carbon Fiber Reinforced Polymer Strips," *Constr. Build. Mater.*, vol. 28, no. 1, pp. 28–37, 2020, doi: 10.1016/j.compstruct.2020.113095.

[41] Y. Zhao, Y. Huang, H. Du, and G. Ma, "Flexural behaviour of reinforced concrete beams strengthened with pre-stressed and near surface mounted steel–basalt-fibre composite bars," *Adv. Struct. Eng.*, vol. 23, no. 6, pp. 1154–1167, 2020, doi: 10.1177/1369433219891595.

[42] F. Bencardino *et al.*, "Near-surface mounted flexural strengthening of reinforced concrete beams with low concrete strength," *Constr. Build. Mater.*, vol. 30, no. 1, pp. 1–13, 2020, doi: 10.1016/j.compstruc.2004.03.047.

[43] L. De Lorenzis, J. G. Teng, and L. Zhang, "Interfacial stresses in curved members bonded with a thin plate," *Int. J. Solids Struct.*, vol. 43, no. 25–26, pp. 7501–7517, 2006, doi: 10.1016/j.ijsolstr.2006.03.014.

[44] M. A. Hosen, M. Z. Jumaat, U. J. Alengaram, and N. H. Ramli Sulong, "CFRP strips for enhancing flexural performance of RC beams by SNSM strengthening technique," *Construction and Building Materials*, vol. 165, pp. 28–44, 2018.

[45] L. De Lorenzis and J. G. Teng, "Near-surface mounted FRP reinforcement: An emerging technique for strengthening structures," *Compos. Part B Eng.*, vol. 38, no. 2, pp. 119–143, 2007, doi: 10.1016/j.compositesb.2006.08.003.

[46] F. Bencardino *et al.*, "Near-surface mounted flexural strengthening of reinforced concrete beams with low concrete strength," *Constr. Build. Mater.*, vol. 30, no. 1, pp. 1–13, 2020, doi:

[47] ASTM International, "ASTM C 33 : Concrete Aggregates 1," vol. i, no. C, pp. 1–11, 2010.

[48] ASTM, "Standard Specification for Deformed and Plain Carbon Steel Bars for Concrete," *B. Stand. Vol. 01.04*, pp. 1–6, 2004.

[49] S. B. TRUST, "Sheet PD. Sikadur®-330," 2020.

[50] ASTM International, "Standard Test Method for Slump of Hydraulic-Cement Concrete," *Astm C143-10a*. pp. 1–4, 2010.

[51] American Society for Testing and Materials (ASTM), "Astm C78/C78M -18:," *Stand. Test Method Flexural Strength Concr. (Using Simple Beam with Third-Point Loading)ASTM Int. USA*, vol. 04.02, pp. 1–3, 2002.

[52] ASTM C496, "Standard Test Method for Splitting Tensile Strength of Cylindrical Concrete Specimens," *Manual on Hydrocarbon Analysis, 6th Edition*. pp. 545-545–3, 2008.

[53] ASTM C 192/C 192M-02, "Standard Practice for Making and Curing Concrete Test Specimens in the Laboratory," *American Society of Testing and Materials*, vol. 04, no. 02. 2002.

[54] B. S. I. Standards, "Testing concrete — compressive strength of concrete cubes," *Br. Stand. Inst.*, no. 1, pp. 1–10, 1983.

[55] S. H. R. Chair *et al.*, "Guide Test Methods for Fiber-Reinforced Polymers (FRPs) for Reinforcing or Strengthening Concrete Structures ACI 440.3R-04," 2004.

[56] Maiti and Bidinger, "Guide for the Design and Construction of Concrete Reinforced with FRP Bars (ACI 440.1R-03)," *J. Chem. Inf. Model.*, vol. 53, no. 9, pp. 1689–1699, 1981.

[57] A. Safaa, H. Abboud, and P. D. A. Y. Ali, "Behavior of Reinforced Concrete Thin Beams with Vertical and Horizontal Openings," Babylon University / College of Engineering, 2019.

[58] A. D. Canonsburg, "Known Issues and Limitations," vol. 15317, no. January, pp. 724–746, 2015.

[59] A. Ansys Release Documentation, "ANSYS Workbench Release 10.0," *ANSYS Work. Release 10.0*, 2005, [Online]. Available: http://kashanu.ac.ir/Files/Content/ANSYS Workbench.pdf.

[60] A. Majid and A. Aoun, "Comparative Study for Different Types of Reinforced Concrete Spliced Girders," 2018.

[61] P. D. P. Kohnke, *ANSYS*, 275 techno. ULregistered ISO 9001, 1994.

[62] A. A. C. I. Standard, *Building Code Requirements for Structural Concrete (ACI 318-08)*, vol. 2007. 2007.

APPENDIX A Design of Control Beam

A.1 Analysis of Reinforced Concrete Beams

All beams were design according to ACI 318M-19 Code and ACI318M-99 Code. The control beam was designed in such a way to ensure flexural failure. The control beam is without any strengthen as a reference beam, all beams have a rectangle cross-section of 150×300 mm, with a total length of 1500mm, span length 1300 mm, strengthen length 1200mm and tested under one point load. All beams had a similar clear cover of 30 mm from the bottom and 25mm from each exterior concrete face to the longitudinal reinforcement, the details of reinforcement included (3Ø12mm) diameter of deformed bars were provided as longitudinal tension reinforcement. Reinforcing bars (2Ø12mm) were used as compressive reinforce at top to prevent compression zone and (Ø10@120 mm) used as stirrups bars to hold compressive bars as shown below: -

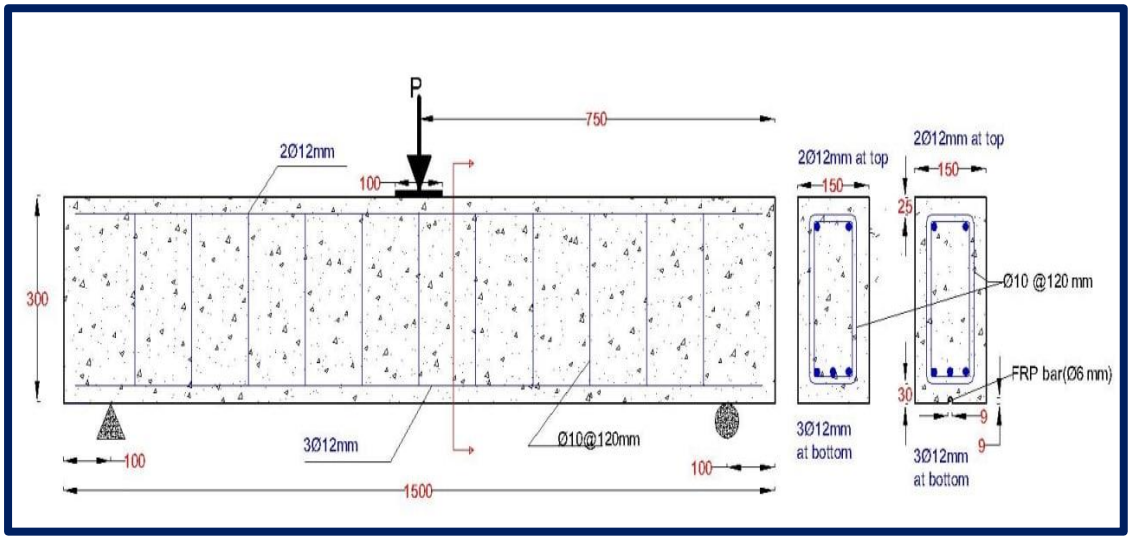

Flexural analysis for control beam in figure (1):

L=1500mm, h =300 mm, b =150 mm, f'_c = 35Mpa, Fy = 678Mpa

$f_y = 580\ Mpa$

d = $300 - 30 - 10 - 6 = 254$ mm

Check for Flexure

$$\beta = 0.85 - 0.05 * \left(\frac{fc - 28}{7}\right) \geq 0.65 \quad , \beta = 0.8$$

As*f_y =0.85 *f'_c * β *c* b + As′ ($\frac{c-\mathrm{d}'}{7}$)*600

C=40.56

a= β*c=0.8*40.54 = 32.43

fs`= $\frac{\mathrm{c}-\mathrm{d}`}{\mathrm{c}}$* 600 = 229.9 = 300 ∴ used

As2 = $\frac{\mathrm{As}`*fc`}{fy}$ = $\frac{226.2*35}{580}$ =13.65

As1 = As – As2 = 325.65 mm^2

$$\in s` = \frac{d - c}{c} * 0.003 = \frac{254 - 40.54}{40.54} * 0.003$$

=0.01 > 0.005 ∴

$M_n = A_s.f_y\left(d - \frac{a}{2}\right)$+ As′ ∗ fs′ $(d - \mathrm{d}')$

$M_n = 325.65 * 280\left(254 - \frac{32.43}{2}\right) + 226.2 * 300\ (254 - 25)$

Mn= 60. 45 kN.m

$$\mathrm{Mn} = \frac{Pn * \mathrm{L}}{4}$$

∴ Pn = 161.2 kN

Check for Shear

$$\boldsymbol{\rho} max = 0.85 * \beta 1 * \left(\frac{\sqrt{f'_c}}{400}\right) * \left(\frac{0.003}{0.007}\right)$$

$$\boldsymbol{\rho} max = 0.027$$

$$\boldsymbol{\rho} min = max\left(\frac{1.4}{400}\right)\left(\frac{\sqrt{f'_c}}{4 * 400}\right) = max(0.0035, 0.00369)$$

$$\boldsymbol{\rho} min = 0.0037$$

For shear Ø10@120mm $Av = \frac{\pi}{4} * d^2 = 78.5mm^2$

$$Vs = \frac{Av * fy * d}{S} * 10^{-3}, \quad S = \frac{d}{2} = \frac{254}{2} = 125.6kN$$

$$Vs = 125.6kN$$

$Vc = 0.17 * \sqrt{f'_c} * bw$*d

$$Vc = 38.318kN$$

$$Vn = Vc + Vs = 163.92kN$$

$$Vn = \frac{Pn}{2}$$

- Pn = 327.84 kN
- used Pn min
- Pn = 161.2 kN

APPENDIX B Material Safety Datasheets

B.1 Data sheet of steel fibers provided by the manufacturer

赣州大业金属纤维有限公司

Ganzhou Daye Metallic Fibres Co., Ltd

Steel fiber for concrete reinforcement

http//: www.gzdymf.com • Email: may@gzdymf.com • Tel: +86-797-8259566 • Fax:+86-797-8259568



Product Description

Micro Steel Fiber	
Type	WSF 0213
Surface	Brass coated

Chemical Composition

C:	MN:	P:	S:	Si:
≈0.80%	≈0.75%	≈0.035%	≈0.035%	≈0.30%

Tensile Strength	Minimum 2300Mpa
Melting Point	1500°C
Length	13mm±1mm
Diameter	≈0.2mm±0.05mm
Form	Straight

This steel fibers can be produced with different length and diameters

Package: By damp-proof poly bag, 25Kg/bag,1800Kg/pallet, 18000Kg/20ft container.

Application: Micro steel fiber is the material of ultra high performance concrete (UHPC), Reactive powder concrete (RPC) and slurry infiltrated concrete(SIFCON) , is well used in the project such as bank cash-box, strong-box, plant , water conservancy, foundation grouting, military project and blast protect panel and etc.


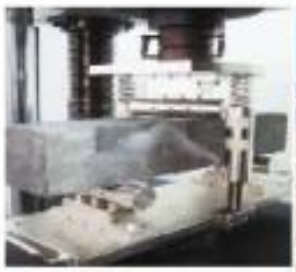


B.2 Data sheet of CFRP provided by the manufacturer

产品型号 Type No.	大小 Size	公称直径 Nominal Diameter (mm)	公称横截面积 Nominal Area (mm^2)	极限抗拉力 Ultimate Tensile Load (KN)	保证抗拉强度 Guaranteed Tensile Strength (MPa)	弹性模量 Modulus of Elasticity (GPa)
B200-6	2	6	31.67	71	2241	124
B200-10	3	10	71.26	154	2172	124
B200-13	4	13	126.7	262	2068	124

产品规格可根据需求定制 / Other types are on request

B.3 Data sheet of GFRP provided by the manufacturer

产品型号 Type No.	大小 Size	公称直径 Nominal Diameter (mm)	公称横截面积 Nominal Area (mm^2)	极限抗拉力 Ultimate Tensile Load (KN)	保证抗拉强度 Guaranteed Tensile Strength (MPa)	弹性模量 Modulus of Elasticity (GPa)	单位重量 Weight (g/m)	剪切强度 Transverse Shear Strength (MPa)
B100-6	2	6	31.67	28	896	46	77.4	150
B100-10	3	10	71.26	59	827	46	159	
B100-13	4	13	126.7	96	758	46	281.3	
B100-16	5	16	197.9	143	724	46	427.1	
B100-19	6	19	285	197	690	46	607.2	
B100-22	7	22	387.9	254	655	46	809.6	
B100-25	8	25	506.7	314	620	46	1046.2	
B100-29	9	29	641.3	376	588	46	1413.7	
B100-32	10	32	791.7	437	551	46	1711.4	
B100-35	11	35	958.1	462	482	46	1934.6	
B100-38	12	38	1160	520	448	46	2455.4	
B100-41	13	41	1338	554	413	46	2872.1	

B.4 Data sheet of CFRP sheet (Sika Warp-C300) provided by the manufacturer

PRODUCT DATA SHEET

SikaWrap®-300 C

WOVEN UNIDIRECTIONAL CARBON FIBRE FABRIC, DESIGNED FOR STRUCTURAL STRENGTHENING APPLICATIONS AS PART OF THE SIKA® STRENGTHENING SYSTEM.

DESCRIPTION

SikaWrap®-300 C is a unidirectional woven carbon fibre fabric with mid-range strengths, designed for installation using the dry or wet application process.

USES

SikaWrap®-300 C may only be used by experienced professionals.
Structural strengthening of reinforced concrete, masonry, brickwork and timber elements or structures, to increase flexural and shear loading capacity for:

- Improved seismic performance of masonry walls
- Replacing missing steel reinforcement
- Increasing the strength and ductility of columns
- Increasing the loading capacity of structural elements
- Enabling changes in use / alterations and refurbishment
- Correcting structural design and / or construction defects
- Increasing resistance to seismic movement
- Improving service life and durability
- Structural upgrading to comply with current standards

CHARACTERISTICS / ADVANTAGES

- Multifunctional fabric for use in many different strengthening applications
- Flexible and accommodating to different surface planes and geometry (beams, columns, chimneys, piles, walls, soffits, silos etc.)
- Low density for minimal additional weight
- Extremely cost effective in comparison to traditional strengthening techniques

APPROVALS / STANDARDS

- Poland: Technical Approval ITB AT-15-5604/2011: Zestaw wyrobów Sika CarboDur do wzmacniania i napraw konstrukcji betonowych
- Poland: Technical Approval IBDiM Nr AT/2008-03-0336/1 „Płaskowniki. pręty, kształtki i maty kompozytowe do wzmacniania betonu o nazwie handlowej: Zestaw materiałów Sika CarboDur® do wzmacniania konstrukcji obiektów mostowych
- USA: ACI 440.2R-08, Guide for the Design and construction of Externally Bonded FRP Systems for strengthening concrete structures, July 2008
- UK: Concrete Society Technical Report No. 55, Design guidance for strengthening concrete structures using fibre composite material, 2012.

PRODUCT INFORMATION

Construction	Fibre orientation	0° (unidirectional)	
	Warp	Black carbon fibres 99 %	
	Weft	White thermoplastic heat-set fibres 1 %	
Fibre Type	Selected mid-range strength carbon fibres		
Packaging		**Fabric length per roll**	**Fabric width**
	10 rolls in cardboard box	≥ 50 m	100 mm
	4 rolls in cardboard box	≥ 50 m	300 mm
	2 rolls in cardboard box	≥ 50 m	600 mm

APPLICATION INFORMATION

Consumption

Dry application with Sikadur®-330

First layer including primer layer	1.0–1.5 kg/m²
Following layers	0.8 kg/m²

Wet application with Sikadur®-300, primer Sikadur®-330

Primer layer	0.4–0.6 kg/m²
Fabric layers	0.6 kg/m²

Please also refer to the relevant Method Statement for further information.

APPLICATION INSTRUCTIONS

SUBSTRATE QUALITY

Minimum substrate tensile strength: 1.0 N/mm² or as specified in the strengthening design.
Please also refer to the relevant Method Statement for further information..

SUBSTRATE PREPARATION

Concrete must be cleaned and prepared to achieve a laitance and contaminant free, open textured surface.
Please also refer to the relevant Method Statement for further information.

APPLICATION METHOD / TOOLS

The fabric can be cut with special scissors or a Stanley knife (razor knife / box-cutter knife). Never fold the fabric.
SikaWrap®-300 C is applied using the dry or wet application process.
Please refer to the relevant Method Statement for details on the impregnating / laminating procedure.

FURTHER DOCUMENTS

Method Statements
Ref. 850 41 02: SikaWrap® manual dry application
Ref. 850 41 03: SikaWrap® manual wet application
Ref. 850 41 04: SikaWrap® machine wet application

LIMITATIONS

- SikaWrap®-300 C shall only be applied by trained and experienced professionals.
- A specialist structural engineer must be consulted for any structural strengthening design calculation.
- SikaWrap®-300 C fabric is coated to ensure maximum bond and durability with the Sikadur® adhesives / impregnating / laminating resins. To maintain and ensure full system compatibility, do not interchange different system components.
- SikaWrap®-300 C can be over coated with a cementitious overlay or other coatings for aesthetic and / or protective purposes. The over coating system selection is dependent on the exposure and the project specific requirements. For additional UV light protection in exposed areas use Sikagard®-550 W Elastic, Sikagard® ElastoColor-675 W or Sikagard®-680 S.
- Please refer to the Method Statement of SikaWrap® manual dry application (Ref. 850 41 02), SikaWrap® manual wet application (Ref. 850 41 03) or SikaWrap® machine wet application (Ref. 850 41 04) for further information, guidelines and limitations.

BASIS OF PRODUCT DATA

All technical data stated in this Product Data Sheet are based on laboratory tests. Actual measured data may vary due to circumstances beyond our control.

LOCAL RESTRICTIONS

Please note that as a result of specific local regulations the performance of this product may vary from country to country. Please consult the local Product Data Sheet for the exact description of the application fields.

ECOLOGY, HEALTH AND SAFETY

REGULATION (EC) NO 1907/2006 - REACH

This product is an article as defined in article 3 of regulation (EC) No 1907/2006 (REACH). It contains no substances which are intended to be released from the article under normal or reasonably foreseeable conditions of use. A safety data sheet following article 31 of the same regulation is not needed to bring the product to the market, to transport or to use it. For safe use follow the instructions given in this product data sheet.Based on our current knowledge, this product does not contain SVHC (substances of very high concern) as listed in Annex XIV of the REACH regulation or on the candidate list published by the European Chemicals Agency in concentrations above 0.1 % (w/w)

LEGAL NOTES

The information, and, in particular, the recommendations relating to the application and end-use of Sika products, are given in good faith based on Sika's current knowledge and experience of the products when properly stored, handled and applied under normal conditions in accordance with Sika's recommendations. In practice, the differences in materials, substrates and actual site conditions are such that no warranty in respect of merchantability or of fitness for a particular purpose, nor any liability arising out of any legal relationship whatsoever, can be inferred either from this information, or from any written recommendations, or from any other advice offered. The

Shelf life	24 months from date of production	
Storage conditions	Store in undamaged, original sealed packaging, in dry conditions at temperatures between +5 °C and +35 °C. Protect from direct sunlight.	
Dry Fibre Density	1.82 g/cm³	
Dry Fibre Thickness	0.167 mm (based on fibre content)	
Area Density	304 g/m² ±10 g/m² (carbon fibres only)	
Dry Fibre Tensile Strength	4 000 N/mm²	(ISO 10618)
Dry Fibre Modulus of Elasticity in Tension	230 000 N/mm²	(ISO 10618)
Dry Fibre Elongation at Break	1.7 %	(ISO 10618)

TECHNICAL INFORMATION

Laminate Nominal Thickness	0.167 mm		
Laminate Nominal Cross Section	167 mm² per m width		
Laminate Tensile Strength	**Average** 3 500 N/mm²	**Characteristic** 3 200 kN/mm²	(EN 2561*) (ASTM D 3039*)
Laminate Modulus of Elasticity in Tension	**Average** 225 kN/mm²	**Characteristic** 220 kN/mm²	(EN 2561*)
	Average 220 kN/mm²	**Characteristic** 210 kN/mm²	(ASTM D 3039*)
	* modification: sample with 50 mm Values in the longitudinal direction of the fibres Single layer, minimum 27 samples per test series		
Laminate Elongation at Break in Tension	1.56 % 1.59 %		(based on EN 2561) (based on ASTM D 3039)
Tensile Resistance	**Average** 585 N/mm	**Characterstic** 534 N/mm	(based on EN 2561) (based on ASTM D 3039)
Tensile Stiffness	**Average** 37.6 MN/m 37.6 kN/m per ‰ elongation	**Characteristic** 36.7 MN/m 36.7 kN/m per ‰ elongation	(based on EN 2561)
	Average 36.7 MN/m 36.7 kN/m per ‰ elongation	**Characteristic** 35.1 MN/m 35.1 kN/m per ‰ elongation	(based no ASTM D 3039)

SYSTEM INFORMATION

System Structure

The system build-up and configuration as described must be fully complied with and may not be changed.

Concrete substrate adhesive primer	Sikadur®-330
Impregnating / laminating resin	Sikadur®-330 or Sikadur®-300
Structural strengthening fabric	SikaWrap®-300 C

For detailed information on Sikadur®-330 or Sikadur®-300, together with the resin and fabric application details, please refer to the Sikadur®-330 or Sikadur®-300 Product Data Sheet and the relevant Method Statement.

user of the product must test the product's suitability for the intended application and purpose. Sika reserves the right to change the properties of its products. The proprietary rights of third parties must be observed. All orders are accepted subject to our current terms of sale and delivery. Users must always refer to the most recent issue of the local Product Data Sheet for the product concerned, copies of which will be supplied on request. It may be necessary to adapt the above disclaimer to specific local laws and regulations. Any changes to this disclaimer may only be implemented with permission of Sika® Corporate Legal in Baar.

Sika Egypt
1st Industrial Zone (A)
Section #10, Block 13035
El Obour City, Egypt
TEL: +202 44810580
FAX: +202 44810459
www.sika.com.eg

B.5 Data sheet of Sika Dur-330 provided by the manufacturer

BUILDING TRUST

PRODUCT DATA SHEET

Sikadur®-330

HIGH-MODULUS, HIGH-STRENGTH, IMPREGNATING RESIN

PRODUCT DESCRIPTION

Sikadur®-330 is a two-component , solvent-free, moisture-tolerant, high strength, high modulus structural epoxy adhesive.

USES

Sikadur®-330 may only be used by experienced professionals.
For use as an impregnating resin with the SikaWrap® Hex 106G, 113C, 117C, 230C and 430G Structural Strengthening Systems.

CHARACTERISTICS / ADVANTAGES

- Long pot life.
- Long open time.
- Easy to mix.
- Tolerant of moisture before, during and after cure.
- High strength, high modulus adhesive.
- Excellent adhesion to concrete, masonry, metals, wood and most structural materials.
- Fully compatible and developed specifically for the SikaWrap® Systems.
- High temperature resistance.
- High abrasion and shock resistance.
- Solvent-free, VOC compliant.

PRODUCT INFORMATION

Packaging	3.2 gal. (12 L) kit / (2) two 1.25 gal. (4.7 L) Component A pails, (2) two 0.35 gal. (1.3 L) Component B pails
Color	Light gray
Shelf Life	2 years in original, unopened container
Storage Conditions	Store dry at 40–95 °F (4–35 °C). Condition material to 65–75 °F (18–24 °C) before using.
Consistency	Non-sag paste

TECHNICAL INFORMATION

Compressive Strength		**60 °F (16 °C)**	**73 °F (23 °C)**	**90 °F (32 °C)**	(ASTM D-695) 50 % R.H.
	8 hour	-	-	8,000 psi (55.2 MPa)	
	1 day	8,100 psi (55.8 MPa)	10,700 psi (73.7 MPa)	10,600 psi (73.1 MPa)	
	3 day	11,200 psi (77.2 MPa)	11,100 psi (76.5 MPa)	11,000 psi (75.8 MPa)	
	7 day	11,600 psi (80.0 MPa)	11,200 psi (77.2 MPa)	11,800 psi (81.3 MPa)	
	14 day	12,400 psi (85.5 MPa)	11,800 psi (81.3 MPa)	11,900 psi (82.0 MPa)	
Flexural Strength	8,800 psi (60.6 MPa) (7 days)				(ASTM D-790) 73 °F (23 °C) 50 % R.H.
Modulus of Elasticity in Flexure	5.06 x 105 psi (3,489 MPa) (7 days)				(ASTM D-790) 73 °F (23 °C) 50 % R.H.
Tensile Strength	4,900 psi (33.8 MPa) (7 days)				(ASTM D-638) 73 °F (23 °C) 50 % R.H.
Elongation at Break	1.2 % (7 days)				(ASTM D-638) 73 °F (23 °C) 50 % R.H.
Heat Deflection Temperature	120 °F (50 °C) (7 days)				(ASTM D-648) [fiber stress loading=264 psi (1.8 MPa)]

APPLICATION INFORMATION

Mixing Ratio	Component 'A' : Component 'B' = 4 : 1 by weight
Coverage	First coat: 40-50 ft²/gal.; Additional coats: 100 ft²/gal.; Final coat: 160 ft²/gal.
Pot Life	57 minutes (325 ml)
Cure Time	**Tack Free Time**: 4–5 hours

APPLICATION INSTRUCTIONS

SUBSTRATE PREPARATION

The concrete surface should be prepared to a minimum concrete surface profile (CSP-3) as defined by the ICRI-surface-profile chips. Localized out-of-plane variations, including form lines, should not exceed 1/32 in. (1 mm). Substrate must be clean, sound, and free of surface moisture. Remove dust, laitance, grease, oils, curing compounds, waxes, impregnations, foreign particles, coatings and disintegrated materials by mechanical means (i.e. sandblasting). For best results, substrate should be dry. However, a saturated surface dry condition is acceptable.

MIXING

Pre-mix each component. Mix entire unit, do not batch. Pour contents of part B to part A. Mix thoroughly for 5 minutes with a 1/2 inch "Jiffy" mixer mounted on a rotary drill and set at a slow speed (400–600 rpm) until uniformly blended. Mix only that quantity that can be used within its pot life.

APPLICATION METHOD / TOOLS

Dry Lay-Up: When installing a SikaWrap® Hex fabric in the dry lay-up process apply the mixed Sikadur®-330 epoxy resin directly onto the substrate at a rate of 40–50 ft.2/gal. (0.95–1.18 m²/L). Coverage rate will depend on the actual surface profile. This equates to a thickness of approximately 32–40 mils. Carefully place the fabric into

the applied resin with gloved hands and smooth out. Work out any irregularities or air pockets with a plastic laminating roller. Let the resin squeeze out between the rovings of the fabric. If more than one layer of fabric is required, apply additional Sikadur®-330 at a rate of 100 ft^2/gal. (2.37 m2/L) and repeat as described above. This equates to a thickness of approximately 16 mils. Add a final layer of Sikadur®-330 onto the exposed surface at a rate of 160 ft^2/gal. (3.79 m^2/L). This equates to a thickness of approximately 10 mils.

Wet Lay-Up: When installing a SikaWrap® Hex fabric vertically or overhead in the wet lay-up process, mixed Sikadur®-330 can be applied to the substrate as a primer/tack coat to prevent the impregnated fabric from sliding down the concrete. Due to its mixed viscosity, do not use Sikadur®-330 with an automatic fabric saturating device. Consult the SikaWrap® Hex fabric technical data sheet for information on saturating/impregnating fabric in a wet lay-up installation.

CLEANING OF TOOLS

Clean all equipment immediately with Sika® Colma Cleaner. Cured material can only be removed mechanically.

LIMITATIONS

- Minimum age of concrete is 21–28 days, depending on curing and drying conditions.
- All repairs required to achieve a level surface must be performed prior to application.
- Do not apply or cure Sikadur®-330 in direct sunlight.
- Minimum substrate temperature 40 °F (4 °C). Maximum application temperature 95 °C (35 °C)
- Do not thin with solvents.
- Material is a vapor barrier after cure.
- Do not encapsulate saturated concrete in areas of freezing and thawing.
- Color of Sikadur®-330 may alter due to variations in lighting and/or UV exposure.
- Due to its mixed viscosity, do not use Sikadur®-330 with an automatic saturating device. Fabric must be saturated/impregnated manually when the wet lay-up process is used.
- At low temperatures and/or high relative humidity, a slight oily residue (blush) may form on the surface of the cured epoxy. If an additional layer of fabric, or a coating is to be applied onto the cured epoxy. This residue must first be removed to ensure adequate bond. The residue can be removed with either a solvent wipe (e.g. MEK) or with water and detergent. In both cases, the surface should be wiped dry prior to application of the next layer or coating.
- Not an aesthetic product. Color may alter due to variations in lighting and/or UV exposure.

BASIS OF PRODUCT DATA

Results may differ based upon statistical variations depending upon mixing methods and equipment, temperature, application methods, test methods, actual site conditions and curing conditions.

OTHER RESTRICTIONS

See Legal Disclaimer.

ENVIRONMENTAL, HEALTH AND SAFETY

For further information and advice regarding transportation, handling, storage and disposal of chemical products, user should refer to the actual Safety Data Sheets containing physical, environmental, toxicological and other safety related data. User must read the current actual Safety Data Sheets before using any products. In case of an emergency, call CHEMTREC at 1-800-424-9300, International 703-527-3887.

LEGAL DISCLAIMER

- **KEEP CONTAINER TIGHTLY CLOSED**
- **KEEP OUT OF REACH OF CHILDREN**
- **NOT FOR INTERNAL CONSUMPTION**
- **FOR INDUSTRIAL USE ONLY**
- **FOR PROFESSIONAL USE ONLY**

Prior to each use of any product of Sika Corporation, its subsidiaries or affiliates ("SIKA"), the user must always read and follow the warnings and instructions on the product's most current product label, Product Data Sheet and Safety Data Sheet which are available at usa.sika.com or by calling SIKA's Technical Service Department at 1-800-933-7452. Nothing contained in any SIKA literature or materials relieves the user of the obligation to read and follow the warnings and instructions for each SIKA product as set forth in the current product label, Product Data Sheet and Safety Data Sheet prior to use of the SIKA product.

SIKA warrants this product for one year from date of installation to be free from manufacturing defects and to meet the technical properties on the current Product Data Sheet if used as directed within the product's shelf life. User determines suitability of product for intended use and assumes all risks. User's and/or buyer's sole remedy shall be limited to the purchase price or replacement of this product exclusive of any labor costs. **NO OTHER WARRANTIES EXPRESS OR IMPLIED SHALL APPLY INCLUDING ANY WARRANTY OF MERCHANTABILITY OR FITNESS FOR A PARTICULAR PURPOSE. SIKA SHALL NOT BE LIABLE UNDER ANY LEGAL THEORY FOR SPECIAL OR CONSEQUENTIAL DAMAGES. SIKA SHALL NOT BE RESPONSIBLE FOR THE USE OF THIS PRODUCT IN A MANNER TO INFRINGE ON ANY PATENT OR ANY OTHER INTELLECTUAL PROPERTY RIGHTS HELD BY OTHERS.**

the applied resin with gloved hands and smooth out. Work out any irregularities or air pockets with a plastic laminating roller. Let the resin squeeze out between the rovings of the fabric. If more than one layer of fabric is required, apply additional Sikadur®-330 at a rate of 100 ft²/gal. (2.37 m2/L) and repeat as described above. This equates to a thickness of approximately 16 mils. Add a final layer of Sikadur®-330 onto the exposed surface at a rate of 160 ft²/gal. (3.79 m²/L). This equates to a thickness of approximately 10 mils.

Wet Lay-Up: When installing a SikaWrap® Hex fabric vertically or overhead in the wet lay-up process, mixed Sikadur®-330 can be applied to the substrate as a primer/tack coat to prevent the impregnated fabric from sliding down the concrete. Due to its mixed viscosity, do not use Sikadur®-330 with an automatic fabric saturating device. Consult the SikaWrap® Hex fabric technical data sheet for information on saturating/impregnating fabric in a wet lay-up installation.

CLEANING OF TOOLS

Clean all equipment immediately with Sika® Colma Cleaner. Cured material can only be removed mechanically.

LIMITATIONS

- Minimum age of concrete is 21–28 days, depending on curing and drying conditions.
- All repairs required to achieve a level surface must be performed prior to application.
- Do not apply or cure Sikadur®-330 in direct sunlight.
- Minimum substrate temperature 40 °F (4 °C). Maximum application temperature 95 °C (35 °C)
- Do not thin with solvents.
- Material is a vapor barrier after cure.
- Do not encapsulate saturated concrete in areas of freezing and thawing.
- Color of Sikadur®-330 may alter due to variations in lighting and/or UV exposure.
- Due to its mixed viscosity, do not use Sikadur®-330 with an automatic saturating device. Fabric must be saturated/impregnated manually when the wet lay-up process is used.
- At low temperatures and/or high relative humidity, a slight oily residue (blush) may form on the surface of the cured epoxy. If an additional layer of fabric, or a coating is to be applied onto the cured epoxy. This residue must first be removed to ensure adequate bond. The residue can be removed with either a solvent wipe (e.g. MEK) or with water and detergent. In both cases, the surface should be wiped dry prior to application of the next layer or coating.
- Not an aesthetic product. Color may alter due to variations in lighting and/or UV exposure.

BASIS OF PRODUCT DATA

Results may differ based upon statistical variations depending upon mixing methods and equipment, temperature, application methods, test methods, actual site conditions and curing conditions.

OTHER RESTRICTIONS

See Legal Disclaimer.

ENVIRONMENTAL, HEALTH AND SAFETY

For further information and advice regarding transportation, handling, storage and disposal of chemical products, user should refer to the actual Safety Data Sheets containing physical, environmental, toxicological and other safety related data. User must read the current actual Safety Data Sheets before using any products. In case of an emergency, call CHEMTREC at 1-800-424-9300, International 703-527-3887.

LEGAL DISCLAIMER

- **KEEP CONTAINER TIGHTLY CLOSED**
- **KEEP OUT OF REACH OF CHILDREN**
- **NOT FOR INTERNAL CONSUMPTION**
- **FOR INDUSTRIAL USE ONLY**
- **FOR PROFESSIONAL USE ONLY**

Prior to each use of any product of Sika Corporation, its subsidiaries or affiliates ("SIKA"), the user must always read and follow the warnings and instructions on the product's most current product label, Product Data Sheet and Safety Data Sheet which are available at usa.sika.com or by calling SIKA's Technical Service Department at 1-800-933-7452. Nothing contained in any SIKA literature or materials relieves the user of the obligation to read and follow the warnings and instructions for each SIKA product as set forth in the current product label, Product Data Sheet and Safety Data Sheet prior to use of the SIKA product.

SIKA warrants this product for one year from date of installation to be free from manufacturing defects and to meet the technical properties on the current Product Data Sheet if used as directed within the product's shelf life. User determines suitability of product for intended use and assumes all risks. User's and/or buyer's sole remedy shall be limited to the purchase price or replacement of this product exclusive of any labor costs. **NO OTHER WARRANTIES EXPRESS OR IMPLIED SHALL APPLY INCLUDING ANY WARRANTY OF MERCHANTABILITY OR FITNESS FOR A PARTICULAR PURPOSE. SIKA SHALL NOT BE LIABLE UNDER ANY LEGAL THEORY FOR SPECIAL OR CONSEQUENTIAL DAMAGES. SIKA SHALL NOT BE RESPONSIBLE FOR THE USE OF THIS PRODUCT IN A MANNER TO INFRINGE ON ANY PATENT OR ANY OTHER INTELLECTUAL PROPERTY RIGHTS HELD BY OTHERS.**

Sale of SIKA products are subject to the Terms and Conditions of Sale which are available at https://usa.sika.com/en/group/SikaCorp/termsandconditions.html or by calling 1-800-933-7452.

Sika Corporation
201 Polito Avenue
Lyndhurst, NJ 07071
Phone: +1-800-933-7452
Fax: +1-201-933-6225
usa.sika.com

Sika Mexicana S.A. de C.V.
Carretera Libre Celaya Km. 8.5
Fracc. Industrial Balvanera
Corregidora, Queretaro
C.P. 76920
Phone: 52 442 2385800
Fax: 52 442 2250537

APPENDIX C Strain Gage for All Specimens

C.1 Data of strain gage for specimen group one

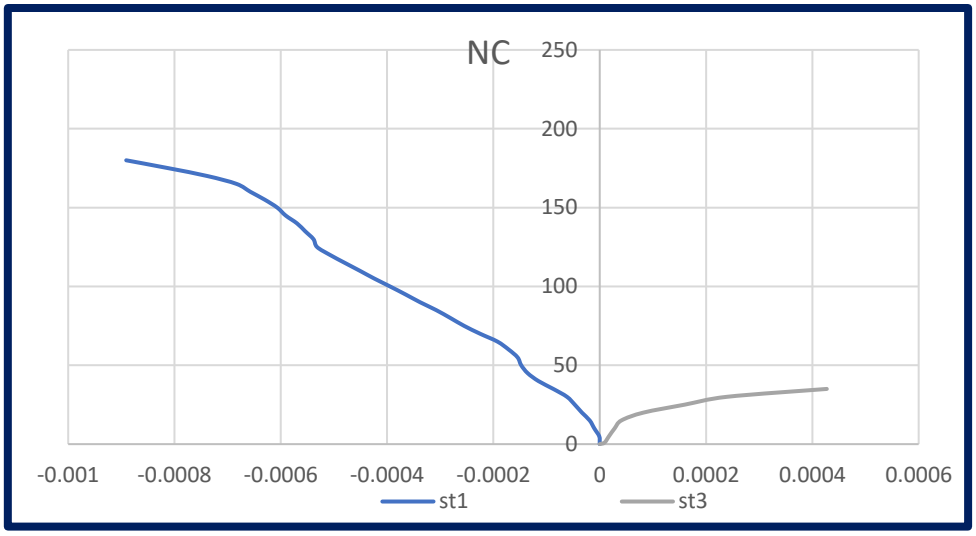

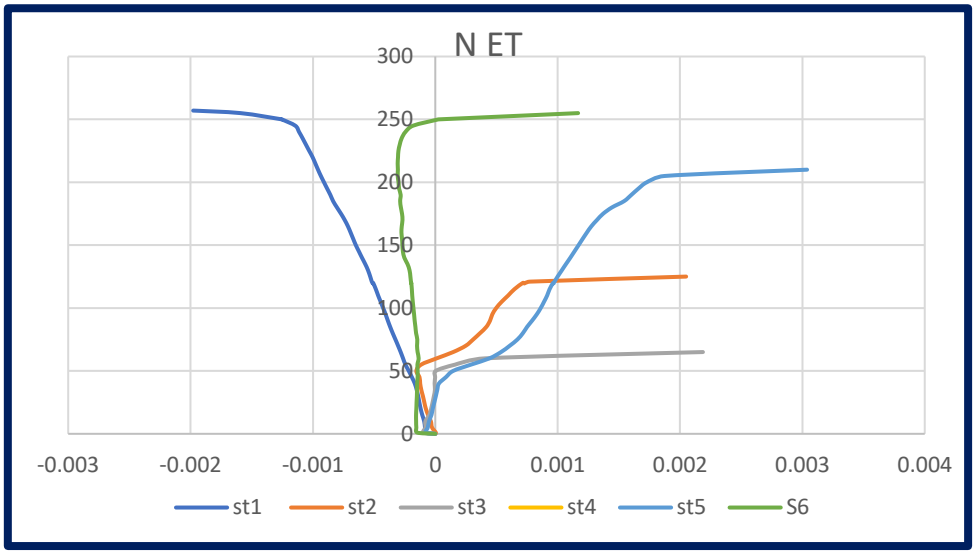

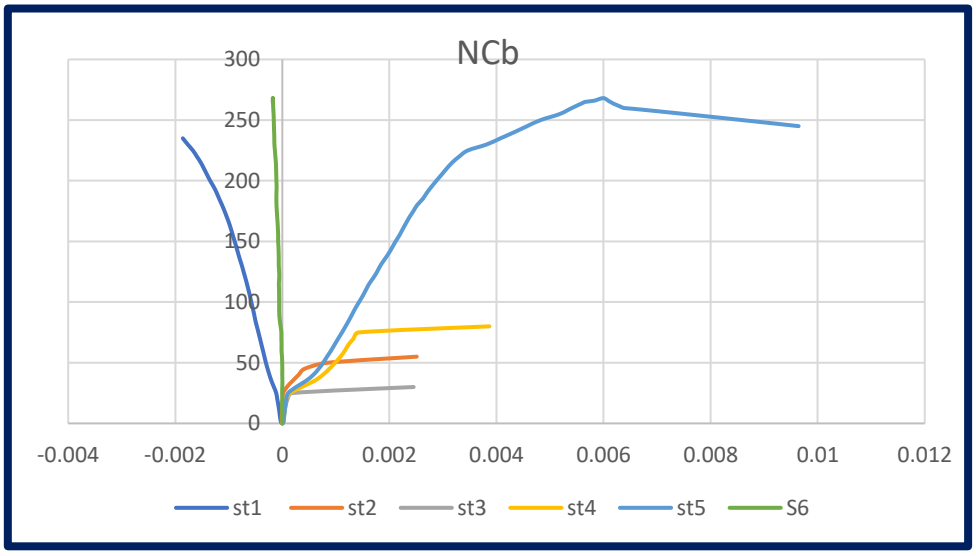

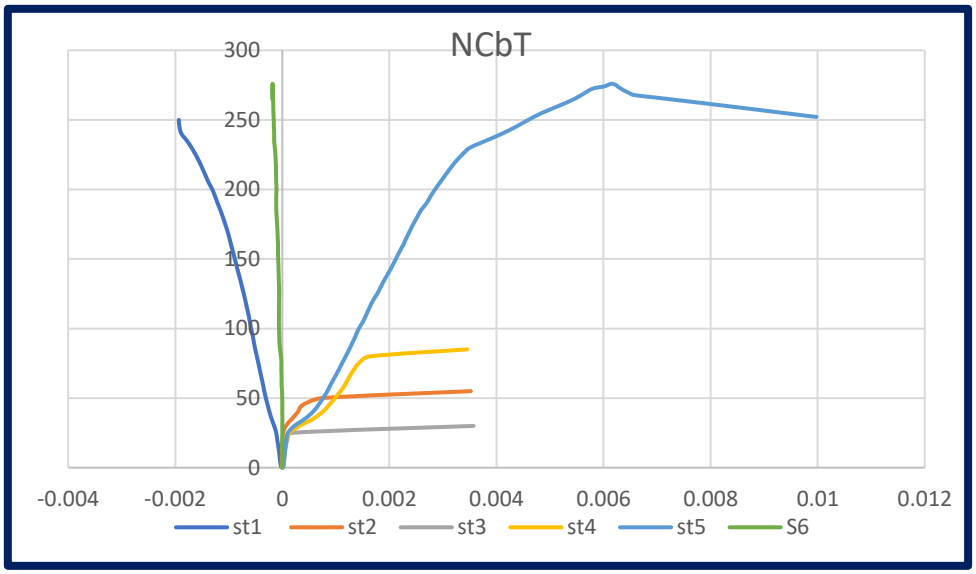
NCbT
300
250
200
150
100
50
0
-0.004
-0.002
0
0.002
0.004
0.006
0.008
0.01
0.012
st1
st2
st3
st4
st5
S6

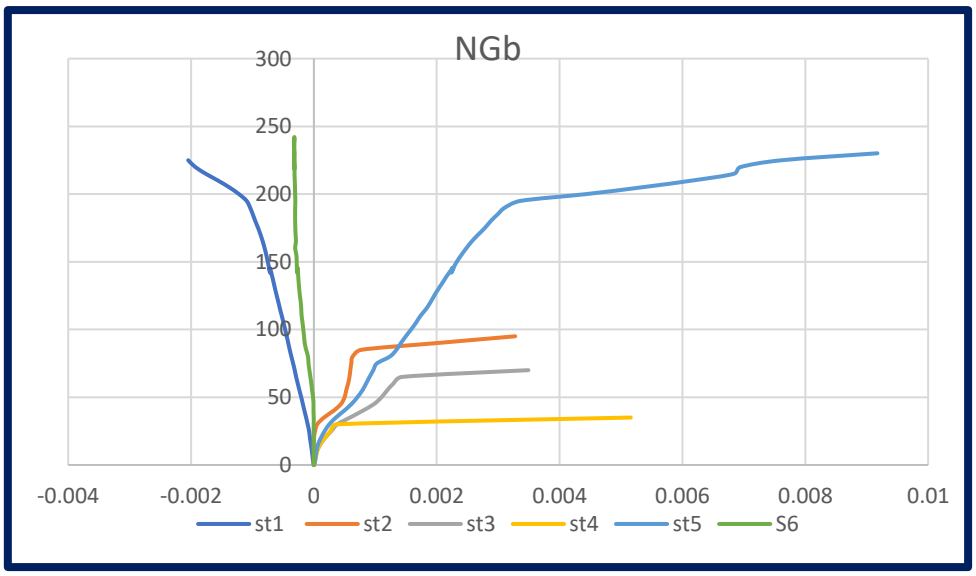
NGb
300
250
200
150
100
50
0
-0.004
-0.002
0
0.002
0.004
0.006
0.008
0.01
st1
st2
st3
st4
st5
S6

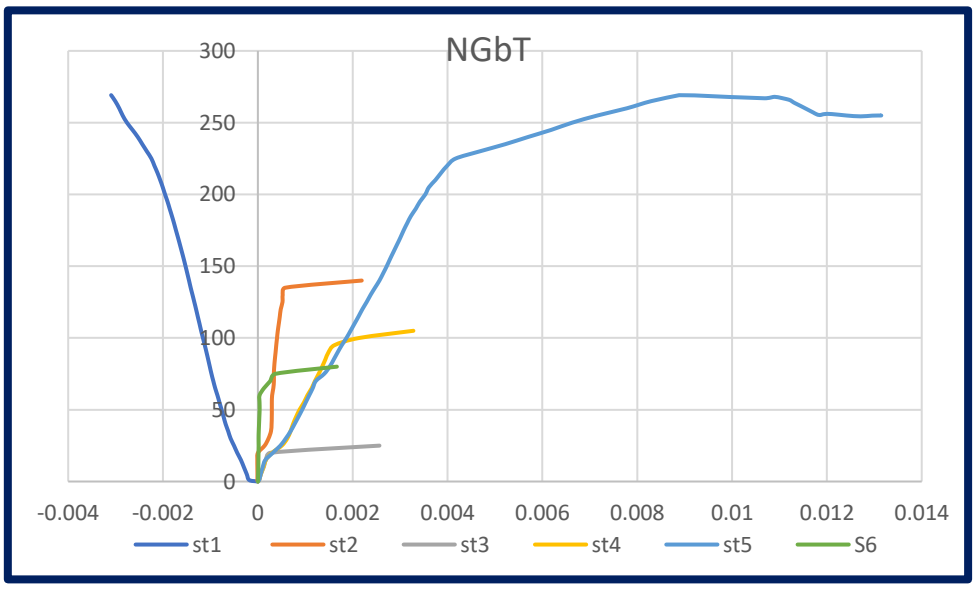
NGbT
300
250
200
150
100
50
0
-0.004
-0.002
0
0.002
0.004
0.006
0.008
0.01
0.012
0.014
st1
st2
st3
st4
st5
S6

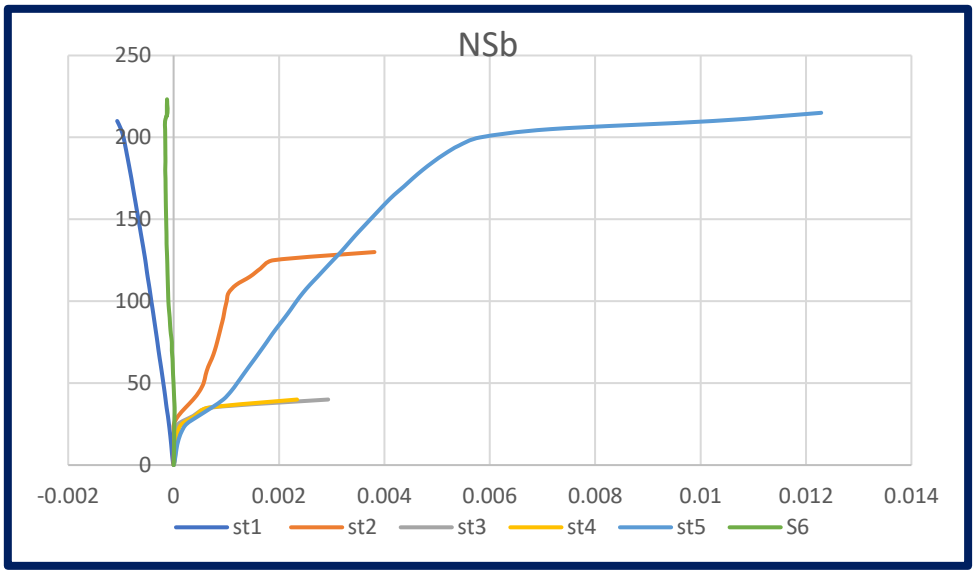

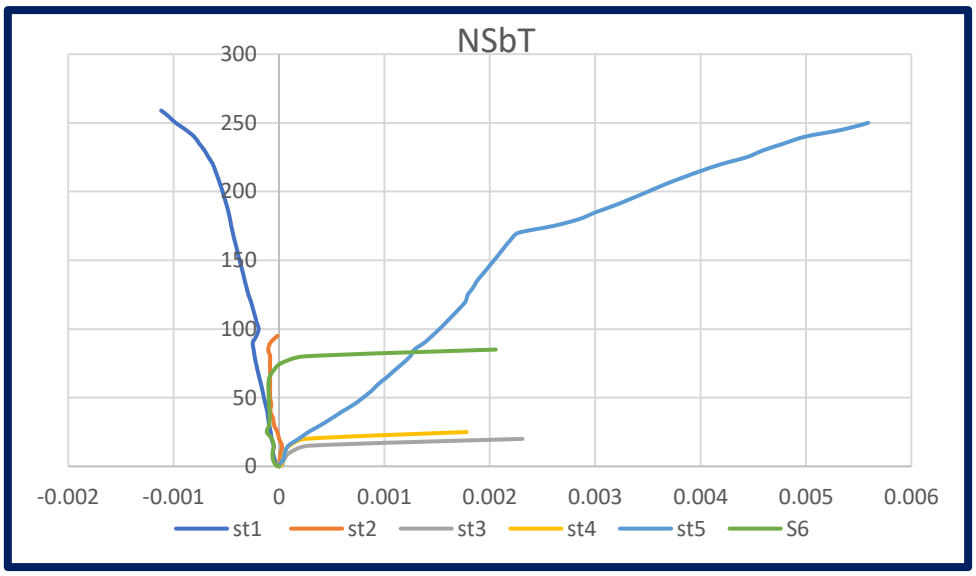

C.2 Data of strain gage for specimen group two

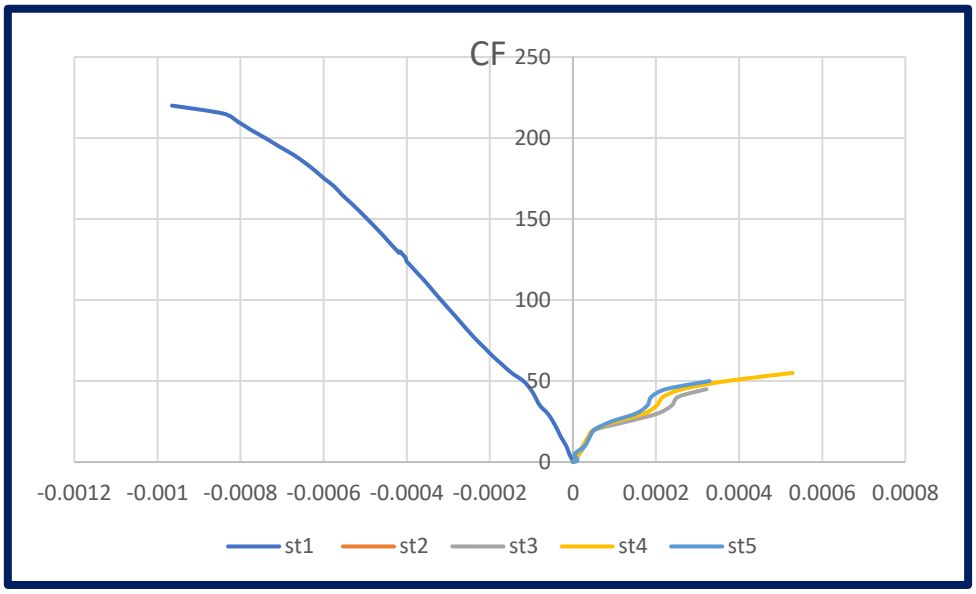

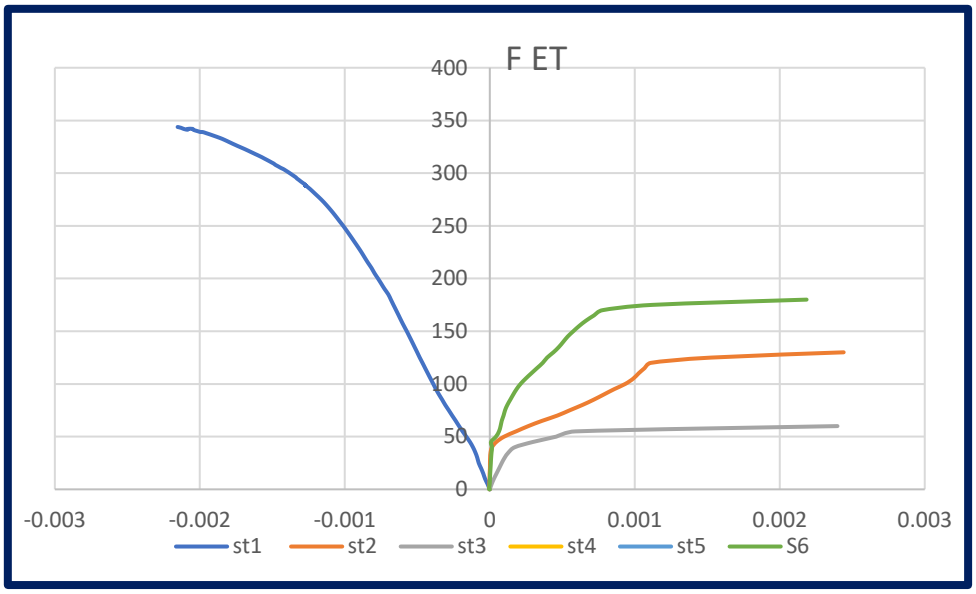
F ET
400
350
300
250
200
150
100
50
0
-0.003
-0.002
-0.001
0
0.001
0.002
0.003
st1
st2
st3
st4
st5
S6

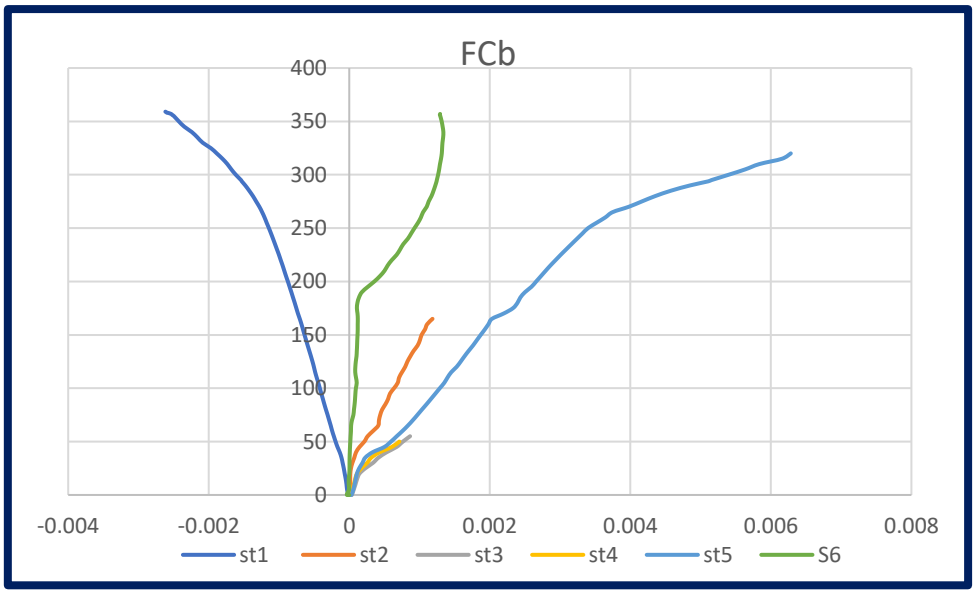
FCb
400
350
300
250
200
150
100
50
0
-0.004
-0.002
0
0.002
0.004
0.006
0.008
st1
st2
st3
st4
st5
S6

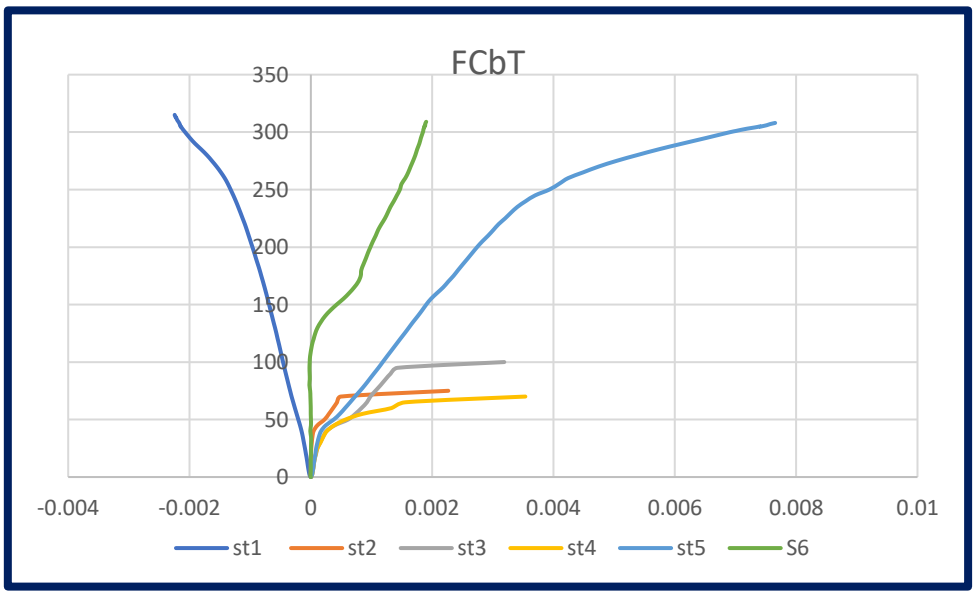
FCbT
350
300
250
200
150
100
50
0
-0.004
-0.002
0
0.002
0.004
0.006
0.008
0.01
st1
st2
st3
st4
st5
S6

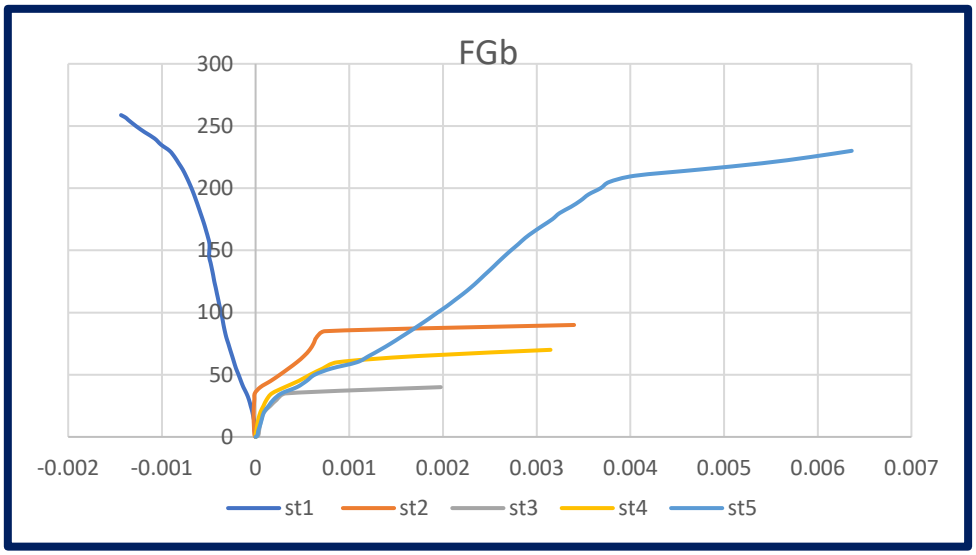
FGb
300
250
200
150
100
50
0
-0.002
-0.001
0
0.001
0.002
0.003
0.004
0.005
0.006
0.007
st1
st2
st3
st4
st5

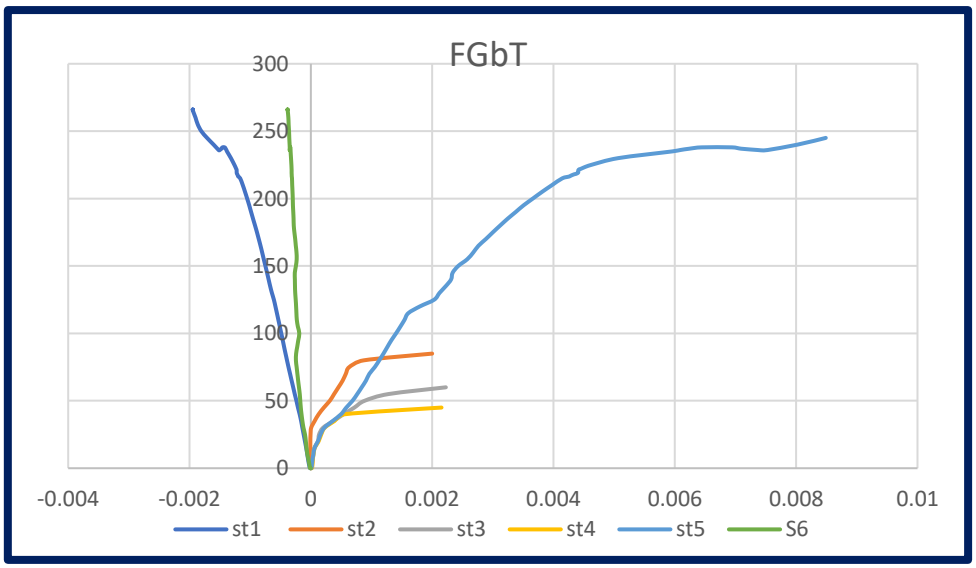
FGbT
300
250
200
150
100
50
0
-0.004
-0.002
0
0.002
0.004
0.006
0.008
0.01
st1
st2
st3
st4
st5
S6

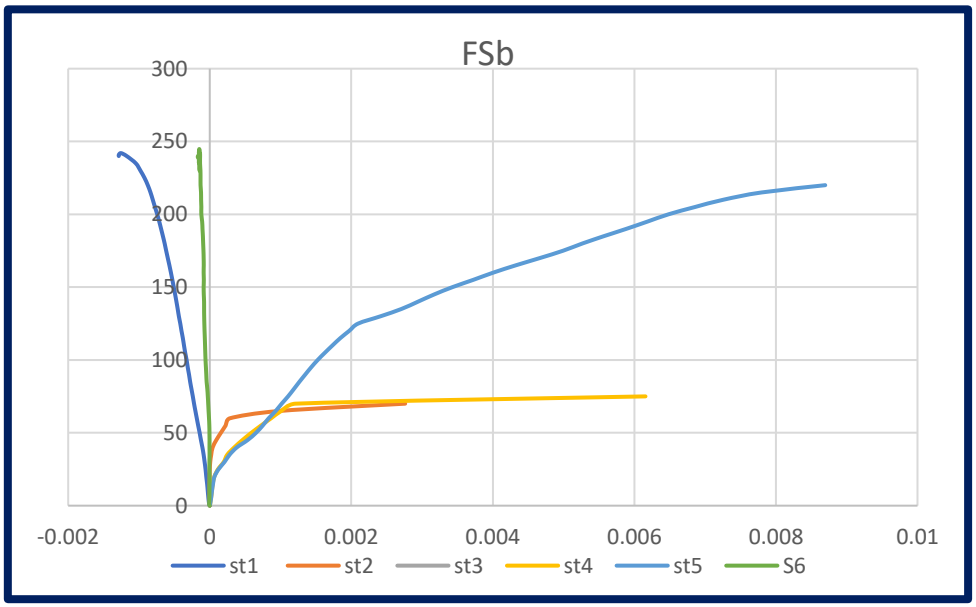
FSb
300
250
200
150
100
50
0
-0.002
0
0.002
0.004
0.006
0.008
0.01
st1
st2
st3
st4
st5
S6

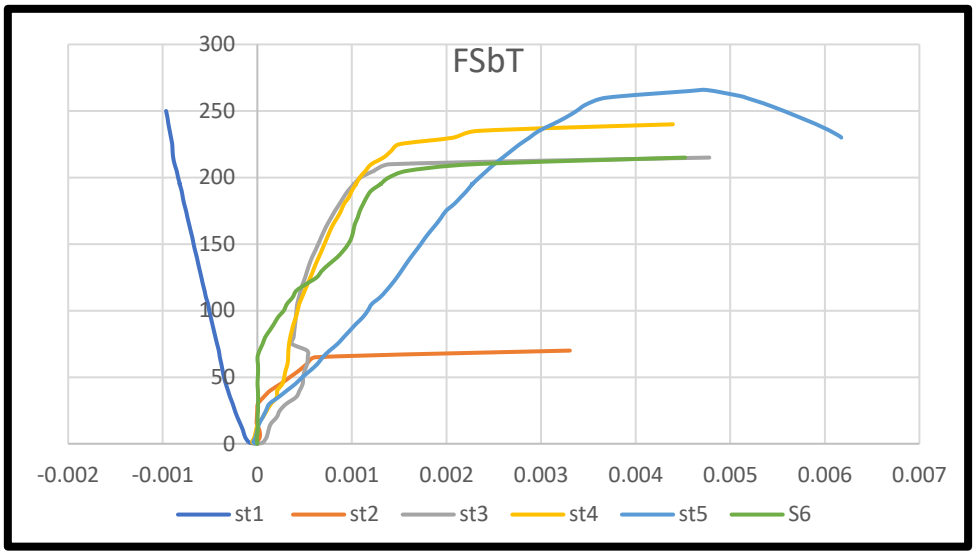

C.3 Compare between strain on bars for group one

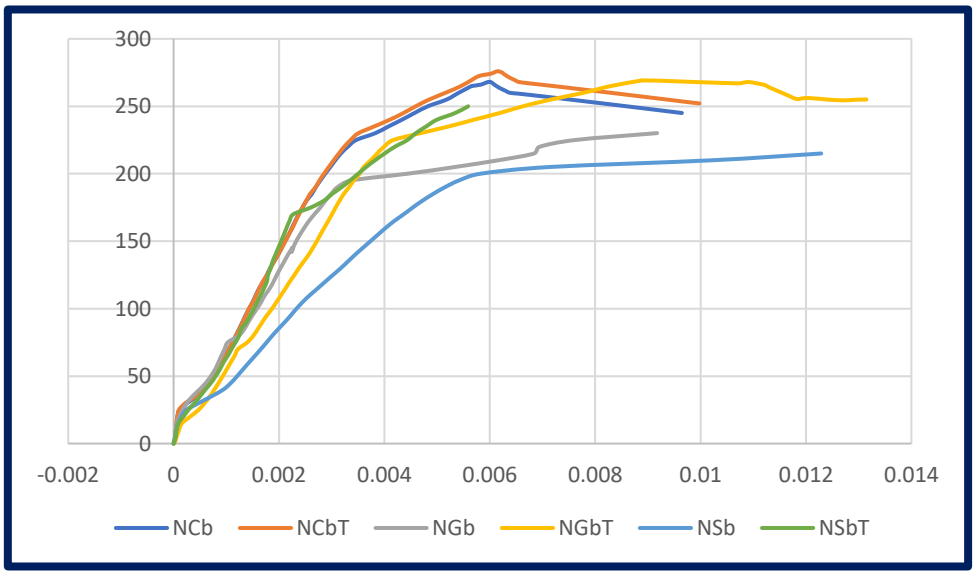

C.4 Compare between strain on bars for group two

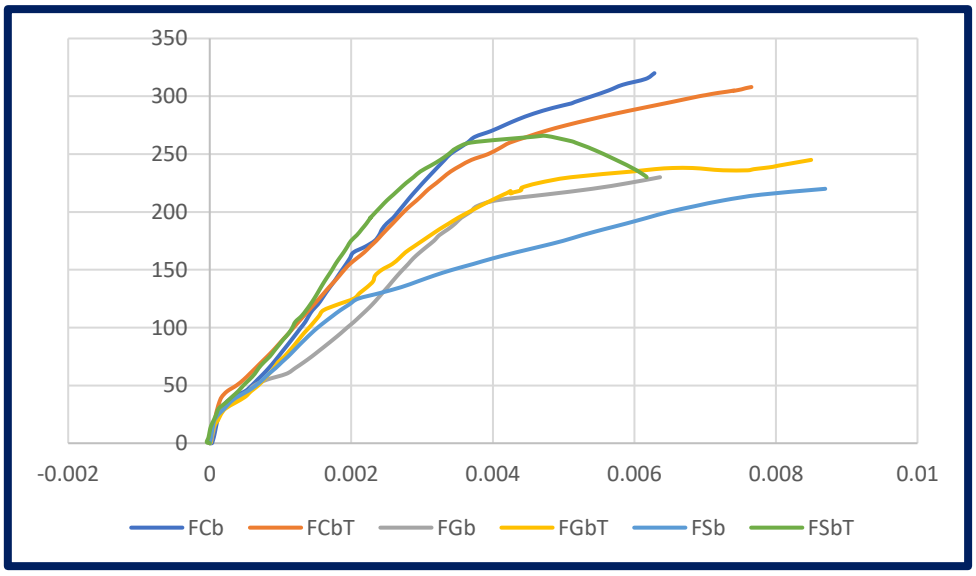

الخلاصة

يمثل تقوية وتعزيز الهياكل جانبًا مهمًا في صناعة البناء بسبب الحاجة المتزايدة لزيادة تحمل المنشأ إلى مستوى معين وضمن أعمال إعادة التأهيل والصيانة المطلوبة. الهدف من هذه الدراسة هو التركيز على سلوك الاعتاب الخرسانية المسلحة المقوى بتقنيتين مركبتين (NSM) و (EBR) في الانثناء. في هذا البحث، تم تخصيص دراسات تجريبية وتحليلية لدراسة سلوك نوعين من الخرسانة (الخرسانة العادية والخرسانة ذات الياف الفايبر) المدعمة ببساطة مع أنواع مختلفة من القضبان والصفائح والمنتجات المركبة.

يتكون العمل التجريبي من تصنيع واختبار ستة عشر عتب من الخرسانة المسلحة بمقطع عرضي (150 × 300 مم) وبطول إجمالي (1500 مم) تم اختبارها تحت حمولة من نقطة واحدة. يتم اختبار جميع العينات إلى الفشل باستخدام أجهزة قياس الضغط وأجهزة تسجيل البيانات وLVDTs، ويتم إعادة تسجيل شكل الفشل وسعة التحمل القصوى.

إلى جانب ذلك، يتم قياس الاجهادات وعرض الشق ونمط الشق في الخرسانة عند مستويات تحميل مختلفة. أظهرت النتائج التجريبية زيادة في سعة التحمل القصوى لجميع الاعتاب المقواة مقارنة بأعتاب التحكم. أيضًا، في المجموعة الأولى، عند استخدام الخرسانة العادية لهذه الاعتاب المقواة، يكون استخدام CFRP أفضل من GFRP وحديد التسليح الصلب بحوالي 2.41٪. يعد استخدام NSM CFRP مع تقوية تقنية CFRP (EBR) أفضل من استخدام CFRP (NSM) فقط، والزيادة في الحمل النهائي حوالي 5.49٪. استخدام الألياف الفولاذية الدقيقة في المجموعة الثانية في التسليح في الاعتاب RC له تأثير على مقاومة الانحناء وانحراف الاعتاب المفحوصة بنسبة (14.94٪) أفضل من المجموعة الأولى. تقوية الاعتاب بواسطة مركبات CFRP يقلل الحد الأقصى للانحراف تحت نفس الانحراف في منتصف فترة الحمل بنسبة 55.92 ٪ للأعتاب مع NSM CFRP.

من ناحية أخرى، تم تقليل الحد الأقصى للانحراف بنسبة 60.02٪ للأعتاب باستخدام EBR. أظهرت النتائج أن ألياف الكاربون لديها قدرة جيدة على إصلاح الاعتاب التالفة، مع تحسن في قدرة تحمل العارضة. طريقة إعادة التأهيل المثلى هي استخدام شريط CFRP مع شريحة CFRP بحوالي (44.08٪ -38.37٪).

يقدم البحث النظري نموذجًا ثلاثي الأبعاد للعناصر المحدودة غير الخطية مناسب لتحليل الاعتاب الخرسانية المسلحة، والذي تم إنتاجه باستخدام برنامج الحاسوب ANSYS (V. 19.2). يفترض وجود رابط تام بين CFRP وGFRP والسطح الخرساني وبين حديد التسليح والخرسانة. تُستخدم عناصر الطوب SOLID65 وSOLID45 لتمثيل العناصر الخرسانية والألواح الفولاذية، على التوالي. بينما تم استخدام LINK180 لتمثيل حديد التسليح وBeam188 CFRP وGFRP bar، على التوالي. تم استخدام Shell 181 لتمثيل مركبات CFRP، على التوالي. بناءً على الحمل النهائي، أظهرت مقارنة النتائج التجريبية والنظرية أنها كانت قريبة جدًا من بعضها البعض.

جمهورية العراق
وزارة التعليم العالي والبحث العلمي
جامعة بابل
كلية الهندسة
قسم الهندسة المدنية

سلوك الأنثناء للاعتاب الخرسانية المسلحة والمقواة بقضبان مثبتة بالقرب من السطح وصفائح الياف الكاربون المسلحة بالبوليمر

رسالة
مقدمة الى كلِّية الهندسة / جامعِة بابل وهي جزءٍ من متطلبات الحصول على درجة الماجستير
في الهندسةِ / الهندسة المدنيِة / انشاءات

من قبل

هديل سمير حمدي حكيم

أشراف

أ. م. د. حيدر محمد جواد علي الخفاجي

2022 A.D **1444 A.H**